Chapter 7
Quantum Communications Systems

7.1 Introduction

The quantum decision theory, developed in the previous two chapters, is now applied to quantum communications systems where the nature of the states that carry the information is specified. A *constellation of K quantum states*, to which to commit a symbol belonging to a K-ary alphabet, corresponds, in the classical version, to a K-ary modulation format. We still consider states that operate at optical frequencies (*optical* quantum systems), because at radio frequencies quantum phenomena are not appreciable. In practice, the quantum states are usually treated as *coherent states* of a coherent monochromatic radiation emitted by a laser. For these states there exists a universal model, proposed by Glauber, that will be introduced in the next section.

Also *squeezed states* as a candidate carrier for quantum communications are considered. Squeezed light is an efficient form of optical radiation, which is obtained from a laser radiation in several ways, mainly based on parametric amplifiers.

In this chapter, we shall first examine *binary* systems, presenting the quantum versions of the OOK (on–off keying) and 2PSK (phase-shift keying) modulations. Then we shall move to *multilevel* systems, and examine the quantum versions of the QAM (quadrature amplitude), PSK, and PPM (pulse position) modulations. All the above-mentioned systems will be examined *in the absence of thermal noise*, which, instead, will be considered in the next chapter. Thus, in this chapter, the scheme of Fig. 7.1 will be followed, in which the channel is ideal and the received state is directly given by the transmitted state. As already observed, neglecting thermal noise does not mean that the analysis will be done in the absence of noise; because we shall take into account the fact that quantum measurements are affected by an intrinsic randomness, corresponding, in the classical model, to *shot noise*.

Organization of the Chapter

The next two sections deal with the definition and properties of coherent states and how to provide a constellation of coherent states. Section 7.5 develops the theory of *classical* optical systems where the decision is based on photon counting.

G. Cariolaro, *Quantum Communications*, Signals and Communication Technology,
DOI 10.1007/978-3-319-15600-2_7

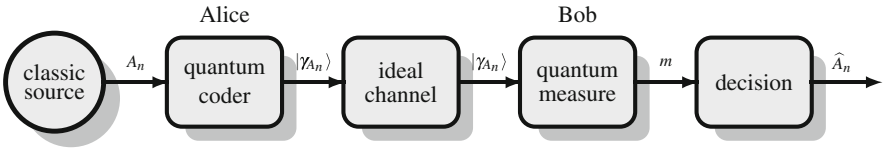

Fig. 7.1 Quantum communications system for digital transmission. $\{A_n\}$ is a sequence of classical symbols of information that Alice conveys into a sequence of quantum states $\{|\gamma_{A_n}\rangle\}$. Bob, in each symbol period, performs a quantum measurement to argue, from the result m of the measurement, which symbol was transmitted

The subsequent sections, from Sects. 7.9 to 7.13, develop the specific quantum communications system with the modulation format listed above.

In the two final sections, we will develop quantum communications with squeezed states with a comparison of the performance with that obtained with coherent states.

As explained in Chap. 4, only digital systems will be considered. For binary systems, we shall use the general theory of binary optimization, essentially Helstrom's theory, developed in Sect. 5.4. For multilevel systems, for which an explicit optimization theory is not available, we shall use the square root measurements (SRM) decision developed in Chap. 6 and, when convenient, we compare SRM results with the ones obtained with convex semidefinite programming (CSP).

7.2 Overview of Coherent States

A general model of the quantum state created by an electromagnetic field at a certain (optical) frequency is given by a coherent quantum state according to Glauber's theory. This model is now formulated in detail in a form suitable to deal with quantum communications systems, but without entering in theoretical considerations. In Chap. 11 coherent states will be fully developed in the framework of quantum information as *continuous quantum states* and also as *Gaussian quantum states*.

7.2.1 Glauber's Representation

The *coherent* radiation emitted by a laser is modeled as a *coherent state*. It has been demonstrated [1–3] that the coherent states of a *single mode* can be represented in a Hilbert space of infinite dimensions, through an orthonormal basis $\{|n\rangle, n = 0, 1, 2, \ldots\}$, where the states are called *number states*, because $|n\rangle$ *contains exactly n photons*. They are also called *number eigenstates* and *Fock states*.

To this basis, the *number operator* is associated, which is defined by

$$N = \sum_{n=0}^{\infty} n|n\rangle\langle n. \tag{7.1}$$

Then N has eigenvectors $|n\rangle$ with eigenvalues n and the spectrum of N is given by the set of naturals, $\sigma(N) = \{0, 1, 2, \ldots\}$.

In this mathematical context, a generic *coherent state* (or Glauber state) is expressed as follows:

$$\boxed{|\alpha\rangle = \mathrm{e}^{-\frac{1}{2}|\alpha|^2} \sum_{n=0}^{\infty} \frac{\alpha^n}{\sqrt{n!}} |n\rangle.} \tag{7.2}$$

where α is a complex amplitude whose meaning is

$$|\alpha|^2 = \text{average number of photons in the state } |\alpha\rangle. \tag{7.3}$$

Therefore, according to (7.2), to each point α of the complex plane $\mathbb{C}$, a coherent state is associated whose physical meaning is given by (7.3). Thus, the more α moves away from the origin of $\mathbb{C}$, the higher becomes the photonic intensity associated to the state $|\alpha\rangle$.

The set of coherent states will be indicated by

$$\mathcal{G} = \{|\alpha\rangle, \alpha \in \mathbb{C}\} \quad : \quad \text{coherent states} \tag{7.4}$$

and then the notation $|\alpha\rangle \in \mathcal{G}$ will be used to distinguish one of these specific kets from the other numerous kets that we will meet. It is interesting to observe that letting $\alpha = 0$ in (7.2) we obtain

$$|\alpha\rangle_{\alpha=0} = |n\rangle_{n=0} \tag{7.5}$$

that is, with $\alpha = 0$ we obtain the state $|0\rangle$ of the Fock basis, called *ground state*.

Remark The notations of Quantum Mechanics are powerful, but sometimes subtle. In this context, it is important to distinguish the complex number $\alpha \in \mathbb{C}$ from the coherent state $|\alpha\rangle \in \mathcal{G}$, which is a ket of the infinite dimensional Hilbert space $\mathcal{H}$, generated by the basis $\{\ |n\rangle | n = 0, 1, 2, \ldots\ \}$. The fundamental relation (7.2) is a mapping $\mathbb{C} \to \mathcal{G}$, where $\mathcal{G} \subset \mathcal{H}$. For instance, $\alpha = 3 - \mathrm{i}4 \in \mathbb{C}$ is mapped onto the coherent state $|3 - \mathrm{i}4\rangle \in \mathcal{G}$, whose full expression is

$$|3 - \mathrm{i}4\rangle = \exp\left[-\frac{1}{2}|3 - \mathrm{i}4|^2\right] \sum_{n=0}^{\infty} \frac{(3 - \mathrm{i}4)^n}{\sqrt{n}} |n\rangle.$$

7.2.2 Link with Poisson's Regime

To find the relationship between the representation of a coherent state $|\alpha\rangle \in \mathcal{G}$ and Poisson's regime, we set up a quantum measurement (Fig. 7.2) with the number

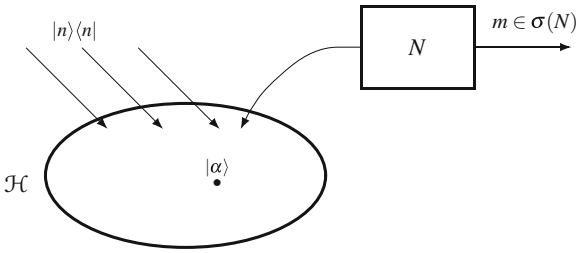

Fig. 7.2 Quantum measurement in a Hilbert space of the coherent state $|\alpha\rangle$ with an observable given by the number operator N. The elementary projectors $|n\rangle\langle n|$ are formed by the number states $|n\rangle$

operator N, interpreted as an *observable* (see Sect. 3.6). The outcome m of the measurement gives the number of photons of the quantum system in the state $|\alpha\rangle$. Then the probability that the measurement gives the outcome $m = i$ turns out to be

$$\begin{aligned} \mathrm{P}[m = i|\alpha] = |\langle i|\alpha\rangle|^2 &= \left| \sum_{n=0}^{\infty} \mathrm{e}^{-\frac{1}{2}|\alpha|^2} \frac{\alpha^n}{\sqrt{n!}} \langle i|n\rangle \right|^2 \\ &= \left| \mathrm{e}^{-\frac{1}{2}|\alpha|^2} \frac{\alpha^i}{\sqrt{i!}} \right|^2 = \mathrm{e}^{-|\alpha|^2} \frac{|\alpha|^{2i}}{i!}. \end{aligned} \tag{7.6}$$

Therefore,

$$\mathrm{P}[m = i|\alpha] = \mathrm{e}^{-N_\alpha} \frac{(N_\alpha)^i}{i!} \quad \text{with} \quad N_\alpha = |\alpha|^2. \tag{7.7}$$

It can also be verified that the average of m is

$$\mathrm{E}[m|\alpha] = \langle \alpha|N|\alpha\rangle = |\alpha|^2 = N_\alpha. \tag{7.8}$$

In conclusion, the outcome of the measurement m is a Poisson random variable with average $N_\alpha = |\alpha|^2$.

7.2.3 Degree of Superposition of Coherent States

It is important to evaluate the degree of superposition of two distinct coherent states $|\alpha\rangle$ and $|\beta\rangle$, within the geometry given by the inner product. We have

Proposition 7.1 *The inner product of two coherent states is given by*

$$\boxed{\langle \alpha|\beta\rangle = \mathrm{e}^{-\frac{1}{2}(|\alpha|^2+|\beta|^2-2\alpha^*\beta)}.} \tag{7.9}$$

Hence **two distinct coherent states are never orthogonal** *(Fig. 7.3).*

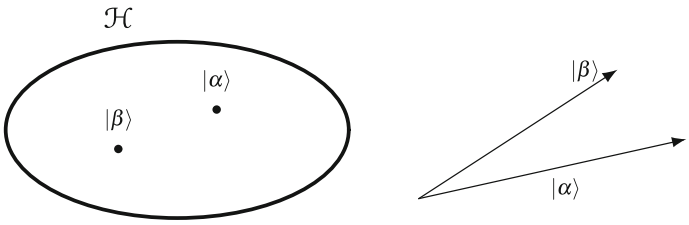

Fig. 7.3 Two distinct coherent states are never orthogonal: $\langle\alpha|\beta\rangle \neq 0$

In fact, from (7.2) we have

$$\begin{aligned}\langle\alpha|\beta\rangle =& \mathrm{e}^{-\frac{1}{2}(|\alpha|^2+|\beta|^2)} \sum_{m=0}^{\infty}\sum_{n=0}^{\infty} \frac{(\alpha^*)^m \beta^n}{\sqrt{m!n!}} \langle m|n\rangle \\ =& \mathrm{e}^{-\frac{1}{2}(|\alpha|^2+|\beta|^2)} \sum_{m=0}^{\infty} \frac{(\alpha^*\beta)^m}{m!} = \mathrm{e}^{-\frac{1}{2}(|\alpha|^2+|\beta|^2)} \mathrm{e}^{\alpha^*\beta}.\end{aligned}$$

and (7.9) follows □

The *(quadratic)* degree of superposition of two states is expressed by

$$\boxed{|X|^2 := |\langle\alpha|\beta\rangle|^2 = \mathrm{e}^{-|\alpha-\beta|^2}, \qquad |\alpha\rangle, |\beta\rangle \in \mathcal{G}} \tag{7.10}$$

where $X = \langle\alpha|\beta\rangle$.

7.2.4 Tensor Product of Coherent States ⇓

The tensor product of two or more coherent states will be particularly relevant to PPM modulation and in general for *vector* modulations.

Let $|\alpha\rangle$ be the tensor product of two coherent states

$$|\alpha\rangle = |\alpha_1\rangle \otimes |\alpha_2\rangle, \qquad |\alpha_1\rangle, |\alpha_2\rangle \in \mathcal{G}.$$

Then, for each of the two factors, the previous result holds: To the state $|\alpha_i\rangle$ a Poisson variable m_i can be associated, with average $\mathrm{E}[m_i|\,\alpha_i] = |\alpha_i|^2$. The global number of photons m associated to the composite state $|\alpha\rangle$ is given by the sum of the two random variables $m = m_1 + m_2$, where m_1 and m_2 are statistically independent. Therefore, m is again a Poisson variable with average $\mathrm{E}[m|\,\alpha] = \mathrm{E}[m_1|\,\alpha_1] + \mathrm{E}[m_2|\,\alpha_2] = |\alpha_1|^2 + |\alpha_2|^2$. This result can be easily generalized to the tensor product of N Glauber states

$$|\alpha\rangle = |\alpha_1\rangle \otimes |\alpha_2\rangle \otimes \cdots \otimes |\alpha_N\rangle$$

and we find, in particular, that the total number of photons $m = m_1 + m_2 + \cdots m_N$ associated to the composite state $|\alpha\rangle$ is still a Poisson variable with average given by

$$\mathrm{E}[m|\,\alpha] = |\alpha_1|^2 + |\alpha_2|^2 + \cdots + |\alpha_N|^2. \tag{7.11}$$

7.2.5 Coherent States as Gaussian States ∇

In Chap. 11, in the framework of continuous quantum variables, coherent states will be defined as eigenkets of the annihilator operator, acting in an infinite dimensional bosonic Hilbert space $\mathcal{H}$. Then, from this abstract definition, the infinite dimensional representation (7.2) is obtained. An alternative representation is considered in the so-called *phase space*, where a quantum state, pure or mixed, is represented by its *Wigner function* $W(x, y)$, a real function of two real variables, having properties similar to the joint probability density of two continuous random variables. Thus we pass from an infinite dimensional Hilbert space $\mathcal{H}$ to the two-dimensional real space $\mathbb{R}^2$, with notable advantages.

The Wigner function $W(x, y)$ allows us to define *Gaussian quantum states*, as the quantum states having as Wigner function the Gaussian bivariate form

$$W(x, y) = \frac{1}{2\pi\sqrt{\det V}} \exp\left[-\frac{1}{2}\frac{V_{22}(x-\overline{q})^2 + V_{11}(y-\overline{p})^2 - 2V_{12}(x-\overline{q})(y-\overline{p})}{\det V}\right] \tag{7.12}$$

where V_{ij} are the covariances and $\overline{q}$, $\overline{p}$ are the mean values ($\det V = V_{11}V_{22} - V_{12}^2$). Hence a Gaussian state is completely specified by the mean vector and by the covariance matrix

$$\bar{X} = \begin{bmatrix} \overline{q} \\ \overline{p} \end{bmatrix}, \qquad V = \begin{bmatrix} V_{11} & V_{12} \\ V_{12} & V_{22} \end{bmatrix}. \tag{7.13}$$

To emphasize this property, a Gaussian state in general represented by a density operator is symbolized as $\rho(\bar{X}, V)$.

We shall see that a coherent state $|\alpha\rangle$ is a special case of Gaussian states with the simple specification

$$\bar{X} = \begin{bmatrix} \overline{q} \\ \overline{p} \end{bmatrix} = \begin{bmatrix} \Re\alpha \\ \Im\alpha \end{bmatrix}, \qquad V = \begin{bmatrix} 1 & 0 \\ 0 & 1 \end{bmatrix} = I_2. \tag{7.14}$$

Then the Wigner function of a coherent state results in

$$W(x, y) = \frac{1}{2\pi} \exp\left[-\frac{1}{2}\left((x-\overline{q})^2 + (y-\overline{p})^2\right)\right] \tag{7.15}$$

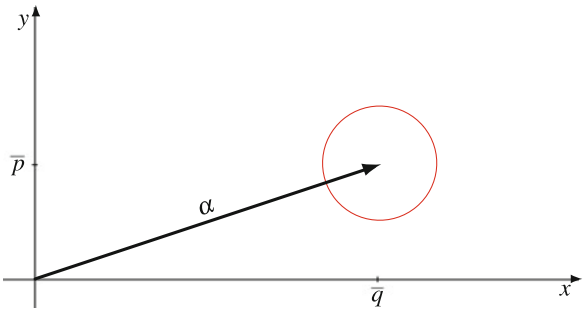

Fig. 7.4 Contour level of the Wigner function $W(x, y)$ of a pure coherent state $|\alpha\rangle$ (in *red*). The mean vector $(\overline{q}, \overline{p}) = (\Re\alpha, \Im\alpha)$ gives the center of the contour

and in the x, y plane it is often represented by a *contour level* obtained by the equation $W(x, y) = L$, where $L > 0$ is a reference level. For a coherent state, this contour is a circle centered at $(\overline{q}, \overline{p})$, as shown in Fig. 7.4.

Problem 7.1 ⋆ Prove that the inner product $X = \langle\alpha|\beta\rangle$ of two coherent states is real if and only if $\arg\alpha - \arg\beta = 0$ or $\arg\alpha - \arg\beta = \pm\pi$.

Problem 7.2 ⋆⋆ The map (7.2) gives for any $\alpha \in \mathbb{C}$ a coherent state $|\alpha\rangle$. Given $|\alpha\rangle$ is it possible to find the complex number α?

Problem 7.3 ⋆⋆ Examine the effect of the introduction of a phasor $z = e^{i\varphi}$ into the complex parameter α that identifies the state $|\alpha\rangle$, that is, evaluate $|e^{i\varphi}\alpha\rangle$.

Problem 7.4 ⋆⋆⋆ Let $|\alpha\rangle = |\alpha_1\rangle \otimes |\alpha_2\rangle$ be a two-mode coherent states. The number of photons m_i associated to each component state is a Poisson variable with mean $\Lambda_i = |\alpha_i|^2$. Considering that m_1 and m_2 are statistically independent (see Sect. 3.10), prove that the total number of photons $m = m_1 + m_2$ is a Poisson variable.

Hint: use the characteristic function given by (4.23).

7.3 Constellations of Coherent States

We recall that the target of a quantum communications system is the transmission of a sequence of classical symbols $\{A_n\}$ through a sequence of quantum states $\{|\gamma_{A_n}\rangle\}$, which in practice are often coherent states. Thus, in general, with a K-ary alphabet $\mathcal{A} = \{0, 1, \ldots, K-1\}$, Alice must be able to prepare a **constellation** of K coherent states

$$\mathcal{S} = \{|\gamma_0\rangle, |\gamma_1\rangle, \ldots, |\gamma_{K-1}\rangle\} \tag{7.16}$$

to realize the c → q mapping

$$A_n \in \mathcal{A} \quad \rightarrow \quad |\gamma_{A_n}\rangle \in \mathcal{S},$$

which must be bijective. This operation may be called *quantum encoding*.

Now a problem to investigate is the choice of the constellation, of course, with the purpose of realizing a high-performance quantum transmission system. One way to decide about the choice, as we shall see in this section, is to get the "inspiration" from the optical transmission systems that we shall briefly call *classical systems*. This approach has also the advantage of allowing us a comparison between the performances of two kinds of systems, classical and quantum.

In Sect. 4.4, we have seen that optical communications use two kinds of modulations, incoherent and coherent; but in the present context, the right comparison is with classical coherent modulations which make use just of a coherent radiation emitted by a laser, as done in quantum communications. A classical K-ary coherent modulation, in general nonlinear, is specified by K complex waveforms

$$\gamma_0(t), \gamma_1(t), \ldots, \gamma_{K-1}(t) \tag{7.17}$$

of duration limited[1] to the signaling interval $[0, T]$, with the rule that if $A_n \in \mathcal{A}$ is the nth source symbol, the modulator forms a signal with *complex envelope*[2] [4]

$$c(t) = \gamma_{A_n}(t) \qquad 0 \le t < T.$$

With a sequence of symbols $\{A_n\}$, the complete expression of the complex envelope becomes

$$c(t) = \sum_{n=-\infty}^{+\infty} \gamma_{A_n}(t - nT)\,, \tag{7.18}$$

from which a real modulated signal is obtained as

$$v(t) = \Re\, c(t)\, \mathrm{e}^{\mathrm{i}2\pi\nu t} \tag{7.19}$$

where ν is the carrier optical frequency. The comparison between a classical modulator and a quantum encoder is depicted in Fig. 7.5.

To proceed from the classical system, characterized by the waveforms $\gamma_i(t)$, $i \in \mathcal{A}$, to the quantum system with coherent state constellation $|\gamma_i\rangle$, $i \in \mathcal{A}$, we must "remove" in some way the time dependence, which is not present in coherent states. For some kinds of modulations the solution is straightforward; for others, it is less obvious.

[1] Some classical coherent modulations use a duration greater than one symbol period.

[2] See Sect. 4.7 for the definition of complex envelope.

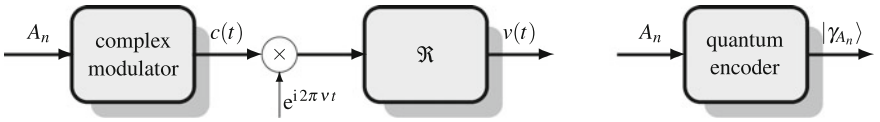

Fig. 7.5 Comparison of a classical modulator (*left*) with a quantum encoder

7.3.1 State Constellations from Scalar Modulations

In some modulations, like PSK and QAM, the waveforms (7.17) are of the form

$$\gamma_i(t) = \gamma_i\, h(t)\,, \qquad i \in \mathcal{A} = \{0, 1, \ldots, K-1\}, \tag{7.20}$$

where $h(t)$ is a real pulse; for example, rectangular between 0 and T, and γ_i are complex numbers. The complex envelope $c(t)$ of the modulated signal is then produced by an encoder, mapping the symbols $i \in \mathcal{A}$ into the complex symbols γ_i, and by an interpolator with impulse response $h(t)$. The resulting complex envelope becomes

$$c(t) = \sum_{n=-\infty}^{+\infty} C_n\, h(t - nT)\,, \tag{7.21}$$

where $\{C_n\}$ is the sequence of complex symbols obtained by the mapping $A_n = i \;\rightarrow C_n = \gamma_i$ (Fig. 7.6).

In this way, a *constellation of complex symbols* is identified

$$\mathcal{C} = \{\gamma_0, \gamma_1, \ldots, \gamma_{K-1}\}\,, \qquad \gamma_i \in \mathbb{C} \tag{7.22}$$

from which one can form the *constellation of coherent states*

$$\mathcal{S} = \{|\gamma_0\rangle, |\gamma_1\rangle, \ldots, |\gamma_{K-1}\rangle\}\,, \qquad |\gamma_i\rangle \in \mathcal{G} \tag{7.23}$$

that are in a one-to-one correspondence with the constellation of complex symbols $\mathcal{C}$ (Fig. 7.7).

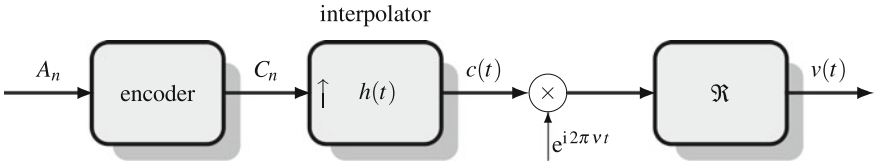

Fig. 7.6 Scheme of a classical **scalar modulator**. The encoder maps the source symbols $A_n \in \mathcal{A}$ into the complex symbols $C_n \in \mathcal{C}$. The interpolator maps the complex symbols into the complex envelope $c(t)$

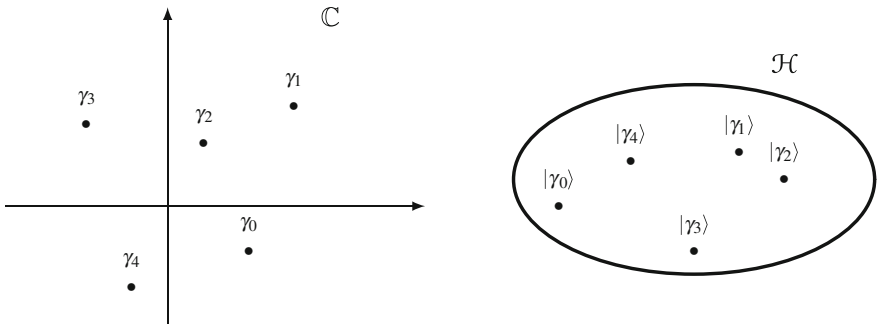

Fig. 7.7 Constellation of complex symbols $\mathcal{C}$ and corresponding constellation of coherent states $\mathcal{S}$: each complex symbol $\gamma \in \mathcal{C}$ is mapped into a coherent state $|\gamma\rangle \in \mathcal{S}$

7.3.2 State Constellations from Vector Modulations ⇓

The previous procedure, consisting in directly creating the constellation of coherent states from the constellation of symbols, is not always possible, because in general the K waveforms (7.17) cannot be expressed in the form (7.20). To remove the time dependence, we can proceed in the following way [4]. We take a basis of functions, $h_1(t), \ldots, h_N(t)$, orthonormal in the interval $[0, T)$, where, in general, $N \leq K$, and we expand the waveforms (7.17) on this basis, namely

$$\gamma_i(t) = \sum_{j=1}^{N} \gamma_{ij}\, h_j(t)\,, \qquad i = 0, 1, \ldots, K-1 \tag{7.24a}$$

where the coefficients are given by

$$\gamma_{ij} = \int_0^T \gamma_i(t)\, h_j^*(t)\, \mathrm{d}\, t\,, \qquad j = 1, \ldots, N. \tag{7.24b}$$

The vectors of the complex coefficients

$$\gamma_i = (\gamma_{i1}, \ldots, \gamma_{iN})\,, \qquad i = 0, 1, \ldots, K-1 \tag{7.25}$$

uniquely identify the waveform $\gamma_i(t)$.

The classical modulator can be implemented as in Fig. 7.8, where the encoder makes the map

$$A_n = i \in \mathcal{A} \quad \rightarrow \quad C_n = \gamma_i \in \mathbb{C}^N$$

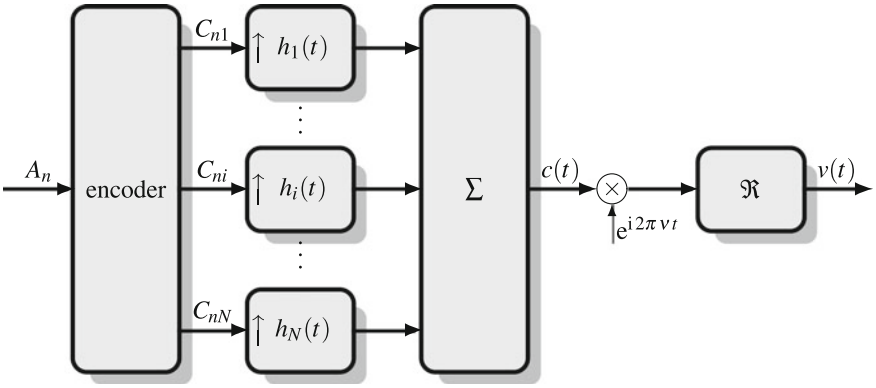

Fig. 7.8 Scheme of a classical **vector modulator**. The encoder maps the source symbols $A_n \in \mathcal{A}$ into a vector of complex symbols $C_n = [C_{n1}, \ldots, C_{ni}, \ldots, C_{nN}]^{\mathrm{T}}$. The bank of interpolators maps the vectors C_n into the complex envelope $c(t)$

with

$$C_n = [C_{n1}, \ldots, C_{nN}], \qquad \gamma_i = [\gamma_{i1}, \ldots, \gamma_{iN}].$$

Then from the vector C_n, a bank of interpolators forms the complex envelope $c(t)$ of the modulated signal, as

$$c(t) = \sum_{n=-\infty}^{\infty} \sum_{i=1}^{N} C_{ni}\, h_i(t - nT). \tag{7.26}$$

This generalizes the scalar modulation, which is obtained with $N = 1$.

The general procedure just described allows us to identify a constellation of complex vectors $\{\gamma_i, i = 0, \ldots, K-1\}$ with $\gamma_i \in \mathbb{C}^N$. Now, to introduce the coherent states, we must consider a composite Hilbert space, given by the tensor product $\mathcal{H} = \mathcal{H}_0 \otimes \mathcal{H}_0 \otimes \cdots \otimes \mathcal{H}_0$ of N equal Hilbert spaces $\mathcal{H}_0$. In this composite space, the states become the *tensor product* of coherent states and, through (7.25), to each symbol $i \in \mathcal{A}$ the **tensor product of coherent states** is associated

$$|\gamma_i\rangle = |\gamma_{i1}\rangle \otimes |\gamma_{i2}\rangle \otimes \cdots \otimes |\gamma_{iN}\rangle \tag{7.27}$$

that, with i varying in $\mathcal{A}$, forms the desired constellation of coherent states. In the context of continuous variables of Chap. 11, the tensor product of N coherent states (7.27) is called N-**mode coherent state**.

An example in which we use this method of forming a composite constellation of coherent states will be seen in PPM modulation developed in Sect. 7.13 (see also Problem 7.5).

7.3.3 Construction of a Symmetric Constellation

An innovative way to obtain a state constellation is based on the geometrically uniform symmetry (GUS), introduced in Sect. 5.13. To this end, it is sufficient finding a unitary operator S having the property of a symmetry operator S

$$S^K = I_{\mathcal{H}} \tag{7.28}$$

that is, S must be a Kth root of the identity operator. Then, fixing an arbitrary state $|\gamma_0\rangle \in \mathcal{H}$, one gets a K-ary constellation of states as

$$|\gamma_i\rangle = S^i\,|\gamma_0\rangle\,, \qquad i = 0, 1, \ldots, K-1. \tag{7.29}$$

More generally, one can fix an arbitrary density operator ρ_0 acting on the Hilbert space $\mathcal{H}$ to get a constellation of density operators as (see (5.123))

$$\rho_i = S^i\,\rho_0\,(S^i)^*\,, \qquad i = 0, 1, \ldots, K-1. \tag{7.30}$$

In this way, we can generate infinitely many constellations having the very useful property represented by the GUS. After the choice of S and of the reference state $|\gamma_0\rangle$ or ρ_0, one achieves "interesting practical properties" for the quantum communications system based on the corresponding constellation. A nontrivial problem is finding a unitary operator with the property (7.28), especially in the case of infinite dimensions, as is for coherent states.

Problem 7.5 ⋆⋆ Show that the PPM must be considered a vector modulation. Find explicitly the waveform $\gamma_i(t)$ and the vector γ_i of the coefficients.

Problem 7.6 ⋆⋆ The n-DFT matrix $W_{[n]}$ is unitary and has the property $W_{[n]}^n = I_n$. Then it allows for the construction of n-ary constellations in $\mathcal{H} = \mathbb{C}^n$. Find a quaternary constellation using $S = W_{[4]}$ and reference state $|\gamma_0\rangle = [1, 1, 0, 0]^{\mathrm{T}}$. Also prove that the four states are linearly independent.

7.4 Parameters in a Constellation of Coherent States

In the previous section, we have investigated how to form interesting constellations of coherent states for quantum communications systems. In this section, we want to clarify how a given constellation format can be parametrized to modify the photonic flux therein, expressed, e.g., in terms of the number of signal photons per symbol. In fact, we are interested in the evaluation of the system performance in a given range of this parameter.

Note that the constellation of coherent states $\mathcal{S}$ given by (7.23) can be structured in matrix form as

$$\Gamma = [|\gamma_0\rangle, |\gamma_1\rangle, \ldots, |\gamma_{K-1}\rangle] \tag{7.31}$$

and becomes the *state matrix*. In practical modulation formats (that will be considered further on), the states of $\mathcal{S}$ are always *independent* (in the sense of vector spaces), and then the state matrix has always full rank, i.e., $\text{rank}(\Gamma) = K$. From the state matrix, we obtain the *Gram's matrix*, a $K \times K$ matrix formed by the inner products between the couples of states

$$G = \Gamma^* \Gamma = \left[\langle \gamma_i | \gamma_j \rangle\right], \qquad |\gamma_i\rangle, |\gamma_j\rangle \in \mathcal{G}$$

that can be calculated using (7.9). Also G has always full rank and, because the states are not orthogonal, all the entries of G are different from zero.

Even in the N-dimensional case, when the states are given by the tensor product of N component states (see (7.27)), to calculate the state superposition, we evaluate the inner products

$$\langle \gamma_i | \gamma_j \rangle = \langle \gamma_{i1} | \gamma_{j1} \rangle \, \langle \gamma_{i2} | \gamma_{j2} \rangle \, \cdots \, \langle \gamma_{iN} | \gamma_{jN} \rangle. \tag{7.32}$$

In this relation we have borne in mind that the inner product of states, given by a tensor product, is obtained as a product of the inner products of the component states (see relation (2.100)). Each of the inner products of the component states is evaluated from (7.9).

7.4.1 Number of Signal Photons in a Constellation

From (7.8) we have that the average number of photons associated to the coherent state $|\gamma\rangle \in \mathcal{G}$ is given by the squared norm of the complex amplitude γ

$$N_\gamma = |\gamma|^2.$$

In a constellation of coherent states, we introduce the *signal photons per symbol*. To this end, we observe that the generic symbol of the constellation, $C \in \mathcal{C}$, must be considered as a random variable with probability $\text{P}[C = \gamma], \gamma \in \mathcal{C}$, and also the average number of photons N_C associated to C becomes a random variable; the statistical average of N_C,

$$N_s = \text{E}[N_C] = \sum_{\gamma \in \mathcal{C}} \text{P}[C = \gamma] N_\gamma = \sum_{\gamma \in \mathcal{C}} \text{P}[C = \gamma] |\gamma|^2, \tag{7.33}$$

defines the *average number of photons per symbol*, briefly **number of signal photons per symbol**. Now, given the one-to-one correspondence $A = i \Leftrightarrow C = \gamma_i$, the probability of these two events turns out to be equal to the prior probability q_i. Therefore, we have

$$N_s = \sum_{i \in \mathcal{A}} q_i |\gamma_i|^2 \quad \text{(photons/symbol)}.$$

In particular, with equally likely symbols, the number of signal photons per symbol becomes

$$\boxed{N_s = \frac{1}{K} \sum_{i \in \mathcal{A}} |\gamma_i|^2 = \frac{1}{K} \sum_{\gamma \in \mathcal{C}} |\gamma|^2.} \tag{7.34}$$

Finally, remembering that, with equiprobable symbols, there are $\log_2 K$ bit/symbol, we find that the **number of signal photons per bit** is given by

$$N_R = \frac{N_s}{\log_2 K} \quad \text{(photons/bit)}. \tag{7.35}$$

⇓ We have seen above that in an N-dimensional constellation $\mathcal{C}$, whose states are N-mode coherent states, $|\gamma\rangle = |\gamma_1\rangle \otimes |\gamma_2\rangle \otimes \ldots \otimes |\gamma_N\rangle$, the average number of photons associated to the composite state $|\gamma\rangle$ results in (see (7.11))

$$N_\gamma = |\gamma_1|^2 + |\gamma_2|^2 + \cdots + |\gamma_N|^2 \tag{7.36}$$

where $\gamma = [\gamma_1, \gamma_2, \ldots, \gamma_N]$. Consequently, the number of signal photons per symbol must be evaluated according to

$$N_s = \sum_{\gamma \in \mathcal{C}} \mathrm{P}[C = \gamma] N_\gamma \tag{7.37}$$

with N_γ given by (7.36), and the sum is extended to the N-dimensional constellation. Of course, with equiprobable symbols we have $\mathrm{P}[C = \gamma] = 1/K$ and the number of signal photons per bit is still given by (7.35).

Sensitivity of a receiver. In telecommunications an important parameter is the sensitivity, which is defined as the minimum value of a parameter of the receiver that guarantees a given value of the error probability P_e, typically $P_e = 10^{-9}$. In optical communications (classical or quantum), the parameter is often given by the number of photons per bit N_R. Thus we say, e.g., that a quantum receiver has the sensitivity of $N_R = 11.5$ photons/bit.

7.4.2 Scale Factor and Shape Factor of a Constellation

The constellation (7.22) of complex symbols $\mathcal{C}$, from which we can *directly* obtain the constellation (7.23) of coherent states $\mathcal{S}$, contains a scale factor linked to the photonic intensity, but modulation formats are usually specified in a normalized form. In the evaluation of a system's performance, it is worthwhile to underline this aspect by expressing the symbols γ_i in the form $\bar{\gamma}_i \Delta$, where $\bar{\gamma}_i$ are *normalized* symbols and Δ is the **scale factor**. Then it is convenient to introduce a *normalized* constellation

$$\mathcal{C}_0 = \{\bar{\gamma}_0, \bar{\gamma}_1, \ldots, \bar{\gamma}_{K-1}\}$$

from which one obtains the scaled constellation as $\mathcal{C} = \{\bar{\gamma}_0 \Delta, \bar{\gamma}_1 \Delta, \ldots, \bar{\gamma}_{K-1} \Delta\}$ and hence the constellation of coherent states as

$$\mathcal{S} = \{|\bar{\gamma}_0 \Delta\rangle, |\bar{\gamma}_1 \Delta\rangle, \ldots, |\bar{\gamma}_{K-1} \Delta\rangle\}.$$

The scale factor appears in the number of signal photons per symbol, given by (7.34), which can be written in the form

$$N_s = \frac{1}{K} \sum_{\gamma \in \mathcal{C}} |\gamma|^2 = \Delta^2 \frac{1}{K} \sum_{\bar{\gamma} \in \mathcal{C}_0} |\bar{\gamma}|^2 = \mu_K \Delta^2 \tag{7.38}$$

where

$$\mu_K := \frac{1}{K} \sum_{\bar{\gamma} \in \mathcal{C}_0} |\bar{\gamma}|^2 \tag{7.39}$$

is a characteristic parameter of the constellation, which we call **shape factor**. For example, in the PSK modulation, the normalized constellation consists of K points on the *unit* circle

$$\mathcal{C}_0 = \{e^{i2\pi m/K} \,|\, m = 0, 1, \ldots, K-1\}$$

whereas the scaled constellation is given by K points on the circle of radius Δ

$$\mathcal{C} = \{\Delta\, e^{i2\pi m/K} \,|\, m = 0, 1, \ldots, K-1\}.$$

In this case, the shape factor is $\mu_K = 1$. An example where $\mu_K \neq 1$ is given by the QAM modulation.

7.4.3 Summary of Constellation Formats

To conclude these two sections on constellations of coherent states, it is convenient to recall that the target of a quantum communications system is the transmission of a classical information, encoded in a *classical* symbol sequence $\{A_n\}$, through a sequence of *quantum* states $\{|\gamma_{A_n}\rangle\}$, as illustrated in Fig. 7.1. Thus, a key operation is the c $\rightarrow$ q mapping $A_n \rightarrow |\gamma_{A_n}\rangle$. This finally explains why we have constellations in both classical and quantum domain.

Here, we wish to summarize the constellations introduced above which are all useful to proceed on. Starting from a symbol alphabet, which was indicated in the form $\mathcal{A} = \{0, 1, \ldots, K-1\}$, we have introduced:

- a constellation of *normalized complex symbols* $\mathcal{C}_0 = \{\bar{\gamma}_0, \bar{\gamma}_1, \ldots, \bar{\gamma}_{K-1}\}$,
- a constellation of *scaled complex symbols* $\mathcal{C} = \{\gamma_0, \gamma_1, \ldots, \gamma_{K-1}\}$, with $\gamma_i = \bar{\gamma}_0 \Delta$, where Δ is a scale factor,
- a constellation of *coherent states* $\mathcal{S} = \{|\gamma_0\rangle, |\gamma_1\rangle, \ldots, |\gamma_{K-1}\rangle\}$, where $|\gamma_i\rangle$ is the coherent state uniquely determined by the scaled complex symbol γ_i, according to relation (7.2).

Note that $\mathcal{C}_0$ and $\mathcal{C}$ live in the field of complex numbers $\mathbb{C}$, while $\mathcal{S}$ lives in the infinite dimensional Hilbert space $\mathcal{H}$.

Problem 7.7 $\star\star\ \nabla$ Find the shape factor μ_k of the 16-QAM constellation (see Fig. 7.28).

7.5 Theory of Classical Optical Systems

We want to compare the performance of a quantum communications system with that of the *corresponding* classical communications system, i.e., not based on quantum measurements, but on an optical detection (see semiclassical detection in Chap. 4).

In the formulation of the transmitter and the receiver, it is convenient to introduce two distinct schemes: One working at the level of *instantaneous optical power* and the other one working on the *complex envelope*. In fact in the semiclassical theory of an optical system, both the optical power and the complex envelope must be jointly considered, as remarked in Sect. 4.7.

7.5.1 Scheme for Instantaneous Optical Powers

We recall that a monochromatic radiation at the optical frequency ν can be modeled as an *instantaneous optical power*, which is formed by the energy quanta of size $h\nu$ and has the impulsive expression

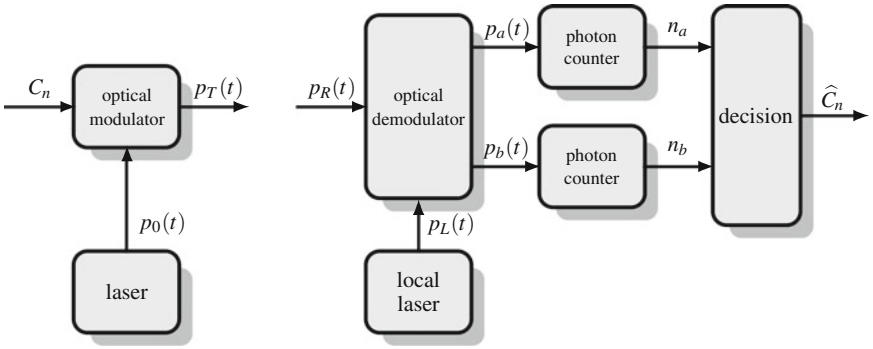

Fig. 7.9 Scheme of a classical modulator and demodulator for the instantaneous optical power. In the figure, the initial encoder $A_n \rightarrow C_n$ and the final decoder $\widehat{C}_n \rightarrow \widehat{A}_n$ are omitted

$$p(t) = \sum_k (h\nu)\, \delta(t - t_k) \tag{7.40}$$

where the arrival instants $\{t_k\}$ are represented by a *doubly stochastic Poisson process*, specified by its random intensity $\lambda(t)$.

Referring to digital systems, the information to be transmitted is first conveyed in a sequence of symbols $\{A_n\}$, $A_n \in \{0, 1, \ldots, K-1\}$ and then, for convenience, in a sequence of complex symbols $\{C_n\}$ belonging to a given (normalized) constellation $\mathcal{C}_0$. Then the first part of the transmitter is an encoder, which provides the map $A_n \rightarrow C_n$. The task of a digital modulator is to modify the laser beam in each symbol period $(nT, nT + T)$ in dependence of the symbol C_n falling in this period.[3] If there are no further processing, as we suppose, the output of the modulator gives the instantaneous transmitted power $p_T(t)$, as shown in Fig. 7.9.

In the receiver, the incoming instantaneous power $p_R(t)$, an attenuated version of $p_T(t)$, is combined with the instantaneous power $p_L(t)$ of a local laser tuned at the same frequency ν as the laser in the transmitter (homodyne detection) or at a different frequency (etherodyne detection). The task of the demodulator is the production of two distinct instantaneous powers $p_a(t)$ and $p_b(t)$ to feed two photon counters, which count the photon numbers in each symbol period as

$$n_a = \frac{1}{h\nu} \int_{nT}^{nT+T} p_a(t)\, \mathrm{d}\, t\,, \qquad n_b = \frac{1}{h\nu} \int_{nT}^{nT+T} p_b(t)\, \mathrm{d}\, t\,.$$

The reason of this double path is due to the fact that n_a and n_b are real (integer) and the receiver has to give an estimated version $\{\widehat{C}_n\}$ of the complex sequence $\{C_n\}$.

In the case of binary systems, where the symbols C_n are real, the double path is not necessary and the detection is based only on a single photon counting. In the following, for brevity, we will consider only homodyne detection.

[3] The practical implementation of this operation will be seen in Sect. 9.2.

7.5.2 Scheme for Complex Envelopes

In an optical system, the complex envelope $V(t)$ (denoted by $c_v(t)$ in Sect. 4.7) contains all the information useful both for the signal analysis and the statistical analysis. In fact from $V(t)$, we can obtain the *signal* $v(t)$, present in the form of electric field, as

$$v(t) = \Re V(t)\, \mathrm{e}^{\mathrm{i}\, 2\pi\, \nu\, t}\,. \tag{7.41}$$

Also, the average power $P(t)$ is proportional to $|V(t)|^2$ and, by appropriate normalization of the electric field, it can be directly written as

$$P(t) = |V(t)|^2\,. \tag{7.42}$$

On the other hand, the average power is connected to the instantaneous power, modeled as a doubly stochastic filtered Poisson process, through Campbell's theorem according to

$$P(t) = \mathrm{E}[p(t)|\lambda] = (h\nu)\,\lambda(t)\,, \tag{7.43}$$

where $\mathrm{E}[\cdot|\lambda]$ denotes the conditional expectation "with a given $\lambda(t)$." This holds for the powers $p_T(t)$, $p_R(t)$, $p_a(t)$, and $p_b(t)$ in the scheme of Fig. 7.9. The fundamental remark is that from the complex envelope $V(t)$, we can obtain the intensity $\lambda(t)$ which gives the full statistical description of the doubly stochastic Poisson processes involved.

At the level of complex envelope, the modulator scheme is essentially the one anticipated in Fig. 7.6, where, starting from the complex sequence $\{C_n\}$, the complex envelope of the modulated signal is obtained with an interpolator according to (7.21), that is,

$$V_T(t) = \sum_{n=-\infty}^{+\infty} C_n V_0\; h(t - nT) \tag{7.44}$$

where V_0 is the amplitude of the carrier produced by the laser. This corresponds to the transmitter instantaneous power $p_T(t)$.

The scheme of the demodulator is extremely simple. To the incoming complex envelope $V_R(t)$, corresponding to the received instantaneous power $p_R(t)$, the amplitude V_L is added for the upper path and the amplitude $\mathrm{i}\, V_L$ to the lower path to get

$$V_a(t) = V_R(t) + V_L, \quad V_b(t) = V_R(t) + \mathrm{i}\, V_L \tag{7.45}$$

as shown in Fig. 7.10.

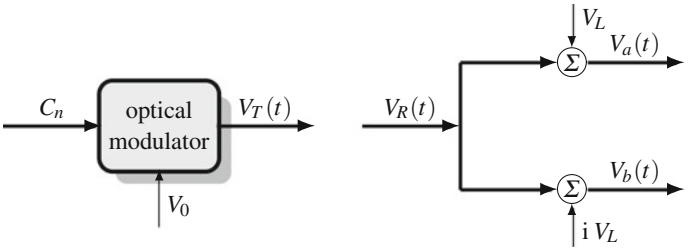

Fig. 7.10 Scheme of a classical modulator and demodulator for the complex envelopes

In the following, we make the assumption that the interpolator impulse response $h(t)$ is unitary in $(0, T)$, so that $V_T(t)$ is simplified as

$$V_T(t) = C_0\, V_0, \quad 0 < t < T. \tag{7.46}$$

Correspondingly (7.45) become

$$V_a(t) = C_0\, V_R + V_L, \quad V_b(t) = C_0\, V_R + \mathrm{i} V_L \tag{7.47}$$

where V_R is the amplitude of the received carrier.

7.5.3 Scheme for Signals. Quadrature Modulator

The scheme for the complex envelope is sufficient for the analysis of an optical system. Now we consider the scheme for the *signal*, which is more detailed and may have interest for the implementation of the system.

Signals are obtained from complex envelopes according to relation (7.41). Letting $C_n = A_n + \mathrm{i}B_n$, from (7.44); we find that the modulated signal results in

$$\begin{aligned} v_T(t) &= \Re \sum_{n=-\infty}^{+\infty} (A_n + \mathrm{i}B_n)\, h(t - nT)\; V_0\, \mathrm{e}^{\,\mathrm{i}\,2\pi\nu t} \\ &= \sum_{n=-\infty}^{+\infty} [A_n V_0\, h(t - nT)\; \cos 2\pi\nu\, t - B_n V_0\, h(t - nT)\; \sin 2\pi\nu\, t]\,. \end{aligned} \tag{7.48}$$

The interpretation of these relations leads to the scheme of Fig. 7.11, called *quadrature modulator*. The carrier $V_T \cos 2\pi\nu t$ is produced by a laser tuned at the frequency ν and the quadrature carrier $-V_T \sin 2\pi\nu t$ is obtained by shifting the carrier $V_T \cos 2\pi\nu t$.

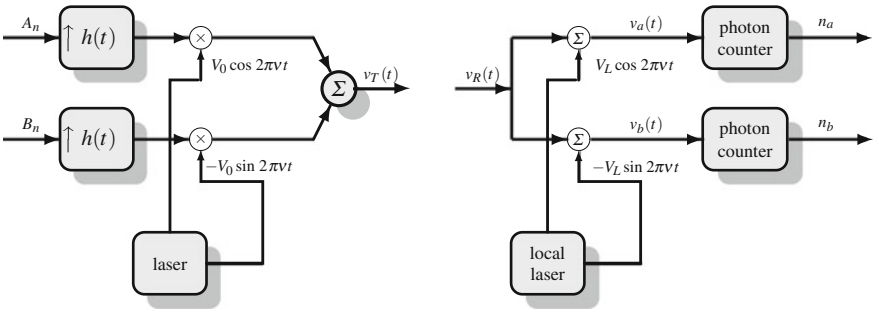

Fig. 7.11 Implementation of a coherent optical system based on a quadrature modulator. On the *left* the transmitter and on the *right* the homodyne receiver

With the simplification of (7.46), (7.48) gives

$$v_T(t) = A_0 V_0 \cos 2\pi\nu t - B_0 V_0 \sin 2\pi\nu t\,, \qquad 0 < t < T. \tag{7.49}$$

At reception, the modulated signal becomes

$$v_R(t) = A_0 V_R \cos 2\pi\nu t - B_0 V_R \sin 2\pi\nu t\,, \qquad 0 < t < T, \tag{7.50}$$

and the constant complex envelopes V_L and i V_L give

$$\Re\ V_L \mathrm{e}^{\mathrm{i}\,2\pi\,\nu\,t} = V_L \cos 2\pi\nu t\,, \qquad \Re\ \mathrm{i}\,V_L \mathrm{e}^{\mathrm{i}\,2\pi\,\nu\,t} = -V_L \sin 2\pi\nu t.$$

These carriers are provided by a local laser, tuned with the transmission laser (homodyne reception). Finally, (7.47) gives for $0 < t < T$

$$\begin{aligned} v_a(t) &= \Re\ [C_0 V_R + V_L]\,\mathrm{e}^{i2\pi\nu t} = (A_0 V_R + V_L)\cos 2\pi\nu t - B_0 V_R \sin 2\pi\nu t \\ v_b(t) &= \Re\ [C_0 V_R + i\,V_L)]\,\mathrm{e}^{i2\pi\nu t} = A_0 V_R \cos 2\pi\nu t - (B_0 V_R + V_L)\sin 2\pi\nu t. \end{aligned} \tag{7.51}$$

These signals feed the photon counters.

7.5.4 Photon Counting and Detection

The count in the interval $(0, T]$ yields two values, n_a and n_b, from which a decision must be taken on the transmitted symbol C_0; n_a and n_b are conditioned Poisson variables and therefore characterized by their averages $\bar{n}_a(C_0) := \mathrm{E}[n_a|C_0]$ and $\bar{n}_b(C_0) := \mathrm{E}[n_b|C_0]$, the condition being "given a transmitted symbol C_0." These averages are obtained dividing the corresponding energies in a symbol period T by

the quantum $h\nu$. Considering that the complex envelopes are constant in $(0, T)$, we have $E_a = P_a T = |V_a|^2 T$ and $E_b = P_b T = |V_b|^2 T$, and then

$$\begin{aligned} \bar{n}_a(C_0) &= H|C_0\, V_R + V_L|^2 = H\left[(A_0 V_R + V_L)^2 + (B_0 V_R)^2\right] \\ \bar{n}_b(C_0) &= H|C_0\, V_R + \mathrm{i}\, V_L|^2 = H\left[(A_0 V_R)^2 + (B_0 V_R + V_L)^2\right] \end{aligned} \tag{7.52}$$

where $H = T/(h\nu)$.

At this point, we assume that the local carrier has an amplitude V_L much greater than V_R, which allows us to get the following approximations

$$\bar{n}(A_0) = H(2A_0 V_R V_L + V_L^2)\,, \qquad \bar{n}(B_0) = H(2B_0 V_R V_L + V_L^2), \tag{7.53a}$$

where now the upper counting depends only on A_0 and the lower counting only on B_0. The averages can be expressed in "numbers" by letting $N_L = HV_L^2$ and $N_R = HV_R^2$ to get

$$\bar{n}(A_0) = 2\sqrt{N_L N_R}\, A_0 + N_L\,, \qquad \bar{n}(B_0) = 2\sqrt{N_L N_R}\, B_0 + N_L. \tag{7.53b}$$

The numbers of photons n_a and n_b can be decomposed as

$$\begin{aligned} n_a &= \bar{n}(A_0) + u_a = A_0\, U_0 + N_L + u_a \\ n_b &= \bar{n}(B_0) + u_b = B_0\, U_0 + N_L + u_b \end{aligned}\,, \qquad U_0 := 2\sqrt{N_L N_R} \tag{7.54}$$

where

- $U_0 A_0$ and $U_0 B_0$ are the *useful signals*,
- N_L is a bias,
- u_a and u_b are the *shot noises*.

We compose for convenience the two countings into a complex one to get

$$z_0 = n_a + \mathrm{i} n_b = C_0\, U_0 + N_L + \mathrm{i}\, N_L + u_a + \mathrm{i} u_b \tag{7.55}$$

which is the standard form of the "signal at the decision point" in a quadrature modulator. Note that

$$\bar{n}(C_0) := \bar{n}(A_0) + \mathrm{i}\,\bar{n}(B_0) = C_0\, U_0 + N_L(1 + \mathrm{i})\,, \qquad C_0 \in \mathcal{C}_0$$

generates a constellation of "received values", with center the point $N_L(1 + \mathrm{i})$ of the complex plane $\mathbb{C}$. The constellation is illustrated in Fig. 7.12 in the case of 8-PSK.

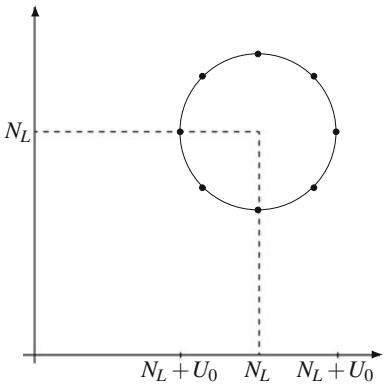

Fig. 7.12 Constellation of "received values" in the complex plane of optical 8-PSK. The points of the constellations are given by $N_L(1+\mathrm{i}) + U_0\,\mathrm{e}^{\mathrm{i}\,2\pi k/8}$, $k = 0, 1 \ldots, 7$

7.5.5 Correct Decision Probability

In principle, it is possible to evaluate the correct decision probability $P_c = \mathrm{P}[\widehat{C}_0 = C_0]$ from the statistical description of the integer random variables n_a and n_b. These variables can be considered statistically independent, and therefore described by two conditioned Poisson distributions $p_{n_a}(k|A_0)$ and $p_{n_b}(k|B_0)$, which in turn are specified by their averages $\bar{n}(A_0)$ and $\bar{n}(B_0)$ given by (7.53). The preliminary step is the choice of the decision regions $\{\mathcal{R}(\gamma)|\gamma \in \mathcal{C}_0\}$, which has to form a partition of the set of integer pairs $\{(k_1, k_2)|k_1, k_2 = 0, 1, 2, \ldots\}$. Then we have the decision criterion

$$\widehat{C}_0 = \gamma \quad \text{if} \quad (n_a, n_b) \in \mathcal{R}(\gamma). \tag{7.56}$$

Correspondingly, the transition probabilities are given by

$$p(\gamma'|\gamma) := \mathrm{P}[\hat{C}_0 = \gamma' \mid C_0 = \gamma] \sum_{(k_1,k_2)\in\mathcal{R}(\gamma')} p_{n_a}(k_1|\Re\gamma)\, p_{n_b}(k_2|\Im\gamma) \tag{7.57}$$

and the correct decision probability, with equally likely symbols, by

$$P_c = \frac{1}{K} \sum_{\gamma\in\mathcal{C}} p(\gamma|\gamma). \tag{7.58}$$

The decision regions should be optimized to maximize P_c.

This procedure will be applied in the next chapter (Sect. 8.6) to a specific case (a BPSK system). In general, it is cumbersome and does not give readable results because only numerical evaluations are possible. The alternative is the **Gaussian approximation**, *where it is assumed that the photon numbers n_a and n_b are independent Gaussian random variables.* This allows us to simplify the analysis and to arrive at very simple results.

Note that n_a and n_b are Poisson random variables and it may appear to be strange that discrete random variables, described by (mass) probability distributions, are

approximated by continuous random variables, described by probability densities. The approximation does not work in counting, but in the evaluation of the transition probabilities and of the error probability. In Sect. 8.6, we will compare the exact evaluation of probabilities, obtained with the Poisson statistics, and the approximate evaluation, obtained with the Gaussian assumption. We will see that the Gaussian approximation gives a very accurate evaluation of the exact probabilities. This conclusion holds in general in the presence of a strong photonic intensity [5] (here ensured by the assumption $V_L \gg V_0$).

With the Gaussian approximation, n_a and n_b become specified by their conditional means $\overline{n}(A_0) := \mathrm{E}[n|A_0]$ and $\overline{n}(B_0) := \mathrm{E}[n_b|B_0]$ and by their variances $\sigma^2(A_0) = \overline{n}(A_0)$ and $\sigma^2(B_0) = \overline{n}(B_0)$. For the latter, a further simplification[4] can be introduced by neglecting in (7.53) $2A_0\sqrt{N_R N_L}$ and $2B_0\sqrt{N_R N_L}$ with respect to N_L, so that they become equal, $\sigma_n^2 := \sigma^2(B_0) = \sigma^2(B_0) = N_L$, and independent of the symbols. Then their joint probability density results in

$$f_{n_a}(a|A_0) f_{n_b}(a|B_0) = \frac{1}{2\pi\sigma_n^2} \exp\left[-\frac{(a-\overline{n}(A_0))^2 + (b-\overline{n}(B_0))^2}{2\sigma_n^2}\right] = \frac{1}{\sigma_n}\phi\left(\frac{a-\overline{n}(A_0)}{\sigma_n}\right)\frac{1}{\sigma_n}\phi\left(\frac{b-\overline{n}(B_0)}{\sigma_n}\right). \tag{7.59}$$

The decision regions $\{R(\gamma) \mid \gamma \in \mathcal{C}_0\}$ become a partition of the complex plane. Then the transition probabilities are given by

$$p_c(\gamma'|\gamma) := \mathrm{P}[\hat{C}_0 = \gamma' \mid C_0 = \gamma] = \int_{R(\gamma')} f_{n_a}(a|\Re\gamma) f_{n_b}(a|\Im\gamma)\,\mathrm{d}a\,\mathrm{d}b. \tag{7.60}$$

The correct decision probability P_c, with equally likely symbols, is still given by (7.58).

The above probabilities depend only on the SNR, which results in

$$\Lambda = \frac{U_0^2}{\sigma_n^2} = 4N_R \tag{7.61}$$

and is related to the number of signal photons contained in the **received power** $P_R = V_R^2$. In fact, considering that $V_R(t) = C_0\, V_R$, the received power is given by $P_R = |C_0|^2 V_R^2$, and therefore the number of signal photons associated to the symbol C_0 is $|C_0|^2 H V_R^2 = |C_0|^2 N_R$. This can be related to the **number of signal photons per symbol** N_s as (see (7.34))

$$N_s = \frac{1}{K}\sum_{\gamma\in\mathcal{C}_0} |\gamma|^2 N_R = \mu_K N_R \tag{7.62}$$

[4] This simplification is not possible for the means given by (7.53) because they represent the useful signal. Otherwise the information on symbols would be lost.

where μ_K is the shape factor of the constellation (see (7.39)). Then $\Lambda = 4N_s/\mu_K$. As we will see, in the cases of interest, with an optimized choice of the decision region, the error probability is a function of the SNR Λ expressed by function $Q(x)$ (see Problem 7.8).

The above theory on classical optical systems is quite long and contains a lot of relations, but the net result for the evaluation of the performance is extremely simple.

Proposition 7.2 *In a classical optical system, where the local carrier has an amplitude V_L much greater than the received carrier amplitude V_R, the shot noise may be considered Gaussian. With equally likely symbols and optimized decision regions $\{R(\gamma), \gamma \in \mathcal{C}_0\}$, the minimum error probability turns out to be a simple function of the SNR*

$$\boxed{\Lambda = \frac{4N_s}{\mu_K}} \tag{7.63}$$

expressed through the complementary normalized Gaussian distribution $Q(x)$. In (7.63) N_s is the number of signal photons per symbol and μ_K is shape factor of the constellation.

Problem 7.8 ⋆ Consider the 4-QAM (which is equivalent to 4-PSK) where the normalized constellation is $\mathcal{C}_0 = \{\gamma = \pm 1 + \pm \mathrm{i}\}$ and the constellation of received values is given by

$$\{(\pm 1 + \pm \mathrm{i})U_0 + (1 + \mathrm{i})N_L\}.$$

Find the optimal decision regions and prove that the minimum error probability P_c is given by $P_c = 1 - \left(1 - Q(\sqrt{\Lambda})^2\right)$ with $\Lambda = 4N_R$.

7.6 Analysis of Classical Optical Binary Systems

In classical optical systems, the transmitted symbol C_0 has in general a complex format; but in the binary case, without restrictions, we can assume a real format. Then the general schemes of the previous section (Figs. 7.9, 7.10, and 7.11) are simplified because the double path is reduced to a single path.

For the sake of comparison with other schemes, it is convenient to express the system performance (error probability) in terms of the *average number of photons per bit N_R*, which is given in general by

$$N_R = q_0\, N_R(0) + q_1\, N_R(1)\,, \qquad q_0 + q_1 = 1$$

where $q_i = \mathrm{P}[A_0 = i]$ are the a priori probabilities and $N_R(i) = \mathrm{E}[n|A_0 = i]$ the average number of photons associated to the symbol $A_0 = i$. Usually we will consider

equiprobable symbols, so that the average number of photon per bit becomes

$$N_R = \frac{1}{2} N_R(0) + \frac{1}{2} N_R(1). \tag{7.64}$$

In the following analysis, we will use the notations for signals and complex envelopes:

- $v_0(t)$ V_0 optical carrier at the transmitter,
- $v_T(t)$ $V_T(t)$ transmitted optical signal,
- $v_R(t)$ $V_R(t)$ received optical signal,
- $v_L(t)$ V_L local optical carrier at the reception.

We assume that the channel is ideal, so that

$$v_R(t) = v_T(t).$$

7.6.1 *Binary System with Incoherent Detection (OOK Modulation)*

In the classical formulation, a monochromatic wave at frequency ν emitted by a laser can be represented by a sinusoidal signal

$$v_0(t) = V_0 \cos 2\pi \nu t \tag{7.65}$$

where the amplitude V_0 gives the optical power as (see Sect. 7.5)

$$P = V_0^2. \tag{7.66}$$

The simplest optical communications system uses amplitude modulation (OOK) and incoherent detection, as shown in Fig. 7.13. The OOK modulator is a special case of the general modulator of Fig. 7.10 with the encoding mapping the identity, $A_0 \rightarrow C_0 = A_0$, which gives the modulated signal

$$v_T(t) = \Re C_0 \, V_0 \, \mathrm{e}^{\mathrm{i}\, 2\pi \nu t} = A_0 \, V_0 \cos 2\pi \nu t \,, \qquad 0 < t < T.$$

In practice, in the symbol period $(0, T)$ the transmitter associates a zero field to the symbol $A_0 = 0$ and the field $V_0 \cos 2\pi \nu t$ to the symbol $A_0 = 1$.

Figure 7.14 shows a sequence of binary symbols and the corresponding modulated signal. This is obtained by amplitude modulating the laser beam of frequency ν or, more simply, by switching on and off the laser itself according to the source symbol to be transmitted. At the receiver, a photodetector transforms the incident field into an electrical current from which a photon counting can be obtained, as seen in Sect. 4.8.

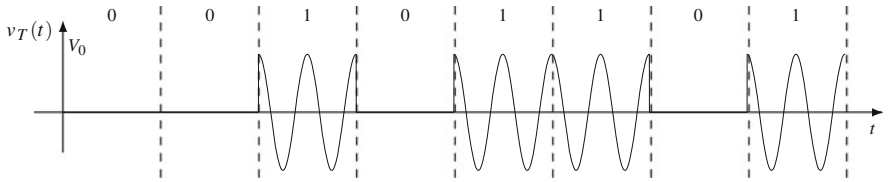

Fig. 7.13 A realization of a binary sequence and corresponding OOK signal

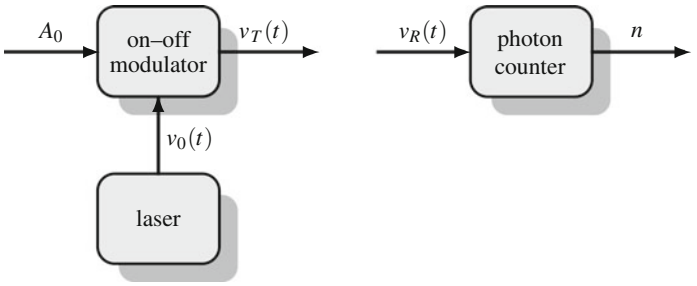

Fig. 7.14 Binary optical system with amplitude on–off modulation and uncoherent detection

Considering that with the transmission of the symbol $A_0 = 0$, the number of photons is null, $n = 0$, in (7.64) we have $N_R(0) = 0$, and therefore

$$N_R = \frac{1}{2} N_R(1).$$

At reception the photon count receiver uses the decision criterion

$$\widehat{A}_0 = \begin{cases} 0 & \text{if } n = 0 \\ 1 & \text{if } n \geq 1, \end{cases} \tag{7.67}$$

where n is the number of photons counted in a symbol period. Then, with the transmission of the symbol $A_0 = 0$, we always have a correct decision

$$P_e(0) = 0. \tag{7.68a}$$

When $A_0 = 1$ the number of arrivals n is a Poisson variable with average $N_R(1)$, and therefore with (conditioned) distribution

$$p_n(k|1) = \mathrm{e}^{-N_R(1)} \frac{N_R(1)^k}{k!}, \qquad k = 0, 1, \ldots$$

and we have an error when $n = 0$, which occurs with probability

$$P_e(1) = p_n(0|1) = \mathrm{e}^{-N_R(1)} = \mathrm{e}^{-2N_R}. \tag{7.68b}$$

The average error probability in the classical system is therefore

$$\boxed{P_{e,\text{classical}} = \frac{1}{2}\mathrm{e}^{-2N_R}} \tag{7.69}$$

where equally likely symbols are assumed.

In optical communications this probability is called the **quantum limit** [6] or **shot noise limit**, and it is the optimum for any detection that does not exploit the coherence property of the optical beam. Notice, in fact, that in this classical context the decision criterion (7.67) is optimal (see Problem 5.4). The receiver scheme is called *direct detection* of the incident light pulses. The main advantage of this approach is its simplicity. In particular, phase and frequency instabilities of the laser source are well tolerated. Moreover, at the receiver direct detection is used and phase sensitive devices are avoided.

7.6.2 Quantum Interpretation of Photon Counting in OOK

The above scheme, known as on–off keying (OOK) modulation, has a simple quantum equivalent, employing the coherent states $|0\rangle$ and $|\alpha\rangle$, with $\alpha > 0$, where the photon counting can be treated as a quantum measurement with not optimal measurement operators.

The quantum measurement realized by the photon counter is obtained with the elementary projectors $|n\rangle\langle n|$, where $|n\rangle$ is the number state (see Fig. 7.2), and the outcome of the measurement is given by the number of photons n. The transition probabilities in the measurement are

$$p(i|\alpha) = \mathrm{P}[n = i|\alpha] = \mathrm{e}^{-|\alpha|^2}\frac{|\alpha|^{2i}}{i!}, \qquad p(i|0) = \mathrm{P}[n = i|0] = \delta_{i0}.$$

The alphabet of the measurement is then $\mathcal{M} = \{0, 1, 2, \ldots\}$, and it is different from the alphabet $\mathcal{A} = \{0, 1\}$ of the source (see Sect. 5.2). To find the global performance, we must introduce a decision criterion consisting in the partitioning of $\mathcal{M}$ into two decision regions $\mathcal{M}_0$ and $\mathcal{M}_1$ to obtain two global measurement operators (see Sect. 5.2.3). The optimal partition is $\mathcal{M}_0 = \{0\}$ and $\mathcal{M}_1 = \{1, 2, \ldots\}$ (Fig. 7.15) and so we have the global projectors

$$Q_0 = |0\rangle\langle 0| \qquad Q_1 = \sum_{n=1}^{\infty} |n\rangle\langle n|. \tag{7.70}$$

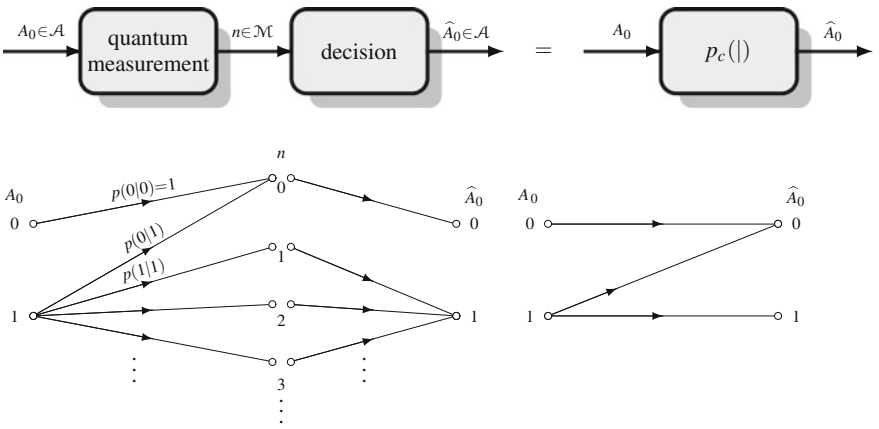

Fig. 7.15 Quantum interpretation of the decision made via a photon counter in an OOK system. The outcome of quantum measurement is given by the number of photons n present in the state $|\alpha\rangle$ or $|0\rangle$. The decision converts the measurement alphabet $\mathcal{M} = \{0, 1, 2, \ldots\}$ into the binary alphabet $\mathcal{A} = \{0, 1\}$, thus realizing a binary channel

The global transition probabilities, from (5.15), are $p_c(0|0) = \mathrm{Tr}[\rho_0\, Q_0]$ and $p_c(0|1) = \mathrm{Tr}[\rho_1\, Q_0]$, where $\rho_1 = |\alpha\rangle\langle\alpha|$ and $\rho_0 = |0\rangle\langle 0|$. Then

$$p_c(0|0) = \langle 0|0\rangle\langle 0|0\rangle = 1$$
$$p_c(0|1) = \langle\alpha|Q_0|\alpha\rangle = |\langle\alpha|0\rangle|^2 = \mathrm{e}^{-|\alpha|^2} = \mathrm{e}^{-2N_R}. \tag{7.71}$$

The performance is lower than that of the quantum version of the OOK, which will be seen in Sect. 7.9, because the projectors (7.70) are suboptimal. We recall, in fact, that with pure states, the optimal measurement operators must be elementary with measurement vectors arranged symmetrically with respect to the coherent states (Fig. 7.16); whereas (7.70) Q_1 has infinite rank and Q_0 is elementary with measurement vector $|\mu_0\rangle$ coinciding with the state $|0\rangle$.

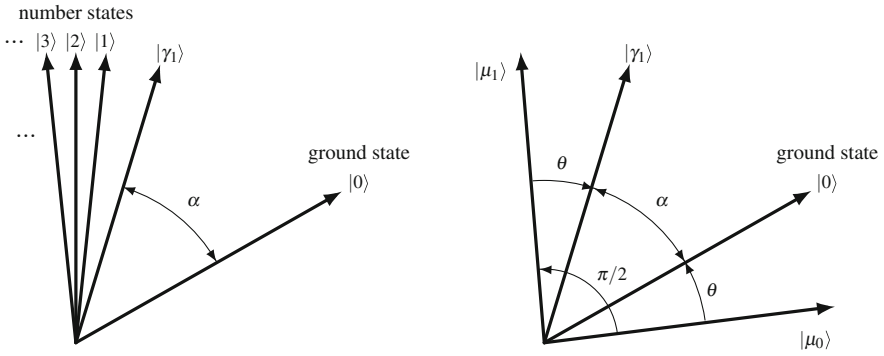

Fig. 7.16 Decision with a photon counter (*left*) and optimal decision

7.6.3 Binary System with Coherent Detection (BPSK Modulation)

A more sophisticated scheme of classical optical communications uses binary phase-shift keying (BPSK) modulation (Fig. 7.17). The BPSK modulator is a special case of the general modulator of Fig. 7.10 with the encoding mapping

$$A_0 \;\rightarrow\; C_0 = \mathrm{e}^{\mathrm{i}A_0\pi} = \begin{cases} +1 & A_0 = 0 \\ -1 & A_0 = 1 \end{cases}$$

which gives the modulated signal

$$v_T(t) = \Re\, C_0\, V_0\, \mathrm{e}^{\mathrm{i}\,2\pi\,\nu\,t} = V_0 \cos(2\pi\,\nu t + A_0\pi)\,, \qquad 0 < t < T \tag{7.72}$$

where V_0 is the amplitude of the carrier $v_0(t) = V_0 \cos 2\pi\,\nu t$. Figure 7.18 shows a sequence of binary symbols and the corresponding BPSK signal, which in the interval $(nT, nT + T)$ is given by $V_0 \cos(2\pi\,\nu t + A_n\,\pi)$.

BPSK with Homodyne Detection

Since the modulated signals $v_R(t) = v_T(t)$ for different symbols have the same optical energy, and hence the same photon counting, direct detection cannot discriminate between them. Then the receiver adds to the incoming field $v_R(t) = V_R \cos(2\pi\,\nu t + A_n\,\pi)$ the field $V_L \cos 2\pi\,\nu t$, generated by a "local" laser tuned at the same frequency as $v_0(t)$, to get the signal

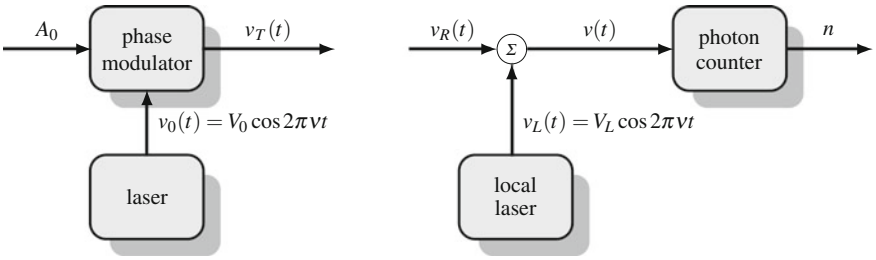

Fig. 7.17 Scheme of a binary coherent optical system with BPSK modulation. The receiver is called *homodyne* because the frequency of the local laser is the same as the frequency of modulation carrier

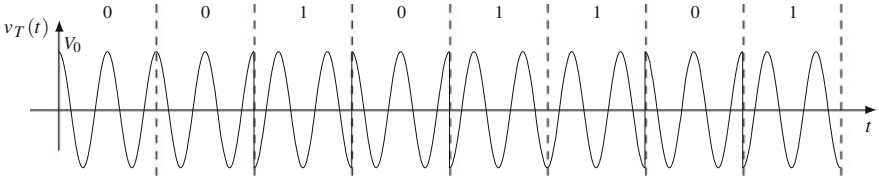

Fig. 7.18 A realization of a binary sequence and corresponding BPSK signal

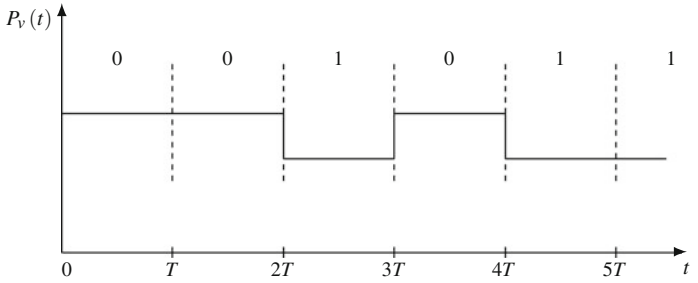

Fig. 7.19 Example of the optical power $P_R(t)$ after the introduction of the local carrier in a homodyne receiver

$$v(t) = V_R \cos(2\pi \nu t + A_0 \pi) + V_L \cos(2\pi \nu t)\,. \tag{7.73}$$

As in Sect. 7.5.4, we assume that the local carrier has an amplitude V_L much greater than that of the received signal, $V_L \gg V_0$. Since $\cos(2\pi \nu t + A_0\pi) = \cos A_0\pi \ \cos 2\pi \nu t$, the power becomes

$$P_v(t) = (V_R \cos \pi A_0 + V_L)^2 = V_R^2 + V_L^2 + 2V_R V_L \cos A_0 \pi \tag{7.74}$$

which is illustrated in Fig. 7.19 for a sequence of source symbols. Applying this power to a photon counter, we obtain a number of arrivals n in a symbol period, which can be decomposed in the form

$$n = \bar{n}(A_0) + u$$

where $\bar{n}(A_0) = \mathrm{E}[n|A_0]$ is the useful signal and the fluctuation u is the shot noise. Now, from the theory of semiclassical detection developed in the previous section, the number of signal photons is given by the photonic intensity $P_v(t)/h\nu$ integrated over $(0, T)$, and therefore it results in

$$\bar{n}(A_0) = H\left(V_L^2 + V_R^2 + 2V_R V_L \cos \pi A_0\right) = N_L + N_R + U_0 \ \cos \pi A_0 \tag{7.75}$$

where $N_L + N_R = H(V_L^2 + V_R^2)$ is a bias term, $U_0 = 2\sqrt{N_L N_R}$, and $U_0 \ \cos \pi A_0$ is the symbol-dependent part. The variance, coinciding with the average, is

$$\sigma_n^2(A_0) = N_L + N_R + U_0 \ \cos \pi A_0 \cong N_L, \tag{7.76}$$

where the approximation follows from the hypothesis $V_L \gg V_0$. In conclusion, the decision on the transmitted symbol A_0 is made on the value

$$\boxed{n = N_L + N_R + U_0 \ \cos(\pi A_0) + u.} \tag{7.77}$$

At this point we introduce the **Gaussian approximation**, *where it is assumed that the photon number n is a Gaussian random variable* and hence specified by the mean $\bar{n}(A_0)$ and by the variance $\sigma^2(A_0) = N_L$, which is independent of the symbol A_0. As seen in the previous section, the Gaussian assumption allows us to simplify the analysis and to arrive at a very simple result.

By choosing the decision rule as

$$\widehat{A}_0 = \begin{cases} 1 & n \le N_L + N_R \\ 0 & n > N_L + N_R \end{cases} \tag{7.78}$$

we obtain the error probability

$$P_e = Q\left(\frac{U_0}{\sigma_n}\right) = Q\left(\sqrt{\Lambda}\right), \tag{7.79}$$

where the SNR is given by $\Lambda = U_0^2/\sigma_n^2 = 4N_R$. Note that $N_R = N_R(0) = N_R(1)$ gives the number of signal photons per bit. In conclusion, the error probability in the classical BPSK with homodyne receiver is given by

$$\boxed{P_{e,\text{classical}} = Q\left(\sqrt{4N_R}\right).} \tag{7.80}$$

This error probability is known as the **standard quantum limit**. The result is in agreement with Proposition 7.2.

Comparison with incoherent detection (OOK) shows that the performances of the homodyne detection are better, as illustrated in Fig. 7.20, where the error probability P_e is plotted versus the average number of signal photons per bit N_R. On the other hand, the implementation of an efficient homodyne scheme implies some complications, in that it requires the presence of a local laser that must be accurately tuned in frequency and phase with the source laser.

BPSK with Superhomodyne Reception

We suppose that at the reception we have available a laser (local oscillator) producing a radiation $v_L(t)$ with the same amplitude, frequency and phase of the carrier at the transmitter, that is,

$$v_L(t) = V_L \cos(2\pi \nu t) \quad \text{with} \quad V_L = V_0. \tag{7.81}$$

This local carrier is added to the received modulated signal, yielding (Fig. 7.21)

$$\begin{aligned} v(t) &= V_0 \cos(2\pi \nu t + A_0 \pi) + V_0 \cos(2\pi \nu t) \\ &= \begin{cases} 2V_0 \cos(2\pi \nu t) & A_0 = 0 \\ 0 & A_0 = 1. \end{cases} \end{aligned} \tag{7.82}$$

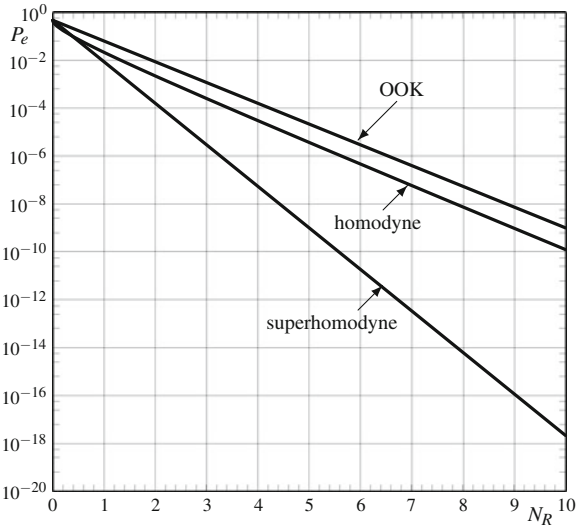

Fig. 7.20 Comparison of error probability P_e versus average number of signal photons per bit N_R in classical binary optical systems

Then the number of signal photons in a symbol period becomes

$$N_v(0) = \frac{4P_R T}{h\nu}, \qquad N_v(1) = 0. \tag{7.83}$$

Using a photon counter, the decision is based on the number of arrivals n by the rule

$$\widehat{A}_0 = \begin{cases} 1 & \text{if } n = 0 \\ 0 & \text{if } n > 0. \end{cases} \tag{7.84}$$

Then, similarly to relation (7.69), we get the error probability

$$P_{e,\text{classical}} = \frac{1}{2} P_e(0) = \frac{1}{2} \mathrm{e}^{-N_v(0)} \tag{7.85}$$

The interesting thing is that the number of signal photons per bit at the reception, i.e., before adding the carrier, is $N_R = P_R T/(h\nu)$ and it is equal to one fourth of $N_v(0)$, so that the relation (7.85) becomes

$$\boxed{P_{e,\text{classical}} = \frac{1}{2} \mathrm{e}^{-4N_R}} \tag{7.86}$$

which represents the *super quantum limit* [6]. So we have a great improvement over the homodyne detection, as shown in Fig. 7.20; because the power introduced by the local oscillator creates a more favorable situation for a correct decision. But the implementation of superhomodyne is very difficult in that it requires the presence of

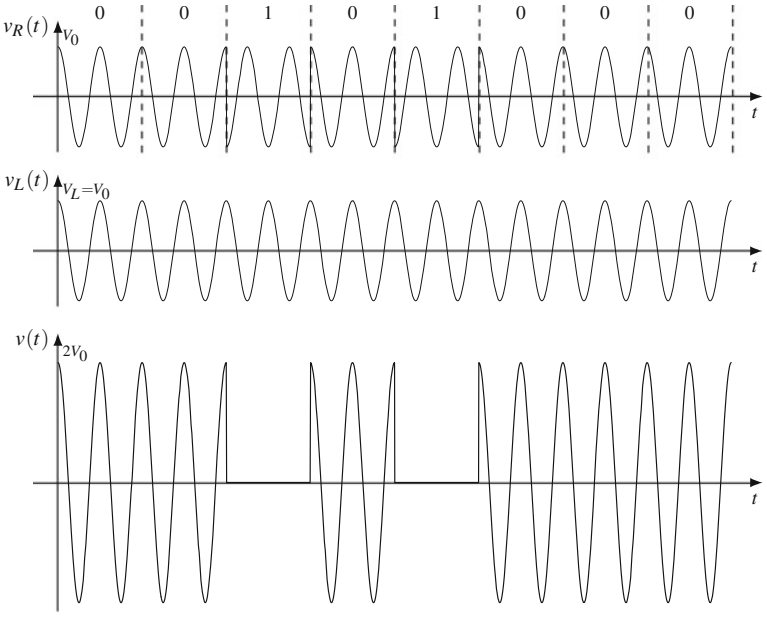

Fig. 7.21 Signals in classical BPSK superhomodyne reception

a local laser that must be accurately tuned with the source laser, not only in frequency and phase but also in amplitude.

Problem 7.9 ⋆⋆⋆ The error probability in classical homodyne BPSK has been evaluated assuming equiprobable symbols. When the symbols are not equiprobable the number of signal photons per bit N_R is still independent of the symbols and gives the SNR as $\Lambda = 4N_R$. The only change is in the evaluation is the decision element, given for equiprobable symbol by (7.78), as

$$\widehat{A}_0 = \begin{cases} 1 & n \leq S \\ 0 & n > S \end{cases}$$

where S is the threshold to be optimized.

Find the optimal decision threshold and prove that the minimum error probability is given by

$$P_e = q_1\, Q\left(\sqrt{\Lambda} + \frac{1}{2\sqrt{\Lambda}} \log \frac{q_1}{q_0}\right) + q_0\, Q\left(\sqrt{\Lambda} - \frac{1}{2\sqrt{\Lambda}} \log \frac{q_1}{q_0}\right). \qquad (7.87)$$

7.7 Quantum Decision with Pure States

In a K-ary quantum communications system, in the absence of thermal noise, we use the quantum decision theory developed in the previous two chapters, limited to *pure states*. We recall the main ideas and the available methods.

The source (Alice) is characterized by a constellation of coherent states $\mathcal{S} = \{|\gamma_0\rangle, |\gamma_1\rangle, ..., |\gamma_{K-1}\rangle\}$, which can be collected in the state matrix

$$\underset{n\times K}{\Gamma} = [|\gamma_0\rangle, |\gamma_1\rangle, ..., |\gamma_{K-1}\rangle] \tag{7.88}$$

where n is the dimension of the underlying Hilbert space (n may be infinite, and it really is infinite in Glauber's representation). The specification of the source requires also the definition of the prior probabilities $q_i = \mathrm{P}[A_0 = i] = \mathrm{P}[C_0 = \gamma_i]$, but usually throughout the chapter we shall assume equiprobable symbols $q_i = 1/K$.

The goal is to find an *optimal* system of measurement operators Q_i, $i \in \mathcal{A}$, that is, minimizing error probability. Kennedy's theorem (Theorem 5.3) states that, with pure states, the optimal measurement operators must be elementary, i.e., in the form $Q_i = |\mu_i\rangle\langle\mu_i|$. We can then limit our search to the measurement vectors, specified by the *measurement matrix*

$$\underset{n\times K}{M} = [|\mu_0\rangle, |\mu_1\rangle, \ldots, |\mu_{K-1}\rangle]. \tag{7.89}$$

These vectors are given as a linear combination of the states, as established by the relation

$$\boxed{M = \Gamma A} \tag{7.90}$$

where A is a $K \times K$ complex matrix.

Kennedy's theorem states also that the optimal measurement vectors $|\mu_i\rangle$ must be orthogonal, and therefore the corresponding measurement operators $Q_i = |\mu_i\rangle\langle\mu_i|$, $i \in \mathcal{A}$ must form a system of projectors. Unfortunately, Kennedy's theorem, as well as Holevo's theorem, do not provide explicit solutions. To compute optimal solutions, we could resort to the numeric programming methods outlined in Sect. 5.8, but, luckily enough, we can get help from the geometrically uniform symmetry (GUS), which is verified in the majority of quantum communications systems. In fact, square root measurement (SRM) decision, which is, in general, suboptimal, with pure states and in the presence of GUS becomes optimal (see Sect. 6.5.4). It is then appropriate to explicitly recall the SRM methodology, that gives good results even in the absence of GUS.

From the measurement vectors, we calculate the transition probabilities $p(j|i) = |\langle\mu_j|\gamma_i\rangle|^2$ and then the probability of correct decision.

7.7.1 Recall of SRM Approach

We summarize the main steps of the SRM theory developed in Sect. 6.3.

Starting from the constellation of K coherent states $\mathcal{C} = \{|\gamma_0\rangle, \ldots, |\gamma_{K-1}\rangle\}$, we evaluate in sequence

(1) Gram's matrix of the inner products $G = [\langle\gamma_i|\gamma_j\rangle|]$, $i, j = 0, 1, \ldots, K-1$, calculated according to (7.9). In the cases of interest, the matrix G, which is $K \times K$, has rank K.

(2) The spectral decomposition (EID) of G

$$G = V \Lambda_G V^* = \sum_{i=0}^{K-1} \sigma_i^2 \, |v_i\rangle\langle v_i| \, . \tag{7.91}$$

From this EID we find the eigenvalues σ_i^2 and the orthonormal basis $\{|v_i\rangle\}$.

(3) The square roots of G

$$G^{\pm\frac{1}{2}} = V \Lambda_G^{\pm\frac{1}{2}} V^* . \tag{7.92}$$

(4) The transition probabilities according to (see (6.29))

$$p_c(i|j) = \left| \left(G^{\frac{1}{2}}\right)_{ij} \right|^2 \tag{7.93}$$

and the error probabilities (with equiprobable symbols)

$$P_e = 1 - \frac{1}{K} \sum_{i=0}^{K-1} \left| \left(G^{\frac{1}{2}}\right)_{ii} \right|^2 . \tag{7.94}$$

(5) The measurement vectors as linear combination of the states according to

$$M = \Gamma \, G^{\frac{1}{2}} \quad \rightarrow \quad |\mu_i\rangle = \sum_{j=0}^{K-1} \left(G^{-\frac{1}{2}}\right)_{ij} |\gamma_j\rangle . \tag{7.95}$$

With geometrically uniform symmetry (GUS). If the states $|\gamma_i\rangle$ have the GUS, Gram's matrix becomes *circulant* and its EID is given by

$$G = W_{[K]} \, \Lambda_G \, W_{[K]}^* = \sum_{i=0}^{K-1} \sigma_i^2 |w_i\rangle\langle w_i| , \tag{7.96}$$

where the vectors $|w_i\rangle$ are the columns of the DFT matrix $W_{[K]}$

$$|w_i\rangle = \frac{1}{\sqrt{K}}\left[W_K^{-i}, W_K^{-2i}, \ldots, W_K^{-i(K-1)}\right]^{\mathrm{T}}, \qquad i = 0, 1, \ldots, K-1 \tag{7.97}$$

and the eigenvalues are given by the DFT of the first row $[r_0, r_1, \ldots, r_{K-1}]$ of the matrix G

$$\lambda_i = \sigma_i^2 = \sum_{k=0}^{K-1} r_k W_K^{-ki}, \qquad r_k = \langle \gamma_0 | \gamma_k \rangle. \tag{7.98}$$

The square roots of G have elements

$$\left(G^{\pm\frac{1}{2}}\right)_{ij} = \frac{1}{K}\sum_{p=0}^{K-1} \lambda_p^{\pm\frac{1}{2}}\, W_K^{-p(i-j)} \tag{7.99}$$

and in particular the diagonal elements are all equal. Therefore, the error probability is simply given by

$$P_e = 1 - \left|\left(G^{\frac{1}{2}}\right)_{00}\right|^2. \tag{7.100}$$

7.8 Quantum Binary Communications Systems

We develop the analysis of a quantum binary system, in which the information is carried by two coherent states. In this section, we assume that the constellation of the two states be generic; whereas, in the subsequent sections, two specific modulation formats will be developed (OOK and BPSK).

In the binary case, the optimal decision can be obtained in explicit form by Helstrom's theory and also by the geometric approach, seen in Sect. 5.4. With equiprobable symbols, we can also use the SRM method, which provides an optimal decision (see Sect. 6.5).

7.8.1 Binary Systems with Coherent States

To implement a Quantum Communications binary system, the transmitter (laser) is placed in one of two distinct coherent states $|\gamma_0\rangle$, $|\gamma_1\rangle \in \mathcal{G}$, which can be collected in the state matrix $\Gamma = [|\gamma_0\rangle, |\gamma_1\rangle]$. The geometry is completely specified by the inner product $X := \langle \gamma_0 | \gamma_1 \rangle$, which can be calculated explicitly from (7.9).

The optimal decision is based on two measurement operators Q_0 and Q_1, with $Q_0 + Q_1 = I$, which, by Kennedy's theorem (see Sect. 5.11), must be in the form $Q_0 = |\mu_0\rangle\langle\mu_0|$ e $Q_1 = |\mu_1\rangle\langle\mu_1|$, and therefore are identified by two measurement

vectors $|\mu_0\rangle$ and $|\mu_1\rangle$, which form the measurement matrix

$$M_{\text{opt}} = [|\mu_0\rangle, |\mu_1\rangle].$$

Still by Kennedy's theorem, the two measurement vectors must be orthogonal, $\langle\mu_0|\mu_1\rangle = 0$, so that the quantum measurement is always projective.

7.8.2 Recall of Helstrom's Theory and of Geometric Approach

We briefly recall the theory of optimal binary decision developed in Sects. 5.3 and 5.4. The results of this theory are completely specified by the a priori probabilities q_0 and q_1 and by the (quadratic) superposition degree of the states $|X|^2 = |\langle\gamma_0|\gamma_1\rangle|^2$, which can be calculated in explicit form from (7.9), obtaining

$$|X|^2 = \mathrm{e}^{-|\gamma_0-\gamma_1|^2}. \tag{7.101}$$

The optimal measurement matrix is related to the state matrix as $M = \Gamma A$ where the matrix A is given explicitly by (5.39).

The error probability, known as the Helstrom bound, is given by

$$\boxed{P_e = \frac{1}{2}\left(1 - \sqrt{1 - 4q_0q_1|X|^2}\right).} \tag{7.102}$$

Case of Equiprobable Symbols

When the symbols are equiprobable, which is the case of main interest, we have a few simplifications. The matrix A becomes

$$A = \frac{1}{2}\begin{bmatrix} \frac{1}{\sqrt{1+|X|}} + \frac{1}{\sqrt{1-|X|}} & \frac{1}{\sqrt{1+|X|}} - \frac{1}{\sqrt{1-|X|}} \\ \frac{1}{\sqrt{1+|X|}} - \frac{1}{\sqrt{1-|X|}} & \frac{1}{\sqrt{1+|X|}} + \frac{1}{\sqrt{1-|X|}} \end{bmatrix}. \tag{7.103}$$

The error probability is simplified as

$$\boxed{P_e = \tfrac{1}{2}\left[1 - \sqrt{1 - |X|^2}\right].} \tag{7.104}$$

Problem 7.10 ⋆⋆ Prove that with the optimization the a posteriori probabilities $q(i|i) := \mathrm{P}[A_0 = i|\hat{A}_0 = i]$ are equal and coincide with the correct decision probability P_c.

Problem 7.11 ⋆ Prove that in a binary system with equiprobable symbols, the error probability can be expressed as function of $N_R(0)$, $N_R(1)$, and of the relative phase of the complex parameters γ_0 and γ_1. that determine the coherent states.

7.9 Quantum Systems with OOK Modulation

The constellation consists of the states (Fig. 7.22)

$$|\gamma_0\rangle = |0\rangle \ , \ |\gamma_1\rangle = |\Delta\rangle \ \in \mathcal{G} \tag{7.105}$$

where $|0\rangle$ is the ground state and the state $|\Delta\rangle$ is determined by the number Δ which is not restrictive to assume real and positive. The quadratic superposition of the two states is $|\langle 0|\Delta\rangle|^2 = \mathrm{e}^{-\Delta^2}$. The number of signal photons associated to the symbol $A_0 = 0$ is $N_R(0) = 0$, while the one associated to the symbol $A_0 = 1$ is $N_R(1) = \Delta^2$. The number of signal photons per bit is then

$$N_R = \tfrac{1}{2} N_R(0) + \tfrac{1}{2} N_R(1) = \tfrac{1}{2} N_R(1)$$

and the quadratic superposition of the two states can be written in the meaningful form

$$|X|^2 = \mathrm{e}^{-2N_R}.$$

From (7.104), we obtain that the error probability of the OOK quantum system with equiprobable symbols becomes

$$\boxed{P_e = \tfrac{1}{2}\left[1 - \sqrt{1 - \mathrm{e}^{-2N_R}}\right].} \tag{7.106}$$

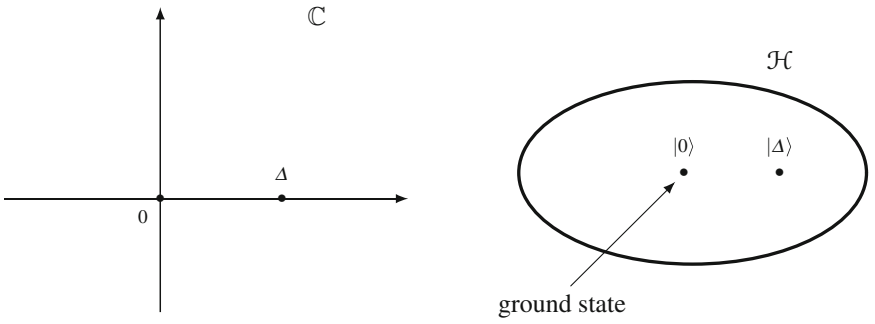

Fig. 7.22 Constellation of symbols and states in OOK modulation

The evaluation of the measurement vectors does not exhibit any specific simplification in (7.103), where now the inner product X can be expressed in the form $X = \mathrm{e}^{-N_R}$.

7.9.1 Comparison with Classical OOK Optical Systems

The *classical* OOK system was developed in Sect. 7.6.1, where we found that the error probability, with equiprobable symbol, is given by

$$\boxed{P_{e,\text{classical}} = \tfrac{1}{2}\,\mathrm{e}^{-2N_R}.} \tag{7.107}$$

The comparison between the $P_{e,\text{classical}}$ of the classical receiver, given by (7.107), and the P_e of the quantum receiver, given by (7.106), is shown in Fig. 7.23 as a function of the average number of photons per bit N_R. The asymptotic behavior of (7.106) becomes (by the approximation $1 - \sqrt{1-x} \simeq \frac{1}{2}x$ for x small)

$$P_e = \tfrac{1}{4}\mathrm{e}^{-2N_R} \qquad N_R \gg 1$$

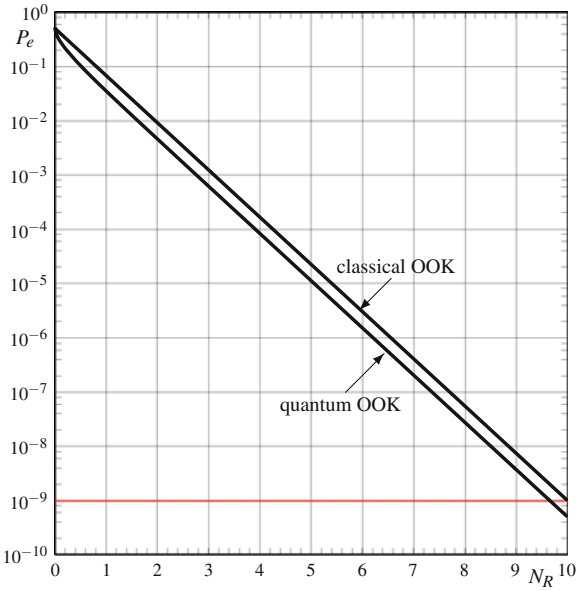

Fig. 7.23 Comparison of quantum and classical OOK

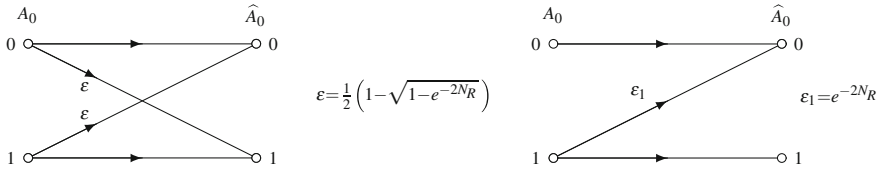

Fig. 7.24 Symmetric binary channel realized by the quantum optimal decision and asymmetric binary channel realized by photon count decision

that is, one half of the classical case. Thus we not have a great improvement in quantum OOK with respect to classical OOK (in error probability a relevant improvement is expressed in decades). The sensititvities in the two kinds of OOK are

$$N_R = 9.668 \text{ photons/bit}\,, \qquad N_{R,\text{classical}} = 10.015 \text{ photons/bit}.$$

Another comparison is between the channels realized by the two kinds of receiver: With the quantum receiver (optimized with equiprobable symbols) we obtain a symmetric channel, notwithstanding that the constellation is unbalanced, while, with the receiver based on photon count, the channel turns out to be very asymmetric (Fig. 7.24).

7.10 Quantum Systems with BPSK Modulation

In the BPSK quantum system, the symbol $A_0 = 0$ (phase $\varphi = 0$) is encoded into a coherent state $|\Delta\rangle$ with a given amplitude Δ and the symbol $A_0 = 1$ (phase $\varphi = \pi$) into the coherent state $|-\Delta\rangle$ (Fig. 7.25)

$$|\gamma_0\rangle = |\Delta\rangle\,, \;\; |\gamma_1\rangle = |-\Delta\rangle \;\in \mathcal{G}. \tag{7.108}$$

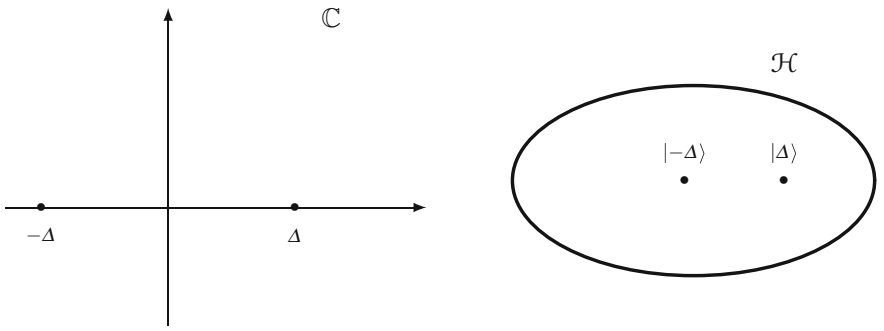

Fig. 7.25 Constellation of symbols and states in 2-PSK modulation

Obviously, the number of signal photons associated to the two states is equal

$$N_R(0) = N_R(1) = |\Delta|^2 = N_R$$

and the (quadratic) superposition degree of the two states becomes

$$|X|^2 = \mathrm{e}^{-|\Delta-(-\Delta)|^2} = \mathrm{e}^{-4|\Delta|^2} = \mathrm{e}^{-4N_R}$$

which yields the error probability

$$\boxed{P_e = \frac{1}{2}\left[1 - \sqrt{1 - \mathrm{e}^{-4N_R}}\right].} \tag{7.109}$$

Compared to the quantum OOK modulation, we have an improvement, because the term at the exponent $4N_R$ in place of $2N_R$.

7.10.1 Comparison with Classical BPSK Optical System

The *classical* BPSK system was developed in Sect. 7.6.2, where we found that the error probability, with equiprobable symbols, is given by

$$\boxed{P_{e,\text{classical}} = Q\left(\sqrt{4N_R}\right)} \tag{7.110}$$

where $Q(x)$ is the normalized complementary Gaussian distribution. The Fig. 7.26 shows the comparison between the P_e of the classical homodyne receiver and the P_e of the quantum receiver.

In this case, the improvement is relevant. For instance for $N_R = 5$ photons per bit, we have $P_e = 0.515\ 10^{-9}$ and $P_{e,\text{classical}} = 0.387\ 10^{-5}$, and the improvement is of the order of four decades! The sensititvities in the two kinds of BPSK are

$$N_R = 4.837 \text{ photons/bit}\,, \qquad N_{R,\text{classical}} = 8.913 \text{ photons/bit}.$$

Generic a Priori Probabilities

Usually we consider equally probable symbols, but it may be interesting to see the comparison when the a priori probabilities q_0 and $q_1 = 1 - q_0$ are different.

In both quantum and classical BPSK we have $N_R(0) = N_R(1)$ and then the number of signal photons per bit $N_R = q_0 N_R(0) + q_1 N_R(1)$ is independent of q_0. In the classical BPSK, the error probability is given by (7.87) of Problem 7.9, that is,

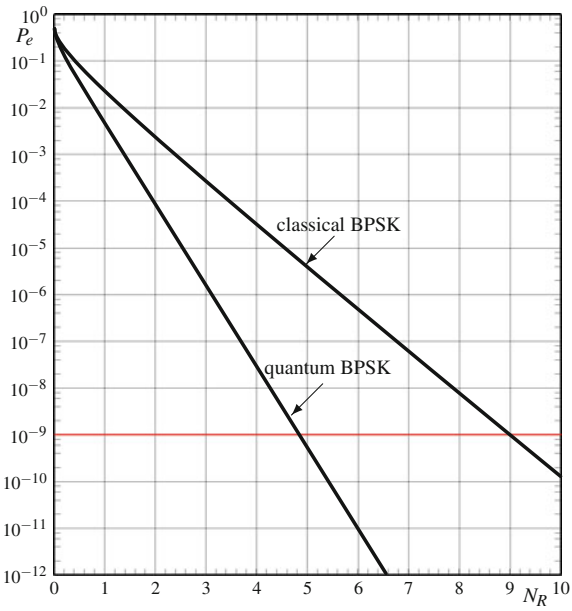

Fig. 7.26 Comparison between quantum and classical BPSK (with equal a priori probabilities)

$$P_{e,\text{classical}} = q_1\, Q\left(\sqrt{4N_R} + \frac{1}{2\sqrt{4N_R}} \log \frac{q_1}{q_0}\right) + q_0\, Q\left(\sqrt{4N_R} - \frac{1}{2\sqrt{4N_R}} \log \frac{q_1}{q_0}\right). \tag{7.111}$$

In the quantum BPSK (7.109) becomes

$$P_e = \frac{1}{2}\left[1 - \sqrt{1 - q_0 q_1 \mathrm{e}^{-4N_R}}\right]. \tag{7.112}$$

The comparison is shown in Fig. 7.27. Note in particular that for $N_R = 0$ in both systems the error probability becomes $P_e = q_0$, so that it reduces with q_0 and also for $N_R > 0$ it is reduced when q_0 becomes smaller. This may lead to think that the performance of a quantum BPSK improves when the a priori probabilities are unbalanced. This is not true because the performance of a system is given not only by the error probability, but also by the entropy and by the capacity (see Chap. 12). With $q_0 = \frac{1}{2}$ the entropy H of a binary source is $H = 1$ bit per symbol, while with $q_0 = 0.01$ the entropy is reduced to $H = 0.08$ bit per symbol.

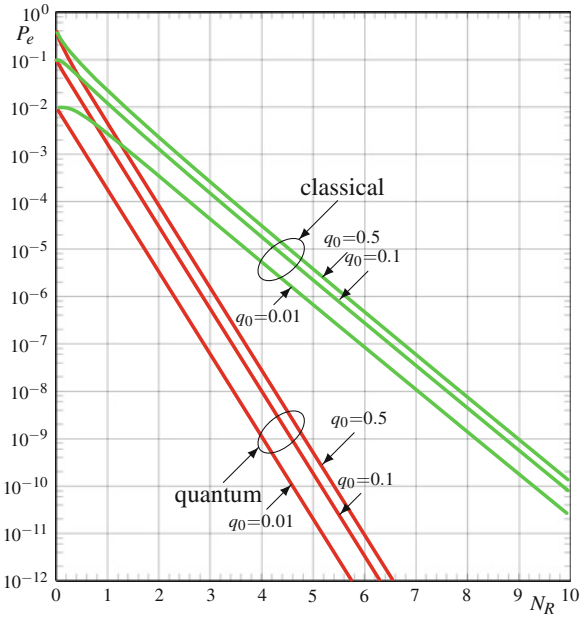

Fig. 7.27 Comparison between quantum and classical BPSK with non equiprobable symbols. The error probability P_e is reduced when q_0 becomes smaller

7.11 Quantum Systems with QAM Modulation

Quadrature amplitude modulation (QAM) is one of the most interesting format in radio frequency (RF) transmission, and can also be proposed for coherent optical modulation (classical system) and for quantum modulation.

QAM is the first example of *multilevel* modulation we are considering, with typically $K = L^2$ levels, that is, $K = 4$, $K = 9$, $K = 16$, and so on. For this format, the optimal quantum detection is not available, and suboptimal solutions must be adopted. We will apply the SRM technique which gives a good overestimate of the error probability [7], with a check by convex semidefinite programming (CSP).

7.11.1 Classical and Quantum QAM Formats

The alphabet of QAM modulation consists of a constellation of $K = L^2$ equally spaced points on a square grid of the complex plane, which can be defined starting from the L–ary balanced alphabet

$$\mathcal{A}_L = \{-(L-1) + 2(i-1) |\ i = 1, 2, \ldots, L\} \qquad \text{with} \quad L = 2, 3, 4, \ldots$$

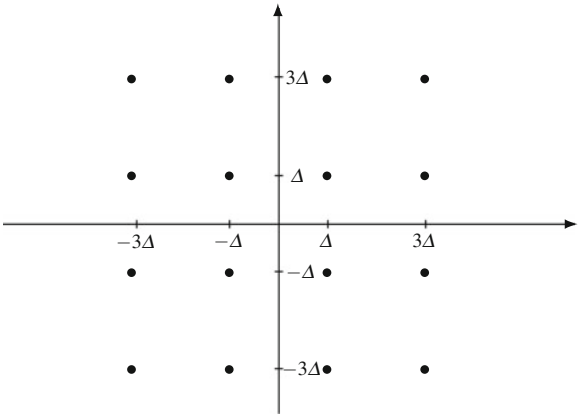

Fig. 7.28 Constellation of 16-QAM with scale factor Δ

In particular

$$\begin{aligned}\mathcal{A}_3 &= \{-2, 0, +2\}\\ \mathcal{A}_4 &= \{-3, -1, +1, +3\}\\ \mathcal{A}_5 &= \{-4, -2, 0, +2, +4\}.\end{aligned}$$

The K-ary QAM constellation is then formed by the complex numbers

$$\mathcal{C} = \{\Delta(u + \mathrm{i}v) |\ u, v \in \mathcal{A}_L\}$$

where Δ is the scale factor and 2Δ gives the spacing of symbols in the constellation, with Δ real and positive. Figure 7.28 illustrates the constellation for $L = 4$ (16-QAM). Notice that the 4-QAM, obtained with $L = 2$, is equivalent to the 4-PSK, which will be developed in the next section.

To obtain the constellation of the coherent states in quantum QAM it suffices to assign to each symbol γ of the constellation $\mathcal{C}$ the corresponding coherent state $|\gamma\rangle$. Then the constellation of the coherent states becomes

$$\mathcal{S} = \left\{ |\gamma_{uv}\rangle = |\Delta(u + \mathrm{i}v)\rangle \ \middle|\ u, v \in \mathcal{A}_L \right\}.$$

For example, for the 16-QAM, where $L = 4$ and $\mathcal{A}_4 = \{-3, -1, +1, +3\}$, we have the following coherent states listed in *lexicographic* order (see Sect. 2.13)

$$\begin{aligned}&u = -3 \quad v = -3 \quad |\gamma_0\rangle = |\gamma_{-3,-3}\rangle = |\Delta(-3 - 3\mathrm{i})\rangle\\ &u = -3 \quad v = -1 \quad |\gamma_1\rangle = |\gamma_{-3,-1}\rangle = |\Delta(-3 - \mathrm{i})\rangle\\ &u = -3 \quad v = +1 \quad |\gamma_2\rangle = |\gamma_{-3,+1}\rangle = |\Delta(-3 + \mathrm{i})\rangle\end{aligned}$$

$$
\begin{array}{llll}
u=-3 & v=+3 & |\gamma_3\rangle = |\gamma_{-3,+3}\rangle = |\Delta(-3+3\mathrm{i})\rangle \\
u=-1 & v=-3 & |\gamma_4\rangle = |\gamma_{-1,-3}\rangle = |\Delta(-1-3\mathrm{i})\rangle \\
\vdots & \vdots & \\
u=+3 & v=-3 & |\gamma_{12}\rangle = |\gamma_{+3,-3}\rangle = |\Delta(3-3\mathrm{i})\rangle \\
u=+3 & v=-1 & |\gamma_{13}\rangle = |\gamma_{+3,-1}\rangle = |\Delta(3-\mathrm{i})\rangle \\
u=+3 & v=+1 & |\gamma_{14}\rangle = |\gamma_{+3,+1}\rangle = |\Delta(3+\mathrm{i})\rangle \\
u=+3 & v=+3 & |\gamma_{15}\rangle = |\gamma_{+3,+3}\rangle = |\Delta(3+3\mathrm{i})\rangle
\end{array}
$$

7.11.2 Performance of Quantum QAM Systems

We consider the decision based on the SRM method, recalled in Sect. 7.7.1. We start from the construction of Gram's matrix G, whose elements are the inner products

$$\langle \gamma_{uv} | \gamma_{u'v'} \rangle = \langle \Delta(u+\mathrm{i}v) | \Delta(u'+\mathrm{i}v') \rangle .$$

Remembering (7.9), we get

$$\langle \gamma_{uv} | \gamma_{u'v'} \rangle = \exp\{-\tfrac{1}{2}\Delta^2[(u'-u)^2+(v'-v)^2-2\mathrm{i}(u'v-v'u)]\} \qquad u, v, u', v' \in \mathcal{A}_L . \tag{7.113}$$

The only problem in building the Gram matrix G is the ordering of the four-index elements in a standard (bidimensional) matrix. To this end, we can use the *lexicographic order* indicated above.

The main point of the SRM technique is the spectral decomposition of G, according to (7.91), namely,

$$G = V \Lambda_G V^* = \sum_{i=0}^{K-1} \sigma_i^2 \, |v_i\rangle\langle v_i|$$

which identifies the eigenvalues σ_i^2 and the orthonormal basis $|v_i\rangle$, $i = 1, 2, \ldots, K$, and also the square roots $G^{\pm\frac{1}{2}} = V \Lambda_G^{\pm\frac{1}{2}} V^*$. We can then compute the transition probabilities from (7.93) and the error probability from (7.94), that is,

$$p(j|i) = |(G^{\frac{1}{2}})_{ij}|^2 , \qquad P_e = 1 - \frac{1}{K} \sum_{i=0}^{K-1} \left[(G^{\frac{1}{2}})_{ii} \right]^2 . \tag{7.114}$$

As usual, the performance is evaluated as a function of the number of signal photons per symbol N_s, given in general by (7.34). For the QAM we find

$$\begin{aligned} N_s &= \frac{1}{K}\sum_{i=0}^{K-1}|\gamma_i|^2 = \frac{1}{K}\sum_{u\in\mathcal{A}_L}\sum_{v\in\mathcal{A}_L}|\gamma_{uv}|^2 \\ &= \frac{1}{K}\Delta^2\sum_{u\in\mathcal{A}_L}\sum_{v\in\mathcal{A}_L}(u^2+v^2) = \frac{2L}{K}\Delta^2\sum_{u\in\mathcal{A}_L}u^2 \\ &= \frac{2L}{K}\Delta^2\sum_{i=1}^{L}[-(L-1)+2(i-1)]^2. \end{aligned}$$

The result is[5]

$$N_s = \frac{2}{3}(L^2-1)\Delta^2 = \frac{2}{3}(K-1)\Delta^2 \tag{7.115}$$

so that the *shape factor* (7.39) of the QAM constellation is given by

$$\mu_K = \frac{2}{3}(K-1). \tag{7.115a}$$

For example, for the 16-QAM we have $N_s = 10\Delta^2$ and $\mu_K = 10$.

Finally, from N_s, we get the number of signal photons per bit as

$$N_R = N_s/\log_2 K.$$

Remark As noted above, the 4-QAM may be viewed as a 4-PSK, for which an exact (non-numerical) evaluation of the SRM is possible. This exact evaluation can be used as a test to check the numerical accuracy of higher order QAM.

7.11.3 An Alternative Evaluation Using the Generalized GUS

The QAM modulation has not the ordinary GUS, but it verifies the first form of generalized GUS introduced in Sect. 5.13, where there are L reference states $|\gamma_0\rangle, \ldots, |\gamma_L\rangle$, instead of a single state $|\gamma_0\rangle$, and the K-ary constellation is subdivided into L subconstellations generated by a common symmetry operator S in the form $|\gamma_{ik}\rangle = S^i|\gamma_k\rangle$, $k = 1, \ldots, L, \quad i = 0, 1, \ldots, K/L-1$.

[5] Using the identities [8]

$$\sum_{i=1}^{n} i = \frac{1}{2}n(n+1), \qquad \sum_{i=1}^{n} i^2 = \frac{1}{6}n(n+1)(2n+1).$$

.

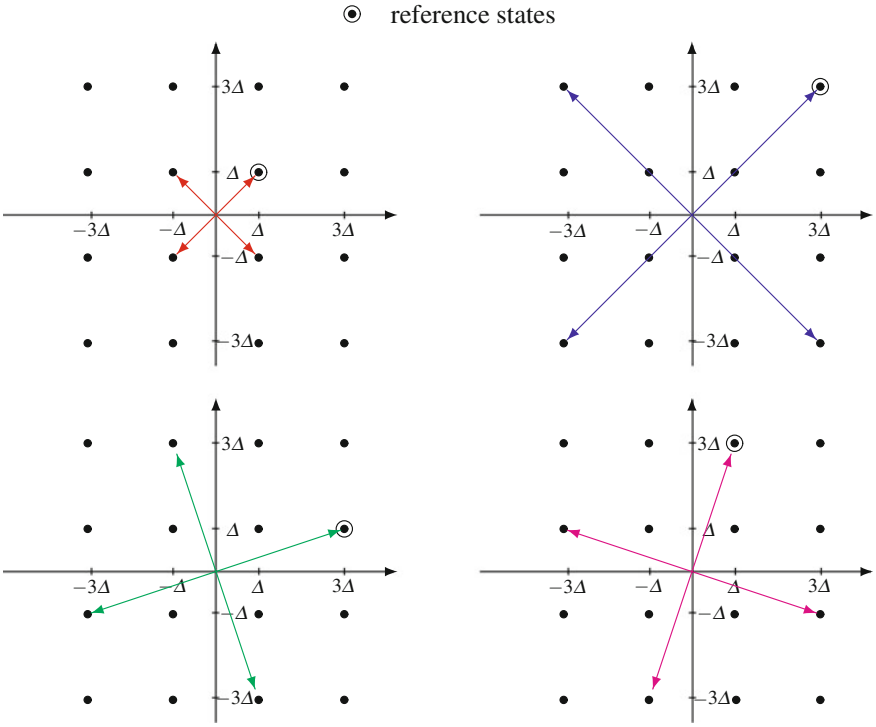

Fig. 7.29 Constellation of 16-QAM and its decomposition into four 4-PSK constellations

In particular, the 16-QAM constellation can be decomposed into 4-PSK constellations, as shown in Fig. 7.29. The reference states are the states belonging to the first quadrant of the complex plane, namely

$$|\gamma_0\rangle = |\Delta(1+\mathrm{i})\rangle\ ,\ |\gamma_1\rangle = |\Delta(3+3\mathrm{i})\rangle\ ,\ |\gamma_2\rangle = |\Delta(3+\mathrm{i})\rangle\ ,\ |\gamma_3\rangle = |\Delta(1+3\mathrm{i})\rangle. \tag{7.116}$$

The symmetry operator is the rotation operator of 4-PSK, $S = R(\pi/2)$, which allows us to generate all the other states of the 16-QAM by rotating the reference states into the other three quadrants. In fact, if we consider the state vector of the reference states $\tilde{\gamma}_0 = [|\gamma_0\rangle, |\gamma_1\rangle, |\gamma_2\rangle, |\gamma_3\rangle]$ and apply the rotation operator in the form

$$\tilde{\Gamma} = [\tilde{\gamma}_0, S\tilde{\gamma}_0, S^2\tilde{\gamma}_0, S^3\tilde{\gamma}_0]$$

we obtain a 16×16 Gram matrix $\tilde{G} = \tilde{\Gamma}^* \tilde{\Gamma}$, which contains the same inner products of the Gram matrix of the previous approach. But, for the different ordering, $\tilde{G}$ turns out to be **block circulant**.

At this point, although we are dealing with pure states, we can represent the 16 states through four density operators, ρ_0, ρ_1, ρ_2, and ρ_3, where ρ_0 collects the four reference states with a fictitious probability 1/4, that is,

$$\rho_0 = \gamma_0\,\gamma_0^* = \tfrac{1}{4}(|\gamma_0\rangle\langle\gamma_0| + |\gamma_1\rangle\langle\gamma_1| + |\gamma_2\rangle\langle\gamma_2| + |\gamma_3\rangle\langle\gamma_3|)$$

and the other density operators are obtained by the GUS relation

$$\rho_i = S^i\,\rho_0\,S^{-i}\,, \qquad i - 1, 2, 3.$$

Hence we can apply the theory of the SRM with GUS for **mixed states** (see Proposition 6.3), which requires the evaluation of the matrices (where now K becomes L)

$$D_k = \sum_{i=0}^{L-1} \gamma_0^* \gamma_i W_L^{-ki} \tag{7.117}$$

and of their square roots $D_k^{1/2}$, where in the present case $L = 4$. Finally, one gets the the correct decision probability as

$$P_c = \mathrm{Tr}\left[\frac{1}{L}\sum_{k=0}^{L-1} D_k^{1/2}\right]^2 .$$

This new approach gives exactly the same performance that we find with the previous SRM approach where the generalized GUS was not considered, with the advantage of a reduced computational complexity. In the specific case of 16-QAM, the evaluation is confined to the square roots of 4×4 matrices, instead of the square root of a 16×16 matrix.

The technique developed for the 16-QAM can be applied to constellations of any order. In particular, the constellation of 64-QAM can be decomposed into 16-PSK constellations, and the evaluation of the square roots is still confined to 4×4 matrices, instead of the square root of a 64×64 matrix.

7.11.4 Performance of the Classical Optical QAM System

The scheme of modulation and demodulation falls under the general classical scheme of Fig. 7.11. We have seen that the signal at the decision point is (see (7.55))

$$z = C_0\,U_0 + u_a + \mathrm{i}\,u_b$$

where $C_0 = A_0 + \mathrm{i}\,B_0$ is the transmitted symbol, U_0 is the amplitude, u_a and u_b are statistically independent Gaussian noises with null average and the same variance σ_u^2.

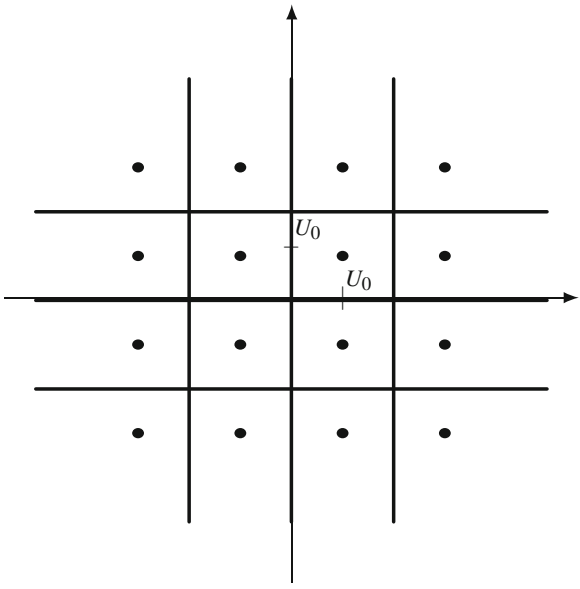

Fig. 7.30 Decision regions for the 16-QAM system constellation

To calculate the error probability, we must choose the decision regions on the complex plane. With equiprobable symbols, the optimal decision regions are found in a straightforward way, as illustrated in Fig. 7.30 for the 16-QAM. In particular for the *inner* symbols of the constellation, the decision regions are squares with sides of length $2U_0$, centered in the corresponding symbols. Using the procedure outlined in Sect. 7.5, one obtains the following expression for the error probability [9]

$$P_{e,\text{classical}} = 1 - \left[1 - 2\left(1 - \frac{1}{L}\right) Q\left(\frac{U_0}{\sigma_u}\right)\right]^2 \tag{7.118}$$

where $Q(x)$ is the normalized complementary Gaussian distribution.

The result depends on the cardinality $K = L^2$ and on the SNR ratio $\Lambda = U_0^2/\sigma_u^2$, which can be expressed as a function of the average number of photons per symbol N_s (see (7.63)), that is,

$$\boxed{\Lambda = \frac{4N_s}{\mu_K} \quad \text{with} \quad \mu_K = \frac{2}{3}(K-1).} \tag{7.119}$$

This result is in agreement with the conclusions of Proposition 7.2.

7.11.5 Comparison of Quantum and Classical QAM Systems

We are now able to compare the two QAM systems: The classical optical version, in which the error probability is given by (7.118) and the quantum optical version, in which P_e is evaluated numerically from (7.114) by the SRM procedure. In both cases, the parameters are the number of levels $K = L^2$ and the number of signal photons/symbol N_s.

The comparison, made in Fig. 7.31 for $K = 16$ and $K = 64$, shows the clear superiority of the quantum QAM system with respect to the classical one. For instance in 16-QAM with $N_s = 50$ photons/symbols we find $P_{e,\text{classical}} = 1.161\ 10^{-5}$, while in the quantum system $P_e = 1.546\ 10^{-9}$; in 64-QAM with $N_s = 200$ photons/symbol we find $P_{e,\text{classical}} = 2.231\ 10^{-5}$ and $P_e = 4.674\ 10^{-9}$. In both cases the improvement obtained with the quantum system is of about four decades.

In Fig. 7.32 the 16-QAM is compared to the 64-QAM as a function of the number of signal photons per bit N_R. The sensitivity at $P_e = 10^{-9}$ is $N_R = 12.783$ photons/bit in 16-QAM and $N_R = 36.035$ photons/bit in 64-QAM.

7.11.6 Comparison of CSP and SRM Evaluation

The QAM format does not have the GUS, and therefore the SRM approach does not give the minimum error probability. For this reason, we have evaluated the minimum error probability also by convex semidefinite programming, implemented in MatLab by the CVX procedure, which gives (numerically) this minimum. The results of the two approaches are shown in the following table for the 16-QAM

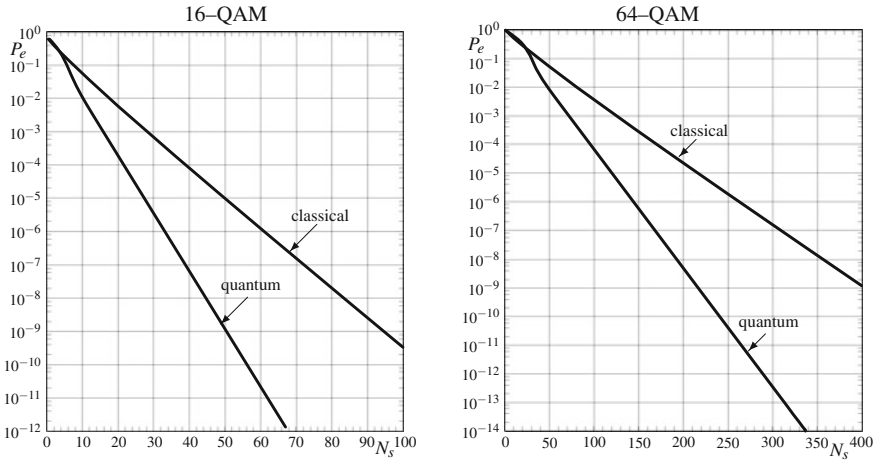

Fig. 7.31 Comparison of quantum and classical 16–QAM and 64–QAM

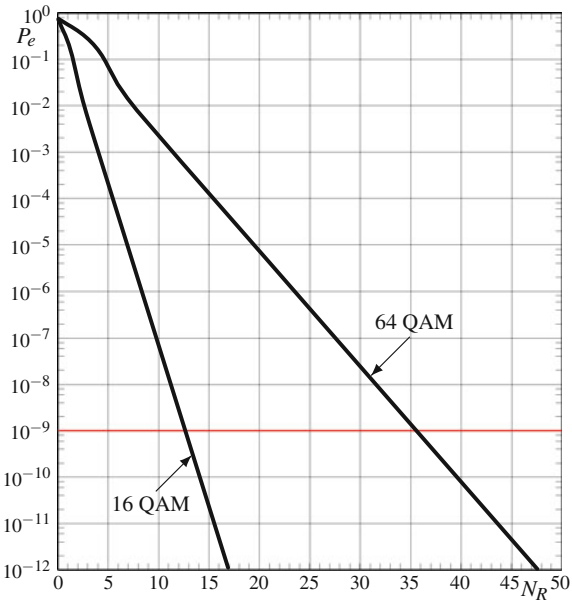

Fig. 7.32 Error probability of quantum QAM versus the *number of signal photons per bit* N_R

N_s	P_e with CSP	P_e with SRM
0.1	0.86919	0.884949
0.5	0.764902	0.784679
1	0.675115	0.690197
1.5	0.597074	0.608958
2.5	0.461457	0.467108
4.5	0.239407	0.240096
6.5	0.0913599	0.0910951
9.5	0.0188974	0.0188975

The two evaluations are very close, especially for large values of N_s, and cannot be distinguished in a log plot (recall that in the evaluation of P_e, decades are relevant, not decimals),

The conclusion is that the SRM approach is recommended also for the QAM (for the other formats the SRM gives the minimum of P_e).

7.12 Quantum Systems with PSK Modulation

Also PSK (phase-shift keying) modulation is one of the best known and most often used formats at radio frequency and at optical frequencies. The BPSK = 2-PSK format has been already seen in Sect. 7.10 as a special case of quantum binary systems.

Quantum K-ary PSK systems were analyzed by several authors and in particular by Kato et al. [7], using the SRM technique. In this case, the constellation of the states enjoys the *geometrically uniform symmetry* and then the SRM technique gives an optimal quantum receiver.

7.12.1 Classical and Quantum PSK Format

The constellation of the PSK modulation consists of K points uniformly distributed along a circle of the complex plane

$$\mathcal{C} = \{\Delta\, W_K^m \mid m = 0, 1, \ldots, K-1\} \tag{7.120}$$

where the scale factor Δ is given by the radius of the circle and $W_K = \mathrm{e}^{\mathrm{i}2\pi/K}$. The constellation is illustrated in Fig. 7.33 for some values of K.

In the quantum version, the states are obtained by simply associating to every complex symbol γ of the constellation (7.120) the corresponding coherent state, which is given by

$$|\gamma_m\rangle = |\Delta\, W_K^m\rangle = \mathrm{e}^{-\frac{1}{2}\Delta^2} \sum_{n=0}^{\infty} \frac{(\Delta\, W_K^m)^n}{\sqrt{n!}} |n\rangle\,, \qquad m = 0, 1, \ldots, K-1. \tag{7.121}$$

In this constellation, all the coherent states have the same number of signal photons given by

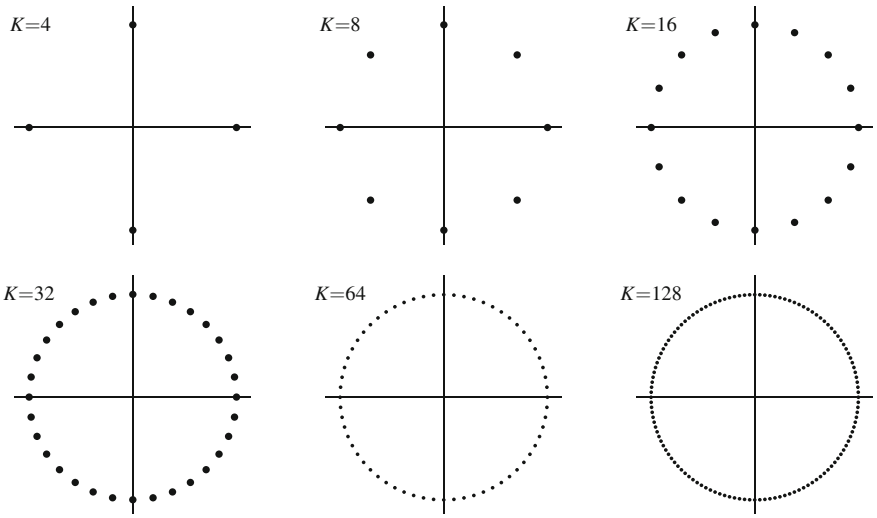

Fig. 7.33 Constellations of PSK modulation

$$N_s = \Delta^2. \tag{7.122}$$

Constellation (7.121) enjoys the GUS, that is, it satisfies the conditions (5.120a) and (5.120b) for an appropriate unitary operator S. In this case S is obtained from the *rotation operator*, which is defined as

$$R(\phi) := \exp(\mathrm{i}\phi N)$$

where N is the number operator given by (7.1). Specifically we have

$$S = R\Big(\frac{2\pi}{K}\Big) = \exp\Big(\frac{\mathrm{i}2\pi}{K}N\Big) = W_K^N. \tag{7.123}$$

The GUS property is verified for all constellations of Gaussian states generated by the rotation operator, as we will prove in Sect. 11.20. In Problem 7.9 we propose a specific proof for the PSK constellations where the key is that the operator $R(\phi)$ rotates a coherent state $|\alpha\rangle$ in the form (see 11.20)

$$R(\phi)\,|\alpha\rangle = |\mathrm{e}^{\mathrm{i}\phi}\alpha\rangle\,, \tag{7.124}$$

and the result is again a coherent state. In other words, the class of coherent states is closed under rotations.

7.12.2 Performance of Quantum PSK Systems

For the decision we apply the SRM, which gives an optimal result. Then, for the performance evaluation, we follow the procedure described in Sect. 7.8.3, taking into account that the PSK constellation satisfies the GUS.

The generic element p, q of Gram's matrix $G = [G_{pq}]$ is the inner product $G_{pq} = \langle\gamma_p|\gamma_q\rangle$ obtained from (7.9) with $\alpha = \Delta W_K^p$ and $\beta = \Delta W_K^q$, namely,

$$G_{pq} = \exp[-\Delta^2(1 - W_K^{q-p})]\,, \qquad p, q = 0, 1, \ldots, K-1. \tag{7.125}$$

As predicted (by the GUS), the element p, q depends only on the difference $q-p$; and therefore Gram's matrix becomes *circulant*. The eigenvalues are obtained computing the DFT of the first row of Gram's matrix, that is,

$$\lambda_i = \sum_{k=0}^{K-1} G_{0k} W_K^{-ki} \tag{7.126}$$

and the corresponding eigenvectors are given by the columns of the DFT matrix

$$|w_i\rangle = \frac{1}{\sqrt{K}}\left[1, W_K^{-i}, W_K^{-2i}, \ldots, W_K^{-(K-1)i}\right]^{\mathrm{T}}.$$

Thus the matrices $G^{\pm\frac{1}{2}}$ are obtained from (7.99), where the element i, j is given by

$$(G^{\pm\frac{1}{2}})_{ij} = \frac{1}{K}\sum_{p=0}^{K-1} \lambda_p^{\pm\frac{1}{2}} W_K^{(j-i)p}.$$

The measurement vectors are computed as linear combination of the states according to (7.95), i.e.,

$$|\mu_i\rangle = \sum_{j=0}^{K-1} \left(G^{-\frac{1}{2}}\right)_{ij} |\gamma_j\rangle.$$

Finally, the error probability with equiprobable symbols is simply

$$P_e = 1 - \frac{1}{K^2}\left(\sum_{i=0}^{K-1}\sqrt{\lambda_i}\right)^2. \tag{7.127}$$

Therefore, to calculate P_e it suffices to evaluate the eigenvalues according to (7.126) and to apply (7.127). As usual, P_e can be expressed as a function of the number of signal photons per symbol N_s, given by (7.122), and of the number of levels K. In fact, the Gram matrix G depends only on $\Delta^2 = N_s$ and K, and so is for the square root of G and subsequent relations. This conclusion is in agreement with Proposition 7.2.

7.12.3 Performance of Classical PSK Systems and Comparison

The classical optical PSK system falls into the general model of quadrature modulation (with homodyne receiver) seen in Sect. 7.5. The signal at the decision point becomes

$$z_0 = C_0\, U_0 + u_a + \mathrm{i}u_b$$

where C_0 is the transmitted symbol, $C_0 \in \mathcal{C}_0 = \{W_K^i \mid i = 1, \ldots, K\}$, u_a and u_b are independent zero-mean Gaussian components with the same variance σ_u^2. At this point, we introduce the count parameters, recalling that

$$U_0 = (2V_R V_L)H \qquad \sigma_u^2 = H\, V_L^2$$

and that in this case the number of signal photons contained in the received power is

$$N_R = N_s = H\, V_R^2.$$

So the SNR becomes

$$\Lambda = \frac{U_0^2}{\sigma_u^2} = 4N_s$$

the shape factor μ_K being unitary.

To find the error probability, we must partition the complex plane into K decision regions. Even in this case, with equiprobable symbols, such regions are easily found, as illustrated in Fig. 7.34 for the 8-PSK, and then we apply the general relation (7.60). Given the nature of the constellation, it is convenient to do a coordinate change in the probability density, from Cartesian to polar coordinates. The exact computation is only known for $K = 2$ and $K = 4$ and it yields (see (7.80))

$$\begin{aligned} K &= 2 \qquad P_{e,\text{classical}} = Q(2\sqrt{N_s}) \\ K &= 4 \qquad P_{e,\text{classical}} = 1 - \left[1 - Q(\sqrt{2N_s})\right]^2 \end{aligned} \tag{7.128}$$

where we recall that for $K = 4$ the PSK coincides with the QAM. For $K > 4$ the exact computation is not known, and we resort to the inequality [10, Chap.10]

$$P_{e,\text{classical}} < P'_e = \exp\left(-\frac{1}{2}\frac{U_0^2}{\sigma_u^2}\sin^2\frac{\pi}{K}\right) = \exp\left(-2N_s \sin^2\frac{\pi}{K}\right). \tag{7.129}$$

The comparison between the classical and the quantum system has been done in Fig. 7.26 for the 2-PSK. The comparison of 4-PSK and 8-PSK is done in Fig. 7.35, where the error probability is plotted as a function of the number of signal photons per symbol N_s. Even in this case we notice a striking superiority of the quantum system. For instance in 4-PSK with $N_s = 10$ photon/symbol we find $P_e = 1.030\ 10^{-9}$ and $P_{e,\text{classical}} = 7.742\ 10^{-6}$; in 8-PSK with $N_s = 30$ photon/symbol we find $P_e = 1.166\ 10^{-8}$ and $P_{e,\text{classical}} = 7.742\ 10^{-6}$. In both cases, the improvement of the quantum system is of several decades.

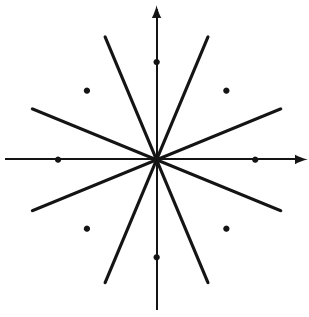

Fig. 7.34 Decision regions in 8-PSK

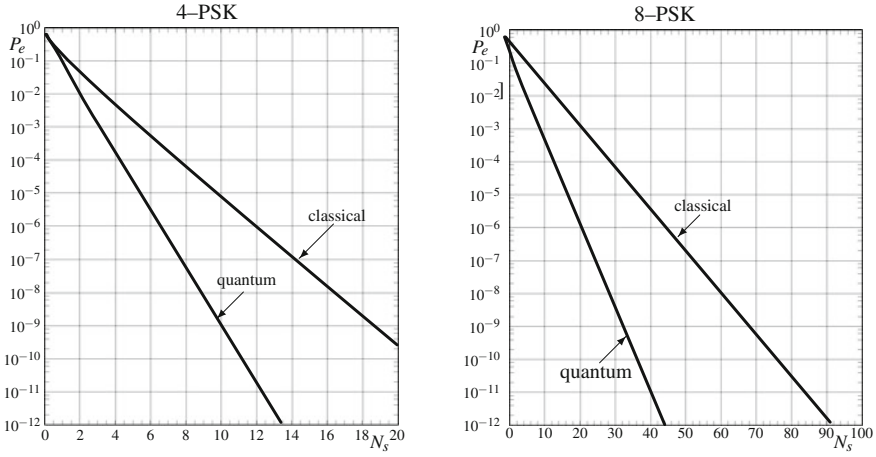

Fig. 7.35 Comparison of quantum and classical 4-PSK and 8-PSK

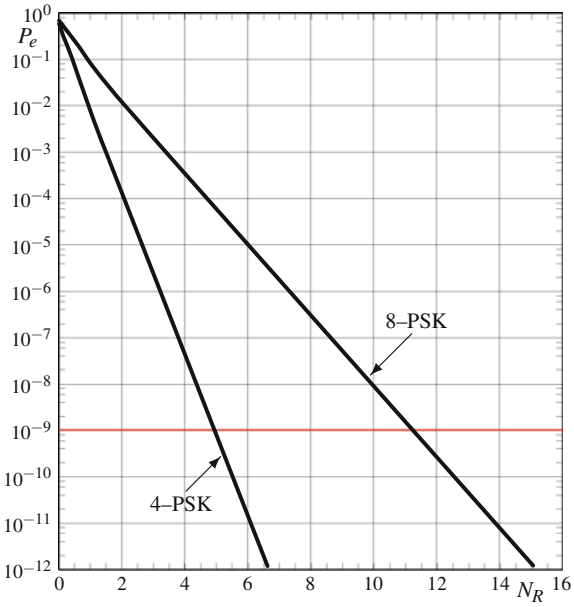

Fig. 7.36 Error probability of quantum PSK versus the *number of signal photons per bit* N_R

Figure 7.36 compares quantum 4-PSK and quantum 8-PSK as a function of the number of signal photons per bit N_R. The sensitivity at $P_e = 10^{-9}$ is $N_R = 5.001$ photons/bit in 4-PSK and $N_R = 11.402$ photons/bit in 8-PSK.

Problem 7.12 ⋆⋆⋆ Prove that the operator S defined by (7.123) is the symmetry operator of the K-PSK modulation.

Problem 7.13 ⋆ Find explicitly the formula for the error probability P_e of quantum 4-PSK system, with the target to show that P_e depends only on $\Delta^2 = N_s$.

7.13 Quantum Systems with PPM Modulation

Pulse position modulation (PPM) is widely adopted in free space optical transmission, and is a candidate for deep-space transmission, also in quantum form [11, 12].

The analysis of a quantum PPM system has been done in a famous article [4] by Yuen, Kennedy and Lax, who found the optimal elementary projectors using an algebraic method developed "ad hoc" for this kind of modulation. Here we shall propose an original method based on the SRM and on the property of quantum PPM of verifying the GUS [13]. It seems odd that such property has not been remarked by other authors; because, on one hand, it is very intuitive, and, on the other hand, it makes it possible to directly achieve the same optimal result.

7.13.1 Classical PPM Format

In the classical version, the symbol period T is subdivided into K parts with spacing $T_0 = T/K$, obtaining K "positions." Then, to the symbol $i \in \mathcal{A} = \{0, 1, \ldots, K-1\}$ the waveform is associated consisting of a rectangle in the ith position iT_0 of the symbol period

$$\gamma_i(t) = \begin{cases} \Delta & iT_0 < t < (i+1)T_0 \\ 0 & \text{elsewhere} \end{cases} \qquad i = 0, 1, \ldots, K-1 \tag{7.130}$$

where $\Delta > 0$ is the scale factor (see Fig. 4.12). But, we will adopt the specular format

$$\gamma_i(t) = \begin{cases} \Delta & (K-1-i)T_0 < t < (K-i)T_0 \\ 0 & \text{elsewhere} \end{cases} \qquad i = 0, 1, \ldots, K-1 \tag{7.131}$$

where the ith position becomes $(K-1-i)T_0$ instead of iT_0, as illustrated in Fig. 7.37 for $K = 4$. The reason of this choice is due to the fact that it simplifies the formulation of the symmetry operator in the quantum version.

To waveforms (7.131), K binary words can be associated of length K

$$\gamma_i = [\gamma_{i,K-1}, \ldots, \gamma_{i,1}, \gamma_{i,0}], \qquad i = 0, 1, \ldots, K-1$$

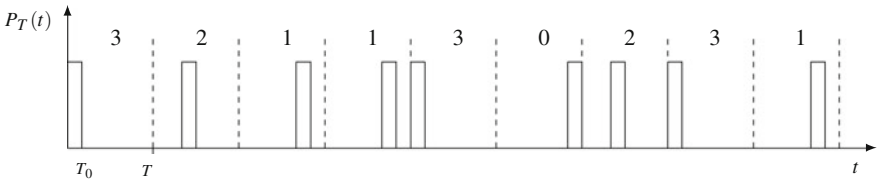

Fig. 7.37 Realization of transmitted symbols and corresponding optical power in classic 4-PPM modulation

where $\gamma_{ij} = \Delta\,\delta_{ij}$. For example, for $K = 4$ the words are

$$\gamma_0 = \begin{bmatrix} 0 & 0 & 0 & \Delta \end{bmatrix} \qquad \gamma_1 = \begin{bmatrix} 0 & 0 & \Delta & 0 \end{bmatrix}$$
$$\gamma_2 = \begin{bmatrix} 0 & \Delta & 0 & 0 \end{bmatrix} \qquad \gamma_3 = \begin{bmatrix} \Delta & 0 & 0 & 0 \end{bmatrix}.$$

As outlined in Problem 7.5, it can be verified that PPM modulation is a special case of *vector* modulation seen in Sect. 7.3.2.

7.13.2 Quantum PPM Format

We have seen in Sect. 7.3.2 that the quantum formulation of a vector modulation must be done over a composite Hilbert space, given by the tensor product $\mathcal{H} = \mathcal{H}_0 \otimes \mathcal{H}_0 \otimes \cdots \otimes \mathcal{H}_0$ of K equal Hilbert spaces $\mathcal{H}_0$, into each of which Glauber's representation must have been introduced, and the states are given by the *tensor product* of K coherent states and become **K–mode Gaussian states**.

In the specific case of PPM, the states become

$$|\gamma_i\rangle = |\gamma_{i,K-1}\rangle \otimes \cdots \otimes |\gamma_{i,1}\rangle \otimes |\gamma_{i,0}\rangle\,, \qquad i = 0, 1, \ldots K-1 \tag{7.132}$$

with

$$|\gamma_{ij}\rangle = \begin{cases} |\Delta\rangle & i = j \\ |0\rangle & i \neq j \end{cases} \tag{7.132a}$$

where $|\Delta\rangle$ is a coherent state with parameter Δ, and $|0\rangle$ is the "ground state". For example, for $K = 4$ we have the four states

$$|\gamma_0\rangle = |0\rangle \otimes |0\rangle \otimes |0\rangle \otimes |\Delta\rangle \qquad |\gamma_1\rangle = |0\rangle| \otimes 0\rangle \otimes |\Delta\rangle \otimes |0\rangle$$
$$|\gamma_2\rangle = |0\rangle \otimes |\Delta\rangle \otimes |0\rangle \otimes |0\rangle \qquad |\gamma_3\rangle = |\Delta\rangle \otimes |0\rangle \otimes |0\rangle \otimes |0\rangle. \tag{7.133}$$

7.13.3 Geometrically Uniform Symmetry (GUS) of PPM

As we shall see in Sect. 11.20, the constellations of Gaussian states generated by the rotation operator $R(\phi)$ verify the GUS, also in the K–mode. This is the case of K-ary PPM. But the parameter ϕ becomes a $K \times K$ Hermitian matrix and the exponential defining $R(\phi)$ becomes difficult to handle. Here we prefer finding directly the symmetry operator S, and in Chap. 11 we will prove that S can be expressed by the K–mode rotation operator.

The symmetry operator S of the quantum PPM format (7.132) can be defined as follows: S is an operator of the composite Hilbert space $\mathcal{H}$ that causes a shift to the left by one position (modulo K) of the factors of the tensor product of the states, moving the first factor to second position, the second to third , and the Kth factor to first. For example, for $K = 4$, the action of S is as follows

$$S|\gamma_{i3}\rangle \otimes |\gamma_{i2}\rangle \otimes |\gamma_{i1}\rangle \otimes |\gamma_{i0}\rangle = |\gamma_{i2}\rangle \otimes |\gamma_{i1}\rangle \otimes |\gamma_{i0}\rangle \otimes |\gamma_{i3}\rangle. \tag{7.134}$$

Then, going on with $K = 4$, with the states of (7.113) we can see that, starting from the state $|\gamma_0\rangle = |0\rangle \otimes |0\rangle \otimes |0\rangle \otimes |\Delta\rangle$, the other states can be obtained in the following way:

$$\begin{aligned} S\,|0\rangle \otimes |0\rangle \otimes |0\rangle \otimes |\Delta\rangle &= |0\rangle \otimes |0\rangle \otimes |\Delta\rangle \otimes |0\rangle = |\gamma_1\rangle \\ S^2|0\rangle \otimes |0\rangle \otimes |0\rangle \otimes |\Delta\rangle &= |0\rangle \otimes |\Delta\rangle \otimes |0\rangle \otimes |0\rangle = |\gamma_2\rangle \\ S^3|0\rangle \otimes |0\rangle \otimes |0\rangle \otimes |\Delta\rangle &= |\Delta\rangle \otimes |0\rangle \otimes |0\rangle \otimes |0\rangle = |\gamma_3\rangle \end{aligned}$$

while the application of S^4 brings back to the initial state, and therefore $S^4 = I_{\mathcal{H}}$.

The considerations we just made "in words" can be translated to "formulas," but this is not so simple, because the symmetry operator S is not separable, but it operates between the K factors of the composite Hilbert space $\mathcal{H} = \mathcal{H}_0^{\otimes K}$. For the symmetry operator, the following result applies, recently demonstrated in [13].

Proposition 7.3 *Let n be the dimension of the component Hilbert spaces $\mathcal{H}_0$, and therefore $N = n^K$ is the dimension of $\mathcal{H}_0^{\otimes K}$. Then the symmetry operator of the K-ary PPM has the following expression*

$$S = \sum_{k=0}^{n-1} w_n(k) \otimes I_L \otimes w_n^*(k), \tag{7.135}$$

where $\otimes$ is Kronecker's product, $w_n(k)$ is a column vector of length n, with null elements except for one unitary element at position k, and I_L is the identity matrix of order $L = n^{K-1}$. □

For example, for $n = 2$ and $K = 3$ (3-PPM) we have

$$w_2(0) = \begin{bmatrix} 1 \\ 0 \end{bmatrix}, \qquad w_2(1) = \begin{bmatrix} 0 \\ 1 \end{bmatrix}, \qquad I_4 = \begin{bmatrix} 1 & 0 & 0 & 0 \\ 0 & 1 & 0 & 0 \\ 0 & 0 & 1 & 0 \\ 0 & 0 & 0 & 1 \end{bmatrix}$$

and therefore from (7.135)

$$\begin{aligned} S &= w_2(0) \otimes I_4 \otimes w_2^*(0) + w_2(1) \otimes I_4 \otimes w_2^*(1) \\ &= \begin{bmatrix} 1 \\ 0 \end{bmatrix} \otimes \begin{bmatrix} 1 & 0 & 0 & 0 \\ 0 & 1 & 0 & 0 \\ 0 & 0 & 1 & 0 \\ 0 & 0 & 0 & 1 \end{bmatrix} \otimes \begin{bmatrix} 1 & 0 \end{bmatrix} + \begin{bmatrix} 0 \\ 1 \end{bmatrix} \otimes \begin{bmatrix} 1 & 0 & 0 & 0 \\ 0 & 1 & 0 & 0 \\ 0 & 0 & 1 & 0 \\ 0 & 0 & 0 & 1 \end{bmatrix} \otimes \begin{bmatrix} 0 & 1 \end{bmatrix} \end{aligned}$$

and, developing the products, we obtain the 16×16 matrix (remember that the tensor product for matrices becomes Kronecker's product, see Sect. 2.13)

$$S = \begin{bmatrix} 1 & 0 & 0 & 0 & 0 & 0 & 0 & 0 & 0 & 0 & 0 & 0 & 0 & 0 & 0 & 0 \\ 0 & 0 & 1 & 0 & 0 & 0 & 0 & 0 & 0 & 0 & 0 & 0 & 0 & 0 & 0 & 0 \\ 0 & 0 & 0 & 0 & 1 & 0 & 0 & 0 & 0 & 0 & 0 & 0 & 0 & 0 & 0 & 0 \\ 0 & 0 & 0 & 0 & 0 & 0 & 1 & 0 & 0 & 0 & 0 & 0 & 0 & 0 & 0 & 0 \\ 0 & 0 & 0 & 0 & 0 & 0 & 0 & 0 & 1 & 0 & 0 & 0 & 0 & 0 & 0 & 0 \\ 0 & 0 & 0 & 0 & 0 & 0 & 0 & 0 & 0 & 0 & 1 & 0 & 0 & 0 & 0 & 0 \\ 0 & 0 & 0 & 0 & 0 & 0 & 0 & 0 & 0 & 0 & 0 & 0 & 1 & 0 & 0 & 0 \\ 0 & 0 & 0 & 0 & 0 & 0 & 0 & 0 & 0 & 0 & 0 & 0 & 0 & 0 & 1 & 0 \\ 0 & 1 & 0 & 0 & 0 & 0 & 0 & 0 & 0 & 0 & 0 & 0 & 0 & 0 & 0 & 0 \\ 0 & 0 & 0 & 1 & 0 & 0 & 0 & 0 & 0 & 0 & 0 & 0 & 0 & 0 & 0 & 0 \\ 0 & 0 & 0 & 0 & 0 & 1 & 0 & 0 & 0 & 0 & 0 & 0 & 0 & 0 & 0 & 0 \\ 0 & 0 & 0 & 0 & 0 & 0 & 0 & 1 & 0 & 0 & 0 & 0 & 0 & 0 & 0 & 0 \\ 0 & 0 & 0 & 0 & 0 & 0 & 0 & 0 & 0 & 1 & 0 & 0 & 0 & 0 & 0 & 0 \\ 0 & 0 & 0 & 0 & 0 & 0 & 0 & 0 & 0 & 0 & 0 & 1 & 0 & 0 & 0 & 0 \\ 0 & 0 & 0 & 0 & 0 & 0 & 0 & 0 & 0 & 0 & 0 & 0 & 1 & 0 & 0 & 0 \\ 0 & 0 & 0 & 0 & 0 & 0 & 0 & 0 & 0 & 0 & 0 & 0 & 0 & 0 & 0 & 1 \end{bmatrix}. \tag{7.136}$$

We leave it to the reader to check that, using the properties of Kronecker's product of Sect. 2.13, from (7.135) we obtain that the matrix S has dimensions $n^K \times n^K$, it is unitary, and has the property $S^K = I_{n^K}$.

For later use it is important to evaluate explicitly the EID of the symmetry operator S in the form (5.128)

$$S = \sum_{i=0}^{K-1} W_K^i \; Y_i \, Y_i^* \tag{7.137}$$

where the columns of the matrices Y_k are formed by the eigenvectors corresponding to the eigenvalues $\lambda_i = W_K^i$. The explicit evaluation of such eigenvectors is long and

cumbersome, and is developed in [13], using the fact that for the PPM the operator S is a *permutation matrix*. The important thing is that this evaluation can be done "analytically" for every n and K, without resorting to numeric evaluation, which could be prohibitive for high values of $N = n^K$. For example, for $K = 4$, $n = 2$, the eigenvalues 1, W_4, W_4^2, W_4^3 have multiplicities respectively 6, 3, 4, and 3, and the corresponding eigenvectors form the matrices

$$Y_0 = \begin{bmatrix} 1&0&0&0&0&0 \\ 0&0&0&\frac{1}{2}&0&0 \\ 0&0&0&\frac{1}{2}&0&0 \\ 0&0&0&0&\frac{1}{2}&0 \\ 0&0&0&\frac{1}{2}&0&0 \\ 0&0&\frac{1}{\sqrt{2}}&0&0&0 \\ 0&0&0&0&\frac{1}{2}&0 \\ 0&0&0&0&0&\frac{1}{2} \\ 0&0&0&\frac{1}{2}&0&0 \\ 0&0&0&0&\frac{1}{2}&0 \\ 0&0&\frac{1}{\sqrt{2}}&0&0&0 \\ 0&0&0&0&0&\frac{1}{2} \\ 0&0&0&0&\frac{1}{2}&0 \\ 0&0&0&0&0&\frac{1}{2} \\ 0&0&0&0&0&\frac{1}{2} \\ 0&1&0&0&0&0 \end{bmatrix} \quad Y_1 = \begin{bmatrix} 0&0&0 \\ -\frac{\mathrm{i}}{2}&0&0 \\ -\frac{1}{2}&0&0 \\ 0&-\frac{\mathrm{i}}{2}&0 \\ \frac{\mathrm{i}}{2}&0&0 \\ 0&0&0 \\ 0&-\frac{1}{2}&0 \\ 0&0&-\frac{\mathrm{i}}{2} \\ \frac{1}{2}&0&0 \\ 0&\frac{1}{2}&0 \\ 0&0&0 \\ 0&0&\frac{1}{2} \\ 0&\frac{\mathrm{i}}{2}&0 \\ 0&0&\frac{\mathrm{i}}{2} \\ 0&0&-\frac{1}{2} \\ 0&0&0 \end{bmatrix}$$

$$Y_2 = \begin{bmatrix} 0&0&0&0 \\ 0&-\frac{1}{2}&0&0 \\ 0&\frac{1}{2}&0&0 \\ 0&0&-\frac{1}{2}&0 \\ 0&-\frac{1}{2}&0&0 \\ -\frac{1}{\sqrt{2}}&0&0&0 \\ 0&0&\frac{1}{2}&0 \\ 0&0&0&-\frac{1}{2} \\ 0&\frac{1}{2}&0&0 \\ 0&0&\frac{1}{2}&0 \\ \frac{1}{\sqrt{2}}&0&0&0 \\ 0&0&0&\frac{1}{2} \\ 0&0&-\frac{1}{2}&0 \\ 0&0&0&-\frac{1}{2} \\ 0&0&0&\frac{1}{2} \\ 0&0&0&0 \end{bmatrix} \quad Y_3 = \begin{bmatrix} 0&0&0 \\ \frac{\mathrm{i}}{2}&0&0 \\ -\frac{1}{2}&0&0 \\ 0&\frac{\mathrm{i}}{2}&0 \\ -\frac{\mathrm{i}}{2}&0&0 \\ 0&0&0 \\ 0&-\frac{1}{2}&0 \\ 0&0&\frac{\mathrm{i}}{2} \\ \frac{1}{2}&0&0 \\ 0&\frac{1}{2}&0 \\ 0&0&0 \\ 0&0&\frac{1}{2} \\ 0&-\frac{\mathrm{i}}{2}&0 \\ 0&0&-\frac{\mathrm{i}}{2} \\ 0&0&-\frac{1}{2} \\ 0&0&0 \end{bmatrix}.$$

7.13.4 Performance of Quantum PPM Systems

Considering that the PPM states have the GUS, the SRM gives an optimal detection, then, in performance evaluation, the same results will have to be found as those of Yuen et al. [4] with a different methodology.

Applying the method summarized in Sect. 7.7.1, about the SRM detection in the presence of GUS, the performance evaluation is articulated as follows. Gram's matrix G has as element i, j the inner product $G_{ij} = \langle \gamma_i | \gamma_j \rangle$, where now the states $|\gamma_i\rangle$ are composite. We recall that the inner product of two states, each generated by the tensor product of K component states, is given by the product of the K inner products of the component states, that is,

$$\langle \gamma_i | \gamma_j \rangle = \langle \gamma_{i0} | \gamma_{j0} \rangle \, \langle \gamma_{i1} | \gamma_{j1} \rangle \, \ldots \, \langle \gamma_{iK-1} | \gamma_{jK-1} \rangle. \tag{7.138}$$

Then, from (7.9), we get

$$\langle \gamma_i | \gamma_j \rangle = \begin{cases} 1 & i = j \\ \mathrm{e}^{-|\Delta|^2} & i \neq j. \end{cases} \tag{7.139}$$

For example, in the case $K = 4$ the inner product $\langle \gamma_0 | \gamma_2 \rangle$ results in

$$\begin{aligned} \langle \gamma_0 | \gamma_2 \rangle &= \langle \Delta | 0 \rangle \ \langle 0 | 0 \rangle \ \langle 0 | \Delta \rangle \ \langle 0 | 0 \rangle \\ &= \mathrm{e}^{-\frac{1}{2}|\Delta|^2} \ \ 1 \ \ \mathrm{e}^{-\frac{1}{2}|\Delta|^2} \ \ 1 = \mathrm{e}^{-|\Delta|^2}. \end{aligned}$$

We observe that the same energy E is associated to all symbols, and, according to (7.132), to each composite state the same signal photons are associated, given by

$$N_s = |\Delta|^2 = \text{number of signal photons/symbol.} \tag{7.140}$$

Therefore Gram's matrix becomes

$$G = \begin{bmatrix} 1 & |X|^2 & \dots & |X|^2 \\ |X|^2 & 1 & \dots & |X|^2 \\ \vdots & & \ddots & \\ |X|^2 & |X|^2 & \dots & 1 \end{bmatrix}$$

where $|X|^2$ is the quadratic superposition degree of the component states ($X = \langle \gamma_i \gamma_j \rangle$, $i \neq j$), given by

$$|X|^2 = |\langle \Delta 0 |^2 = \mathrm{e}^{-|\Delta|^2} = \mathrm{e}^{-N_s} \rangle.$$

Notice that G is a *circulant* matrix, as a consequence of the GUS.

Considering the GUS, the eigenvalues of G are given by the DFT of the first row $[1, |X|^2, \dots, |X|^2]$, and therefore

$$\lambda_i = \sum_{k=0}^{K-1} G_{0k} W_K^{-ki} = 1 + |X|^2 \sum_{k=1}^{K-1} W_K^{-ki}.$$

Recalling the orthogonality condition

$$\sum_{k=0}^{K-1} W_K^{-ki} = \begin{cases} K & i = 0 \\ 0 & i \neq 0 \end{cases} \tag{7.141}$$

we have

$$\lambda_i = \begin{cases} 1 + (K-1)|X|^2 & i = 0 \\ 1 - |X|^2 & i = 1, \dots, K-1. \end{cases}$$

The square roots of G become

$$G^{\pm\frac{1}{2}} = \sum_{i=0}^{K-1} \lambda_i^{\pm\frac{1}{2}} |w_i\rangle\langle w_i|.$$

The transition probabilities are computed from (7.93) and result in

$$p_c(i|j) = \frac{1}{K^2}\left|\sum_{p=0}^{K-1} \lambda_p^{1/2} W_K^{-p(i-j)}\right|^2 = \frac{1}{K^2}\left|\lambda_0^{1/2} + \lambda_1^{1/2}\sum_{p=1}^{K-1} W_K^{-p(i-j)}\right|^2$$

and, from (7.141),

$$p_c(j|i) = \begin{cases} K^{-2}\left(\lambda_0^{1/2} - \lambda_1^{1/2}\right)^2 & i \neq j \\ K^{-2}\left(\lambda_0^{1/2} + (K-1)\lambda_1^{1/2}\right)^2 & i = j \end{cases} \tag{7.142}$$

where

$$\lambda_0 = 1 + (K-1)|X|^2, \qquad \lambda_1 = 1 - |X|^2, \qquad \text{with} \quad |X|^2 = \mathrm{e}^{-N_s}.$$

The error probability is computed from (7.94) and becomes

$$\boxed{P_e = 1 - \frac{1}{K^2}\left(\sqrt{1 + (K-1)|X|^2} + (K-1)\sqrt{1 - |X|^2}\right)^2} \tag{7.143}$$

in perfect agreement with the results of [4].

Finally, the measurement vectors are obtained from (7.95), namely,

$$|\mu_i\rangle = \sum_{j=0}^{K-1} a_{ij}|\gamma_j\rangle \quad , \qquad a_{ij} = \begin{cases} K^{-2}\left(\lambda_0^{-1/2} - \lambda_1^{-1/2}\right)^2 & i \neq j \\ K^{-2}\left(\lambda_0^{-1/2} + (K-1)\lambda_1^{-1/2}\right)^2 & i = j. \end{cases}$$

7.13.5 Performance of Classical PPM Systems

We use the notations

- A_0 transmitted word,
- B_0 received word,
- $\widehat{A}_0$ decided word.

Let us consider, for simplicity, the case $K = 4$ with the standard (non specular) format and with a unitary scale factor ($\Delta = 1$), in which the possible transmitted words A_0 are

$$\gamma_0 = \begin{bmatrix} 1 & 0 & 0 & 0 \end{bmatrix}, \qquad \gamma_1 = \begin{bmatrix} 0 & 1 & 0 & 0 \end{bmatrix}$$
$$\gamma_2 = \begin{bmatrix} 0 & 0 & 1 & 0 \end{bmatrix}, \qquad \gamma_3 = \begin{bmatrix} 0 & 0 & 0 & 1 \end{bmatrix}. \tag{7.144}$$

With a photon counter, the symbol 0 is always received correctly, whereas the symbol 1 may be received as 0, with an error probability e^{-N_s}. Then we have five possible received words: the four correct words (7.144) and the wrong word $\begin{bmatrix} 0 & 0 & 0 & 0 \end{bmatrix}$, and we have to decide to which correct word the wrong word should be associated. The optimum criterion (with equiprobable symbols) is to associate the wrong word $\begin{bmatrix} 0 & 0 & 0 & 0 \end{bmatrix}$ to whatever correct word, for example to γ_0 (Fig. 7.38).
Then the decision criterion becomes

$$\begin{aligned}
&\widehat{A}_0 = \gamma_0 \quad \text{if} \quad B_0 = \begin{bmatrix} 1 & 0 & 0 & 0 \end{bmatrix} \quad \text{or} \quad B_0 = \begin{bmatrix} 0 & 0 & 0 & 0 \end{bmatrix} \\
&\widehat{A}_0 = \gamma_1 \quad \text{if} \quad B_0 = \begin{bmatrix} 0 & 1 & 0 & 0 \end{bmatrix} \\
&\widehat{A}_0 = \gamma_2 \quad \text{if} \quad B_0 = \begin{bmatrix} 0 & 0 & 1 & 0 \end{bmatrix} \\
&\widehat{A}_0 = \gamma_3 \quad \text{if} \quad B_0 = \begin{bmatrix} 0 & 0 & 0 & 1 \end{bmatrix}
\end{aligned}$$

and we can get an error only in the last three cases, each with probability e^{-N_s}. Thus,

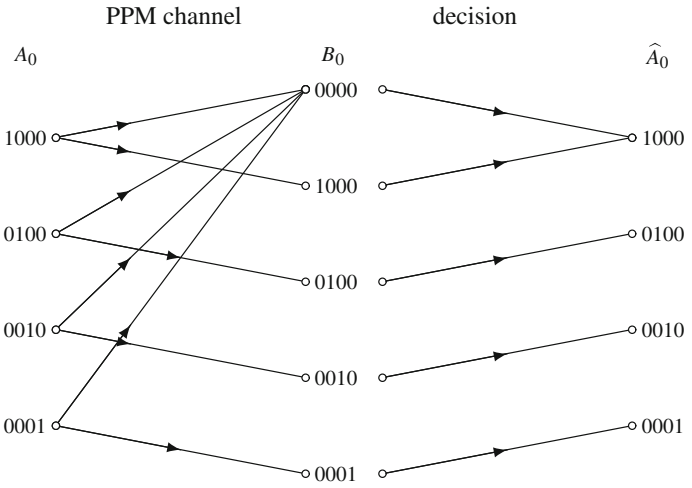

Fig. 7.38 Channel and decision criterion of a classical 4-PPM. A_0 is the transmitted word, B_0 the received word, and $\widehat{A}_0$ the decided word

$$P_{e,\text{classical}} = \frac{1}{4}[P_e(\gamma_1) + P_e(\gamma_2) + P_e(\gamma_3) + P_e(\gamma_4)]$$
$$= \frac{1}{4}[0 + \mathrm{e}^{-N_s} + \mathrm{e}^{-N_s} + \mathrm{e}^{-N_s}] = \frac{3}{4}\mathrm{e}^{-N_s}.$$

The general result is

$$\boxed{P_{e,\text{classical}} = \frac{K-1}{K}\mathrm{e}^{-N_s}.} \tag{7.145}$$

7.13.6 Comparison in the Binary Case

For binary quantum PPM, from (7.143) we get

$$P_c = \frac{1}{4}\left[\sqrt{1-|X|^2} + \sqrt{1+|X|^2}\right]^2 = \frac{1}{2}\left[1 + \sqrt{1-|X|^4}\right]$$

where $|X|^4 = \mathrm{e}^{-2N_s} = \mathrm{e}^{-2N_R}$, with $N_R = N_s$ the number of signal photons per bit. The error probability is therefore

$$P_e = \frac{1}{2}\left[1 - \sqrt{1-\mathrm{e}^{-2N_R}}\right], \tag{7.146}$$

the same result found for the OOK format (see (7.106)).

Instead, in the classical case, from (7.145) we have $P_{e,\text{classical}} = \frac{1}{2}\mathrm{e}^{-N_R}$. The comparison of these results is shown in Fig. 7.39.

7.13.7 Comparison in the K-ary Case

In the quantum case, the error probability is given by (7.143), which can be rewritten in the form

$$P_e = \frac{K-1}{K^2}\left[K - (K-2)(1-|X|^2) + 2\sqrt{(1-|X|^2)(1+(K-1)|X|^2)}\right]$$

where the superposition degree $|X|^2$ can be expressed as a function of the number of signal photons per symbol N_s, or of the number of signal photons per bit N_R

$$|X|^2 = \mathrm{e}^{-N_s} = \mathrm{e}^{-N_R \log_2 K}.$$

In the classical case the error probability is given by (7.145).

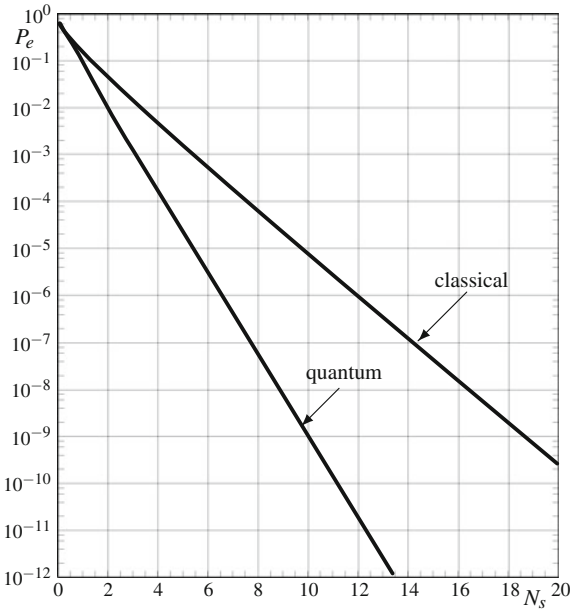

Fig. 7.39 Comparison of quantum and classical 2-PPM

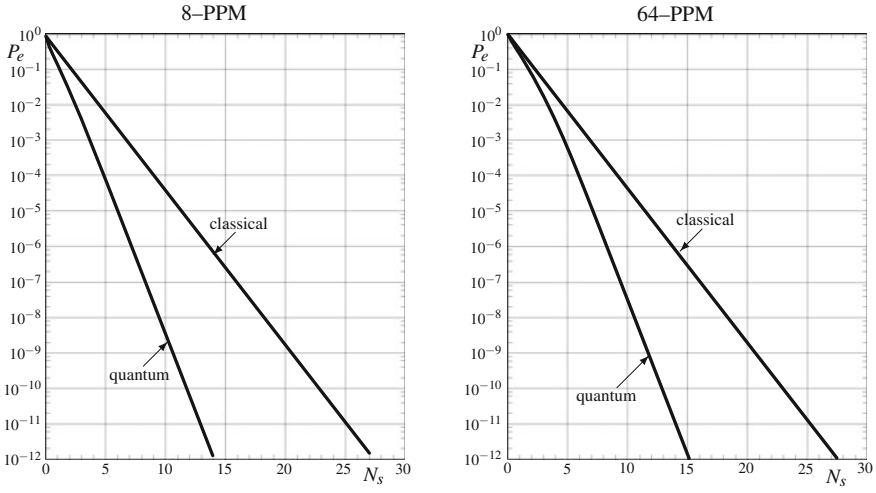

Fig. 7.40 Comparison between quantum and classical 8-PPM and 64-PPM in terms of number of signal photons per symbol N_s

The comparison between the two systems is illustrated for the 8-PPM and 64-PPM in Fig. 7.40 as a function of the number of signal photons per symbol N_s. Even in this case we notice a striking superiority of the quantum system.

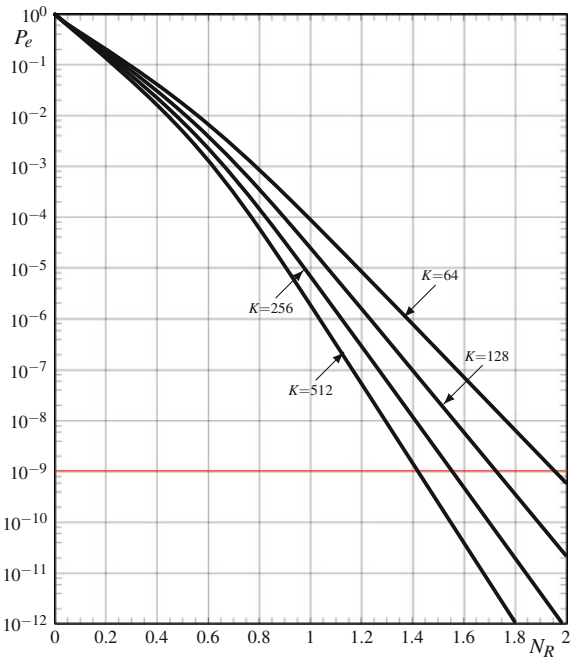

Fig. 7.41 Error probability of quantum PPM as a function of the *number of signal photons per bit* N_R

For instance in 8-PPM with $N_s = 10$ photon/symbol we find $P_e = 3.660\ 10^{-9}$ and $P_{e,\text{classical}} = 3.972\ 10^{-5}$; in 64–PPM with $N_s = 10$ photon/symbol we find $P_e = 3.421\ 10^{-9}$ and $P_{e,\text{classical}} = 4.469\ 10^{-5}$. In both cases the improvement of the quantum system is of several decades.

In Fig. 7.41 the error probability of the quantum PPM is plotted as a function of the number of signal photons per bit N_R for four values of K. We realize that quantum PPM receivers have an extraordinary sensitivity, specifically

2-PPM	$N_R = 9.66849$	photons/bit
4-PPM	$N_R = 5.10889$	photons/bit
8-PPM	$N_R = 3.54713$	photons/bit
16-PPM	$N_R = 2.75561$	photons/bit
32-PPM	$N_R = 2.27708$	photons/bit
64-PPM	$N_R = 1.95665$	photons/bit
128-PPM	$N_R = 1.72722$	photons/bit
256-PPM	$N_R = 1.55486$	photons/bit
512-PPM	$N_R = 1.42072$	photons/bit
1024-PPM	$N_R = 1.31332$	photons/bit

7.14 Overview of Squeezed States

Up to now we have considered Quantum Communications based on coherent states. In these last two sections, we consider the promising possibility to use squeezed states.

We have seen that a coherent state $|\alpha\rangle$ is completely determined by a complex parameter α. A squeezed state, and more precisely, a squeezed-displaced state, say $|z, \alpha\rangle$ may be seen as a generalization of a coherent state, because of the dependence on two complex parameters, the *displacement* α and the *squeeze factor* $z = re^{i\theta}$. In particular, setting z to zero, the squeezed-displaced state gives back the coherent state

$$|0, \alpha\rangle = |\alpha\rangle \in \mathcal{G}. \tag{7.147}$$

This simple property allows us to say that, using squeezed states in quantum communications with appropriate parameters, the performance cannot be worse than with coherent states. As we shall see, the squeeze factor z allows us to control the photon statistic in such a way that, by choosing z in an appropriate range, we get a considerable improvement of the system performance. This opportunity has been long recognized [14].

The theory of **squeezed-displaced states** will be formulated in Sect. 11.15 in the context of continuous variables, where it is shown that they represent the **most general form of Gaussian states**. In this section, we give the essential properties of squeezed states that are needed for Quantum Communications.

We shall use the following notations

- $|z, \alpha\rangle$: squeezed-displaced state
- $|0, \alpha\rangle = |\alpha\rangle$: coherent state
- $|z, 0\rangle$: squeezed state or squeezed vacuum state.

7.14.1 Definition and Properties of Squeezed-Displaced States

Squeezed states live in the same Hilbert space as coherent states, that is an infinite dimensional Hilbert space where the Fock basis has been introduced. Squeezed-displaced states are the result of two distinct operations applied to the vacuum state: A squeezing and a displacement. They may be specified by the Fock expansion, whose Fourier coefficients result in

$$|z, \alpha\rangle_n = \frac{\sqrt{n!}}{\mu} \left(\frac{\beta}{\mu}\right)^n \mathcal{H}_n\left(\frac{\mu\nu}{\beta^2}\right) \exp\left(-\frac{1}{2}|\beta|^2 - \beta^2 \frac{\nu^*}{2\mu}\right). \tag{7.148}$$

where $\mathcal{H}_n(x)$ are the polynomials (of degree $\lfloor n/2 \rfloor$)

$$\mathcal{H}_n(x) := \sum_{j=0}^{\lfloor n/2 \rfloor} \frac{1}{(n-2j)!j!}\, x^j. \tag{7.149}$$

and

$$\mu = \cosh r\,, \qquad \nu = \sinh r \exp(\mathrm{i}\,\theta)\,, \qquad \beta = \mu\alpha - \nu\alpha^*. \tag{7.149a}$$

The deduction of (7.148) from the operations of squeezing and displaciment is made in Sect. 11.15.[6]

The class of squeezed-displaced states has two special subclasses, which are obtained for $z = 0$ (absence of squeezing) and for $\alpha = 0$ (absence of displacement). In the first case we have **coherent states** with coefficients (see (7.2))

$$|0, \alpha\rangle_n = \mathrm{e}^{-\frac{1}{2}|\alpha|^2}\, \frac{\alpha^n}{\sqrt{n!}} \tag{7.150}$$

In the second case we have **squeezed vacuum states** with coefficients

$$|z, 0\rangle_n = \sqrt{\mathrm{sech} r} \sum_{n=0}^{\infty} \frac{\sqrt{(2n)!}}{2^n n!} \lambda^n |2n\rangle \qquad \lambda = \tanh r\, \mathrm{e}^{\mathrm{i}\theta} \tag{7.151}$$

that is, the state $|z, 0\rangle$ is given by a linear combination of *even photon number states*, which means that the probability that the state contains an odd number of photons is zero.

7.14.2 Statistics of Squeezed-Displaced States

The probability distribution of the number of photons in a squeezed state is obtained by squaring the Fourier coefficients (7.148), that is,

$$p_n(i) := \mathrm{P}[n = i] = ||z, \alpha\rangle_i|^2 \tag{7.152}$$

This distribution is illustrated in Fig. 7.42 for $\alpha = 3$ and four values of r with $\theta = 0$. Note that for $r = 0$, absence of squeezing, $p_n(i)$ becomes a Poisson distribution, but in general it may be far form the Poisson shape, and sometimes this is classified as *sub-Poissonian statistic*. Under certain conditions, this statistics may be controlled acting on the squeeze factor [14].

The mean photon number in a squeezed-displaced state is given by [4]

---

[6] The Fock expansion of squeezed-displaced states was first established by [4], who expressed the Fourier coefficients in terms of Hermite polynomials $H_n(x)$. The equivalent formulation in terms of the polynomials $\mathcal{H}_n(x)$ appear to be more direct.

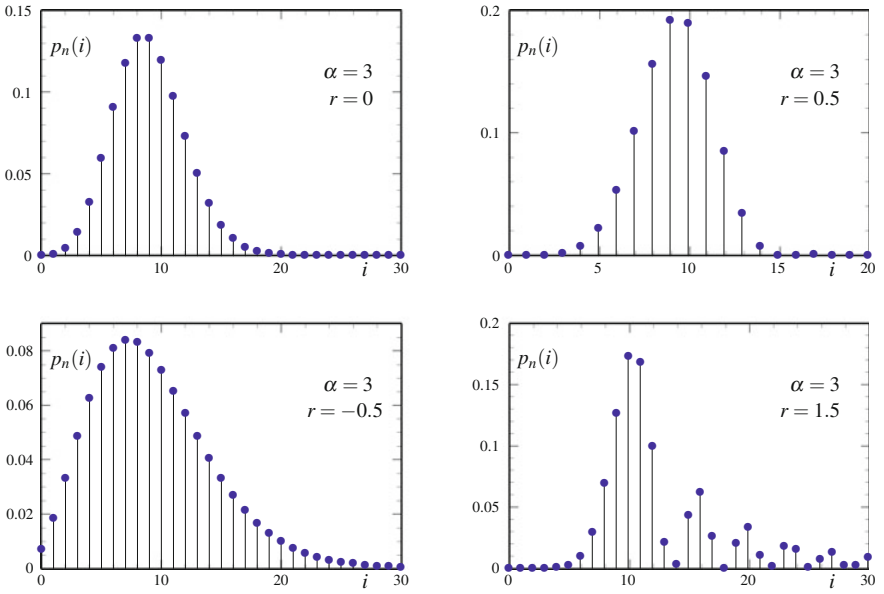

Fig. 7.42 The probability distribution of photon number in squeezed-displaced states, $p_n(i) = \mathrm{P}[n = i \mid |(\alpha, r)\rangle]$, for $\alpha = 3$ and different values of r

$$\bar{n}_{|z,\alpha\rangle} = |\alpha|^2 + \sinh^2 r \tag{7.153}$$

and the variance of the photon number is given by [15]

$$\sigma^2_{n_{|z,\alpha\rangle}} = |\alpha|^2 \left[\mathrm{e}^{-2r}\cos^2\theta + \mathrm{e}^{2r}\sin^2\theta\right] + \frac{1}{2}\sinh^2 2r. \tag{7.154}$$

Clearly these parameters, illustrated in Fig. 7.43, confirm the non-Poissonian statistic, because the mean and the variance are different.

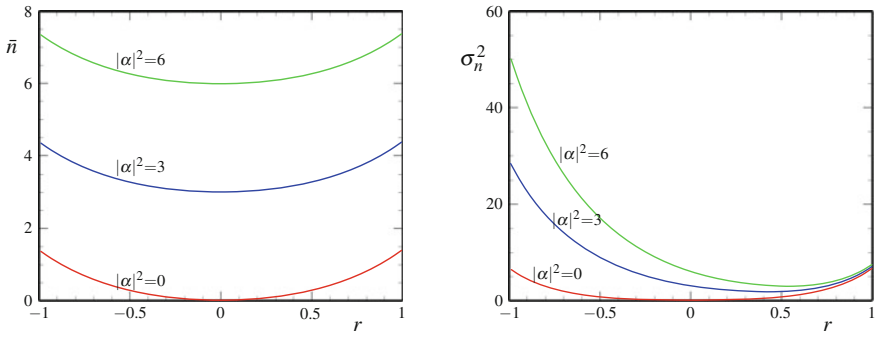

Fig. 7.43 Mean photon number $\bar{n}$ and variance σ_n^2 in squeezed-dispaced states versus the squeeze factor r for three values of $|\alpha|^2$

7.14.3 Degree of Superposition of Squeezed-Displaced States

The most important parameter for Quantum Communications is given by the inner product, which must be studied in detail.

Proposition 7.4 *The inner product of two squeezed-displaced states was evaluated by Yuen [4, Eq. 3.25] and reads*

$$\boxed{\langle z_1, \alpha_1 z_0, \alpha_0 = A^{-\frac{1}{2}} \exp\left[-\frac{A\left(|\beta_1|^2 + |\beta_0|^2\right) - 2\beta_1\beta_0^* + B\,\beta_1^{*2} - B^*\beta_0^2}{2A}\right]} \tag{7.155}$$

where

$$\begin{aligned} &z_i = r_i \mathrm{e}^{\mathrm{i}\theta_i}, \qquad i = 0, 1 \\ &\mu_i = \cosh(r_i), \qquad \nu_i = \sinh(r_i)\mathrm{e}^{\mathrm{i}\theta_i} \\ &\beta_i = \mu_i\alpha_i - \nu_i\alpha_i^* \\ &A = \mu_0\mu_1^* - \nu_0\nu_1^*, \qquad B = \nu_0\mu_1 - \mu_0\nu_1 \end{aligned} \tag{7.155a}$$

To study this complicate expression, we begin with remarking the dependence on the displacements α_i and on the squeeze factors z_i: The parameters β_0 and β_1 depend on both, while *all the other parameters depend only on the squeeze factors*. We can write (7.155) as

$$\langle z_1, \alpha_1 | z_0, \alpha_0 \rangle = A^{-\frac{1}{2}} \exp\left[-\sum_{i=0}^{1}\sum_{j=0}^{1}\left(a_{ij}\,\alpha_i\alpha_j + b_{ij}\,\alpha_i\alpha_j^* + d_{ij}\,\alpha_i^*\alpha_j^*\right)\right]$$

having at the exponent a bi-quadratic structure in α_0, α_1, α_0^*, and α_1^*, whose coefficients a_{ij}, b_{ij}, d_{ij} depend *only on the squeeze factors*.

For $\alpha_0 = \alpha_1 = 0$ (absence of displacement), (7.155) gives

$$\begin{aligned} \langle z_1, 0 | z_0, 0 \rangle &= A^{-\frac{1}{2}} = (\mu_0\mu_1^* - \nu_0\nu_1^*)^{-\frac{1}{2}} \\ &= (\cosh r_0 \cosh r_1 - \sinh r_0\, \sinh r_1 \mathrm{e}^{\mathrm{i}(\theta_0 - \theta_1)})^{-\frac{1}{2}} \end{aligned}$$

which is in agreement with the expression obtained in [16] for the inner product of two squeezed vacuum states

$$\langle z_1, 0 | z_0, 0 \rangle = \sqrt{\operatorname{sech} r\, \operatorname{sech} r_0} \,/\, \sqrt{1 - \mathrm{e}^{\mathrm{i}(\theta_0 - \theta)} \tanh r\, \tanh r_0}. \tag{7.156}$$

For $z_0 = z_1 = 0$ (absence of squeezing) we get $A = 1$, $B = 0$, $\beta_i = \alpha_i$, and then

$$\langle 0, \alpha_1 | 0, \alpha_0 \rangle = \exp\left[-\frac{1}{2} \left(|\alpha_1|^2 + |\alpha_0|^2 - 2\alpha_1 \alpha_0^* \right) \right]$$

which is the formula we got for the inner product of two coherent states (see (7.9)).

7.14.4 Squeezed-Displaced States as Gaussian States

As said above, squeezed-displaced states are the most general Gaussian states. The state $|z, \alpha\rangle$ depends on two complex parameters

$$z = r\, \mathrm{e}^{\mathrm{i}\theta}, \qquad \alpha = \Delta\, \mathrm{e}^{\mathrm{i}\,\varepsilon}. \tag{7.157}$$

We examine in detail the Wigner function $W(x, y)$ of the state (7.157), which is completely determined by the mean value and by the covariance matrix (see Sect. 7.2.5). Now, in $|z, \alpha\rangle$ the squeezing part does not give any contribution to the mean value, so we have

$$\begin{bmatrix} \overline{q} \\ \overline{p} \end{bmatrix} = \begin{bmatrix} \Re\alpha \\ \Im\alpha \end{bmatrix} = \begin{bmatrix} \Delta \cos\varepsilon \\ \Delta \sin\varepsilon \end{bmatrix}. \tag{7.158}$$

On the other hand the covariance matrix of the displacement component is the identity, so that the covariance matrix depends only on the squeeze factor as

$$\begin{aligned} V &= \begin{bmatrix} V_{11} & V_{12} \\ V_{12} & V_{22} \end{bmatrix} \\ &= \begin{bmatrix} \cosh^2 r + \sinh^2 r + \cos\theta \sinh 2r & \sin\theta \sinh 2r \\ \sin\theta \sinh 2r & \cosh^2 r + \sinh^2 r - \cos\theta \sinh 2r \end{bmatrix}. \end{aligned} \tag{7.159}$$

Considering that $\det V = 1$, the Wigner function results in

$$W(x, y) = \frac{1}{2\pi} \exp\left\{ -\frac{1}{2} \left[V_{22} \big(x - \overline{q}\big)^2 + V_{11} \big(y - \overline{p}\big)^2 - 2V_{12} \big(x - \overline{q}\big)\big(y - \overline{p}\big) \right] \right\}. \tag{7.160}$$

A convenient representation of $W(x, y)$ in the x, y plane is given by a *contour level*, which represents the curve given by the relation $W(x, y) = L$, with $L > 0$ real. In general, these curves are *tilted* ellipses as shown in Fig. 7.44. The ellipses have the common center given by the displacement α, and the main axis is tilted by the angle $\frac{1}{2}\theta$. The lengths of the main axis and of the minor axis are proportional to e^{2r} and to e^{-2r}, respectively, and so they are independent of the squeeze phase θ.

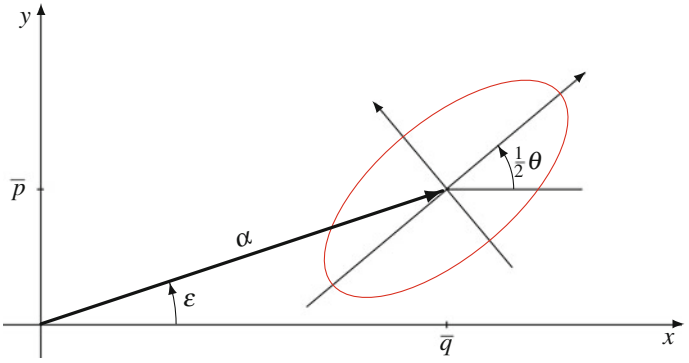

Fig. 7.44 Contour level of the Wigner function W(x,y) (in *red*) of a squeezed-displaced state $|z, \alpha\rangle$ with $z = r\,\mathrm{e}^{\mathrm{i}\theta}$ and $\alpha = \Delta\,\mathrm{e}^{\mathrm{i}\varepsilon}$. The mean vector $(\bar{q}, \bar{p}) = (\Delta\cos\varepsilon, \Delta\sin\varepsilon)$ gives the displacement amount and determines the center of the elliptic countour. The main axis of the *ellipse* is tilted with respect to the x axis of the angle $\frac{1}{2}\theta_0$

7.14.5 Constellations of Squeezed-Displaced States with GUS

In Sect. 11.20, we will prove that the application of the rotation operator $R(\phi)$ to a squeezed-displaced state $|z, \alpha\rangle$, with $z = r\,\mathrm{e}^{\mathrm{i}\theta}$ and $\alpha = \Delta\mathrm{e}^{\mathrm{i}\varepsilon}$, gives back the new squeezed-displaced state

$$R(\phi)|z, \alpha\rangle = |z\mathrm{e}^{\mathrm{i}\,2\phi}, \alpha\mathrm{e}^{\mathrm{i}\,\phi}\rangle = |r\mathrm{e}^{\mathrm{i}\,(2\phi+\theta)}, \Delta\mathrm{e}^{\mathrm{i}\,(\phi+\varepsilon)}\rangle$$

that is, with the modification of squeeze factor $z \to z\mathrm{e}^{\mathrm{i}\,2\phi}$ and of the displacement $\alpha \to \alpha\mathrm{e}^{\mathrm{i}\,\phi}$. In other words, the class of squeezed-displaced states is closed under rotations.

The above properties allow us to construct K-ary PSK constellations having the GUS, using as symmetry operator $S = R(2\pi/K)$. If $|z_0, \alpha_0\rangle$ is a reference squeezed-displaced state, the constellation has the form

$$\mathcal{S} = \{S^k\,|z_0, \alpha_0\rangle = |z_0\mathrm{e}^{\mathrm{i}\,2k\,2\pi/K}\ ,\ \alpha_0\mathrm{e}^{\mathrm{i}\,k\,2\pi/K}\rangle\ ,\ k = 0, 1, \ldots, K-1\}. \quad (7.161)$$

Figure 7.45 shows two 8-PSK constellations having the GUS with coherent states and squeezed-displaced states. The circles and the ellipses around the states represent the contour levels of the Wigner function of each state; the eccentricity of the ellipse depends only the squeeze factor r.

As seen for coherent states the GUS will allow us to find an optimal detection (minimum error probability) with the SRM approach.

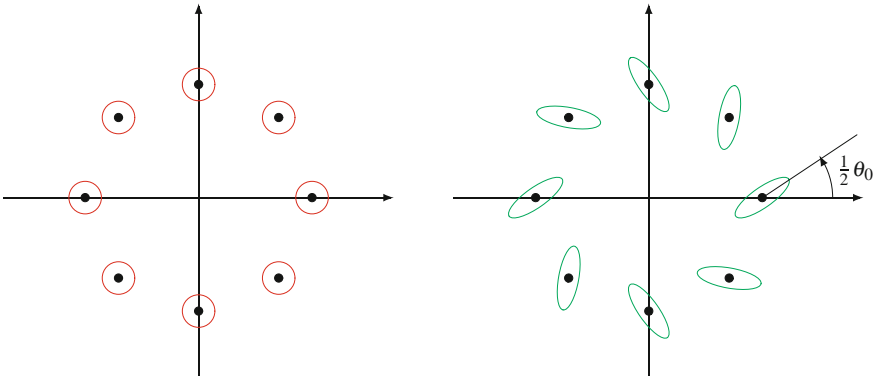

Fig. 7.45 8-PSK constellations of coherent states (*left*) and of squeezed-displaced states (*right*) with the GUS. In both constellations the reference state has a real and positive displacement ($\alpha = \Delta$, $\varepsilon = 0$). The squeeze phase of the reference state is θ_0 and the corresponding *ellipse* is tilted of $\frac{1}{2}\theta_0$

7.15 Quantum Communications with Squeezed States

In this section, we evaluate the performance (error probability) in quantum communications systems where the information carrier is given by squeezed-displaced states instead of coherent states. We consider only PSK communications systems[7]; and therefore it is natural to choose constellations having the GUS. Then, for a given modulation order K, we have to choose a reference state of the constellation, $|z_0, \alpha_0\rangle$, because the other states are generated through the rotation operator, as indicated in (7.161).

In the choice of the reference state $|z_0, \alpha_0\rangle$, where $z_0 = r_0\, \mathrm{e}^{\mathrm{i}\theta_0}$, without restriction we can assume α_0 real and positive. This parameter, together with r_0, determines the average number of photons contained in the state, which is given by

$$\boxed{\overline{n}_{|z_0,\alpha_0\rangle} = |\alpha_0|^2 + \sinh^2 r_0.} \tag{7.162}$$

This number is very important because, in a PSK constellation with equally likely symbols, it also gives the average number of signal photons per symbol N_s. Now, choosing r_0 as a parameter that quantify the squeezing amount, it remains to choose the squeeze phase θ_0 and this will be done by taking θ_0 that minimizes the error probability.

Considering that the performance of PSK essentially depends on the quadratic superposition between the states of the constellation

$$|X|^2 = |\langle r_0 \mathrm{e}^{\mathrm{i}\theta_0}, \alpha_0 | r_1 \mathrm{e}^{\mathrm{i}\theta_1}, \alpha_1 \rangle|^2$$

[7] Recently also the PPM with squeezed-displaced states has been considered [17].

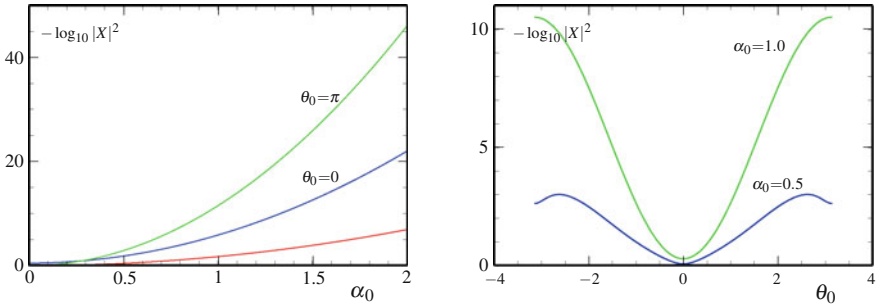

Fig. 7.46 Square of the inner product $X = \langle \alpha_0, r_0 e^{i\theta_0} | \alpha_1, r_1 e^{i\theta_1} \rangle$, represented by $-\log_{10}|X|^2$, for a BPSK constellation. On the *left*, the plot is versus the amplitude α_0 of the displacement for coherent states (*red*) and for squeezed-displaced states with $r_0 = 0.9$ and two values of θ_0. On the *right*, the plot is versus θ_0 with $r_0 = 0.9$ and two values of α_0

it is important to learn how $|X|^2$ depends on squeeze and displacement parameters. This is considered in Fig. 7.46 for the BPSK, where $r_1 e^{i\theta_1} = r_0 e^{i(\theta_0 + 2\pi)}$ and $\alpha_1 = \alpha_0 e^{i\pi}$. On the left of the figure $|X|^2$ is plotted versus α_0 for coherent states (red curve) and also for squeezed-displaced states for a fixed value of r_0 and two values of θ_0. It is remarkable the great improvement obtained with squeezed states, especially at the increase of the displacement amount α_0. The right of the figure shows the strong dependence of $|X|^2$ on the squeeze phase θ_0 and hence the importance of an appropriate choice of this parameter.

7.15.1 BPSK with Squeezed States

The BPSK constellation of squeezed-displaced states is obtained from (7.161) with $K = 2$, namely

$$\mathcal{S} = \{|r_0 e^{i\theta_0}, \alpha_0\rangle, |r_0 e^{i\theta_0} e^{i2\pi}, \alpha_0 e^{i\pi}\}\rangle. \tag{7.163}$$

For the evaluation of the error probability we can apply Helstrom's theory (see (7.102)), which gives, with equally likely symbols,

$$P_e = \frac{1}{2}\left(1 - \sqrt{1 - |X|^2}\right). \tag{7.164}$$

Thus, the only parameter needed is the quadratic superposition $|X|^2$ between the two states of the constellation. We have seen that $|X|^2$ is a function of r_0, α_0, and θ_0. Now, fixing r_0 and α_0, we have the number of signal photons per symbol N_s as

$$N_s = |\alpha_0|^2 + \sinh^2 r_0. \tag{7.165}$$

and we choose the squeeze phase θ_0 that achieves the minimum error probability.

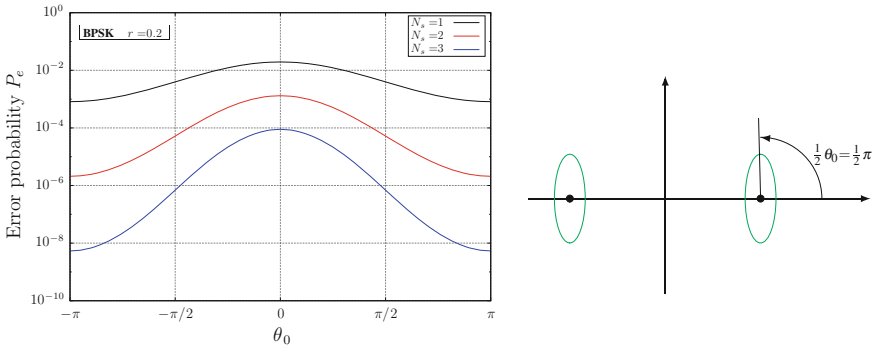

Fig. 7.47 BPSK system with squeezed-displaced states. On the *left*, the error probability P_e versus the squeeze phase θ_0 for three values of the number of signal photons per symbol N_s. All the curves have a minimum for $\theta_0 = \pi$. On the *right*, the optimal BPSK constellation where the ellipse of the reference state is tilted of $\theta_0 = \pi/2$ because the optimal squeeze phase is $\theta_0 = \pi$

In Fig. 7.47 the error probability is plotted versus θ_0 for three values of N_s. Clearly, the minimum of P_e is obtained for $\theta_0 = \pi$, which means that in optimal BPSK constellation the ellipses appear to be vertically tilted, as shown at the right of the figure.

Finally, in Fig. 7.48 we compare the error probability P_e versus N_s obtained with coherent states and squeezed-displaced states. It is remarkable that the performance of the BPSK is highly improved with the presence of squeezing.

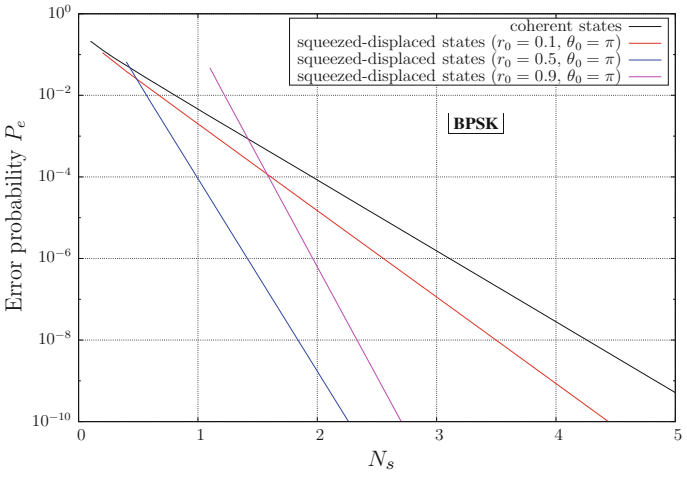

Fig. 7.48 Error probability P_e versus the number of signal photons per symbol N_s in 4-PSK. The *dark curve* refers to coherent states, while the *colored curves* refer to squeezed-displaced states with different values of the squeeze factor r_0 and optimal squeeze phase $\theta_0 = -\pi/2$. The curve do not start at $N_s = 0$, because $N_s = |\alpha_0|^2 + \sinh^2 r_0$ and for $N_s < \sinh^2 r_0$ there is no room for the displacement α_0

7.15.2 4-PSK with Squeezed States

The 4-PSK constellation of squeezed-displaced states is obtained from (7.161) with $K = 4$, namely $\mathcal{S} = \{|z_i, \alpha_i\rangle\}$, where

$$z_i = z_0 \mathrm{e}^{\mathrm{i}\, 2k\, 2\pi/4}, \qquad \alpha_i = \alpha_0 \mathrm{e}^{\mathrm{i}\, k\, 2\pi/2}, \qquad i = 0, 1, 2, 3. \tag{7.166}$$

Considering that the constellation has the GUS, for the evaluation of the error probability we apply the SRM approach, which turns out to be optimum. From Sect. 7.7 we recall that the evaluation of P_e using the SRM is obtained as follows:

(1) Evaluation of the inner products

$$G_{pq} = \langle z_p, \alpha_p | z_q, \alpha_q \rangle, \qquad p, q = 0, 1, 2, 3.$$

(2) Evaluation of the eigenvalues $\lambda_i = \sum_{k=0}^{3} G_{0k}\, W_4^{-ki}$, and finally

$$P_e = 1 - \left(\frac{1}{4} \sum_{i=0}^{3} \sqrt{\lambda_i} \right)^2. \tag{7.167}$$

Also in this case P_e is a function of r_0, α_0, and θ_0 and the number of signal photons per symbol N_s is still given by (7.165). Again, we choose r_0 and α_0 as parameters and we search for the squeeze phase θ_0 that gives the minimum error probability.

In Fig. 7.49 the error probability is plotted versus θ_0 for three values of N_s. Clearly, the minimum of P_e is obtained for $\theta_0 = -\pi/2$, which means that in the optimal 4-PSK constellation the reference ellipse is tilted of $\frac{1}{2}\theta_0 = -\pi/4$, as shown on the right of the figure (see Fig. 7.45).

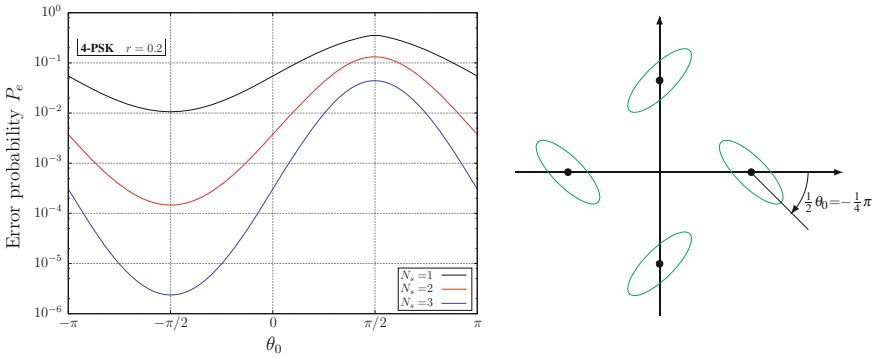

Fig. 7.49 4-PSK system with squeezed-displaced states. On the *left*, the error probability P_e versus the squeeze phase θ_0 for three values of the number of signal photons per symbol N_s All the curves have a minimum for $\theta_0 = -\pi/2$. On the *right* the optimal 4-PSK constellation; the ellipse of the reference state is tilted by $\frac{1}{2}\theta_0 = -\pi/4$ because the optimal squeeze phase is $\theta_0 = -\pi/2$

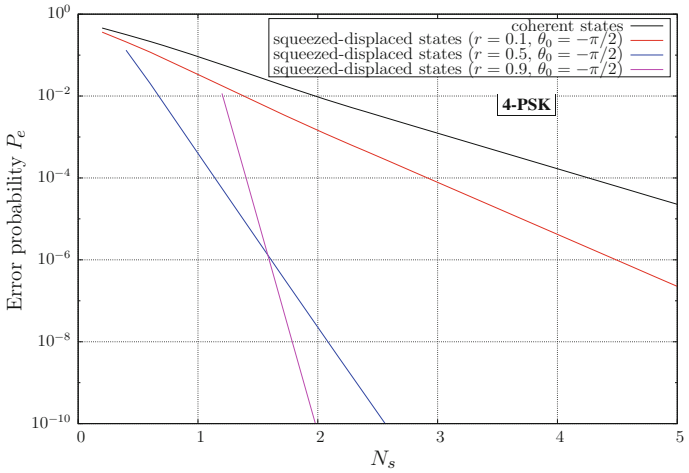

Fig. 7.50 Error probability P_e versus the number of signal photons per symbol N_s in 4-PSK. The *dark curve* refers to coherent states, while the *colored curves* refer to squeezed-displaced states with different values of the squeeze factor r_0 and optimal squeeze phase $\theta_0 = -\pi/2$. The curve do not start at $N_s = 0$, because $N_s = |\alpha_0|^2 + \sinh^2 r_0$ and for $N_s < \sinh^2 r_0$ there is no room for the displacement α_0

Finally, in Fig. 7.50 we compare the error probability P_e versus. N_s obtained with coherent states and with squeezed-displaced states. We realize that also the 4-PSK is highly improved with the presence of squeezing.

7.15.3 Conclusions

In this chapter, we have considered coherent states as the standard carrier for data transmission in quantum communications systems. On the other hand, in this last section, we have seen the possibility of a huge improvement using squeezed light, but we have limited the analysis only to the systems 2PSK and 4PSK for the reason that squeeze technique is not promising for the immediate future because of losses and excess noise present in this technique and because of the complexity and power required. However, quantum optics is making rapid progress so that quantum communications with squeezed states merits a special attention.

References

1. R.J. Glauber, The quantum theory of optical coherence. Phys. Rev. **130**, 2529–2539 (1963)
2. R.J. Glauber, Coherent and incoherent states of the radiation field. Phys. Rev. **131**, 2766–2788 (1963)

3. C.W. Helstrom, J.W.S. Liu, J.P. Gordon, Quantum-mechanical communication theory. Proc. IEEE **58**(10), 1578–1598 (1970)
4. H.P. Yuen, R. Kennedy, M. Lax, Optimum testing of multiple hypotheses in quantum detection theory. IEEE Trans. Inf. Theory **21**(2), 125–134 (1975)
5. J. Shapiro, Quantum noise and excess noise in optical homodyne and heterodyne receivers. IEEE J. Quantum Electron. **21**(3), 237–250 (1985)
6. J.E. Mazo, J. Salz, On optical data communication via direct detection of light pulses. Bell Syst. Tech. J. **55**, 347–360 (1976)
7. K. Kato, M. Osaki, M. Sasaki, O. Hirota, Quantum detection and mutual information for QAM and PSK signals. IEEE Trans. Commun. **47**(2), 248–254 (1999)
8. I.S. Gradshteyn, I.M. Ryzhik, *Tables of Integrals, Series, and Products*, 7th edn. (Elsevier, Amsterdam, 2007)
9. J.G. Proakis, *Digital Communications* (McGraw-Hill, New York, 2001)
10. G. Cariolaro, *Modulazione analogica, discreta e numerica* (Edizioni Progetto, Padova, 1996)
11. A. Waseda, M. Sasaki, M. Takeoka, M. Fujiwara, M. Toyoshima, A. Assalini, Numerical evaluation of PPM for deep-space links. IEEE/OSA J. Opt. Commun. Netw. **3**(6), 514–521 (2011)
12. M. Sasaki, A. Waseda, M. Takeoka, M. Fujuwara, H. Tanaka, Quantum information technology for power minimum info-communications, in *Toward Green ICT*, ed. by R. Prasad, S. Ohmori, D. Simunic (River Publishers, Denmark, 2010). ch. 15
13. G. Cariolaro, G. Pierobon, Theory of quantum pulse position modulation and related numerical problems. IEEE Trans. Commun. **58**(4), 1213–1222 (2010)
14. R.E. Slusher, B. Yurke, Squeezed light for coherent communications. J. Lightwave Technol. **8**(3), 466–477 (1990)
15. M.S. Kim, F.A.M. de Oliveira, P.L. Knight, Properties of squeezed number states and squeezed thermal states. Phys. Rev. A **40**, 2494–2503 (1989)
16. X.B. Wang, T. Hiroshima, A. Tomita, M. Hayashi, Quantum information with Gaussian states. Phys. Rep. **448**(1–4), 1–111 (2007)
17. G. Cariolaro, R. Corvaja, G. Pierobon, Gaussian states and geometrically uniform symmetry. Phys. Rev. A **90**(4), 042309 (2014)